1-1-2013

Renewable Bio-Based Polymers and Degradable Functional Polymers

Kejian Yao
University of South Carolina - Columbia

RENEWABLE BIO-BASED POLYMERS AND DEGRADABLE FUNCTIONAL POLYMERS

by

Kejian Yao

Bachelor of Science
East China University of Science and Technology, 2006

Submitted in Partial Fulfillment of the Requirements

For the Degree of Doctor of Philosophy in

Chemistry

College of Arts and Sciences

University of South Carolina

2013

Accepted by:

Chuanbing Tang, Major Professor

Brian Benicewicz, Committee Member

Richard Adams, Committee Member

Francis Gadala-Maria, Committee Member

Lacy Ford, Vice Provost and Dean of Graduate Studies

DEDICATION

To my mother, my whole family, and all my friends, without their support and encouragement, none of my accomplishments would be possible.

ACKNOWLEDGEMENTS

First I would like to show my deepest appreciation to my advisor, Dr. Chuanbing Tang, who gave me the opportunity to work and learn in his research group and offered me tremendous guidance and support on my research projects. I feel very fortunate to have worked under the guidance of Dr. Tang for the past 4 to 5 years. His enthusiasm for polymer science influenced me a lot and I am grateful for all I have learned from Dr. Tang and hope to learn more from him in the future.

Then I would like to thank Dr. Brian Benicewicz, Dr. Richard Adams and Dr. Francis Gadala-Maria for being my committee members and providing me valuable suggestions on my researches as well as this dissertation. Also I want to express my gratitude to all my Department colleagues, especially the members in Dr. Tang's research group, Dr. Lixia Ren, Dr. Yijun Zheng, Dr. Jifu Wang, Dr. Ying Chen, Dr. Yali Qiao, Dr. Yi Yan, Dr. Alper Nese, Christopher Hardy, Perry Wilbon, Jiuyang Zhang, Jeffery Hayat, Liang Yuan, Mitra Ganewatta, Yupeng Liu and many others. It is a great pleasure to work with all of you and learn from you. Thanks for all your helps and suggestions.

Further, I want to give my sincerest appreciation to my family and friends. Thanks to my family for their unconditional love and support. Thanks to all my friends both in USA and China for their encouragement and help.

Finally, I acknowledge all the funding supports from University of South Carolina, US Department of Agriculture, Kimberly-Clark Corporation, and Chinese Academy of Forestry.

ABSTRACT

In this dissertation, polymers derived from renewable bio-based resources and degradable functional polymers with stimuli-responsive properties by various polymerization techniques were investigated. The properties of these polymeric materials were characterized and discussed.

In Chapter 1, the overall background and recent development of renewable bio-based polymers as well as degradable stimuli-responsive polymers was introduced. Major research objectives of my doctoral work were described.

The first section of the dissertation, on the preparation of renewable bio-based polymers was provided from Chapter 2 to Chapter 4. In Chapter 2, the preparation of novel polymers derived from renewable gum rosin by atom transfer radical polymerization (ATRP) and reversible addition-fragmentation chain-transfer (RAFT) polymerization was described. Chapter 3 described the preparation of different rosin containing polycaprolactone (PCL) by a combination of ring-opening polymerization (ROP) and "click" chemistry. The rosin containing PCL showed excellent hydrophobicity, elevated glass transition temperature, low water uptake and full degradability. Also the polymers exhibited good biocompatibility and low cytotoxicity, suitable for potential biomedical applications. In Chapter 4, sustainable graft copolymers derived from renewable cellulose, rosin and fatty acid as novel thermoplastic elastomers

were accomplished by ATRP and mechanical properties of the polymers were characterized by tensile stress-strain and creep compliance testing.

The second part of the dissertation is the preparation and characterization of degradable salt-responsive polymers. In Chapter 5, degradable cationic random copolymers containing a PCL skeleton and quaternary ammonium side groups were synthesized by a combination of ring-opening polymerization and copper-catalyzed click reaction. These random copolymers exhibited ion strength-dependent solubility in water. In salt-free water or water with low ionic strength, random copolymers were completely soluble while in high salt concentration solution, the solubility of random copolymers decreased. Also these cationic random copolymers showed good degradability in dilute acid solution. Chapter 6 described the preparation of high molecular weight cationic salt-responsive bottle-brush polymers by ring-opening polymerization, ring-opening metathesis polymerization, and click reaction. These cationic bottle brush polymers exhibited not only good salt responsive properties but also better mechanical properties due to the high molecular weight of the polymers. Both the random copolymers and bottle brush polymers with salt responsive properties showed potential applications in personal hygiene products.

Finally, a summary is given in Chapter 7. In addition, some suggestions about future research directions on the renewable polymer materials and degradable stimuli-responsive polymers are provided.

TABLE OF CONTENTS

LIST OF TABLES

LIST OF FIGURES

LIST OF SYMBOLS

T_g	glass transition temperature
M_n	number average molecular weight
J_s^0	elastic creep compliance
η_0	extensional viscosity
τ	relaxation time
χ	percentage of elastic strain recovery

List of Abbreviations

ATRP ..... Atom Transfer Radical Polymerization

ROP ..... Ring-Opening Polymerization

ROMP ..... Ring-Opening Metathesis Polymerization

CuAAC ..... Copper(I)-Catalyzed Azide-Alkyne Cycloaddition

RAFT ..... Reversible Addition-Fragmentation Chain-Transfer

NMP ..... Nitroxide-Mediated Polymerization

GPC ..... Gel Permeation Chromatography

PDI ..... Polydispersity Index

DSC ..... Differential Scanning Calorimetry

TGA ..... Thermogravimetric Analysis

FTIR ..... Fourier Transform Infrared Spectrometry

AFM ..... Atomic Force Microscopy

PCL ..... Poly(ε-caprolactone)

PLA ..... Polylactide acid

PHA ..... Polyhydroxyalkanoate

TPE ..... Thermoplastic Elastomers

QA ..... Quaternary Ammonium

DHAA ..... Dehydroabietic Acid

DAEA ..... Dehydroabietic Ethyl Acrylate

DAEMA ..... Dehydroabietic Ethyl Methacrylate

DABA ..... Dehydroabietic Butyl Acrylate

DAA ..... Dehydroabietic Acrylate

DAPE ..... Dehydroabietic Propargyl Ester

HRPE ..... Hydrogenated Rosin Propargyl Ester

GRPE ..... Gum Rosin Propargyl Ester

BA ..... n-Butyl Acrylate

LMA ..... Lauryl Methacrylate

Cell ..... Cellulose

DBU ..... 1,8-Diazabicyclo[5.4.0]undec-7-ene

PMDETA ..... *N,N,N',N'',N''*-Pentamethyldiethylenetriamine

Me6Tren ..... Tris(2-(dimethylamino)ethyl)amine

AIBN ..... Azobisisobutyronitrile

CDB ..... Cumyl Dithiobenzoate

DMF ..... *N,N*-Dimethylformamide

THF ..... Tetrahydrofuran

CHAPTER 1

GENERAL INTRODUCTION[1]

[1] K. Yao and C. Tang. *Macromolecules* **2013** *46* (5), 1689-1712.

1.1 Renewable bio-based polymers

Currently, most polymers we use are derived from non-sustainable petroleum resources. [1-5] Synthetic plastics account for consumption of ~7% of global fossil fuels. [6-9] Depleting petroleum resources coupled with environmental concerns have led to an increased interest in developing renewable bio-based polymer materials from various natural resources.[10-17] There are two major classes of natural resources. The first class is natural polymers such as cellulose, hemicellulose, lignin and polysaccharides.[11, 17-25] These natural polymers are usually considered as cheap and abundant feedstock. They have been exploited for a long time for different applications in our daily life. Due to their complexity and pre-existing macromolecular structures, these natural polymers usually can only be modified by physical blending or modest chemical modifications to improve their material properties. In contrast, the second class of natural resources is natural molecular biomass including lactic acids, vegetable oils, fatty acids, hydroxyalkanoates and many others. This kind of molecular biomass could be precisely molecular-engineered into monomers for different polymerizations in a way similar to many synthetic polymers prepared from petroleum resources.[16, 26-36] According to the various origins, natural molecular biomass can be classified into four categories based on hydrogen, carbon and oxygen compositions: (1) oxygen-rich molecular biomass with the molar ratio of C/O less than an arbitrary number 5.0; (2) hydrocarbon-rich molecular biomass with the ratio of C/O larger than 5.0; (3) hydrocarbon molecular biomass; and (4) non-hydrocarbon molecular biomass. Figure 1.1 shows some representative molecular biomass of each category.

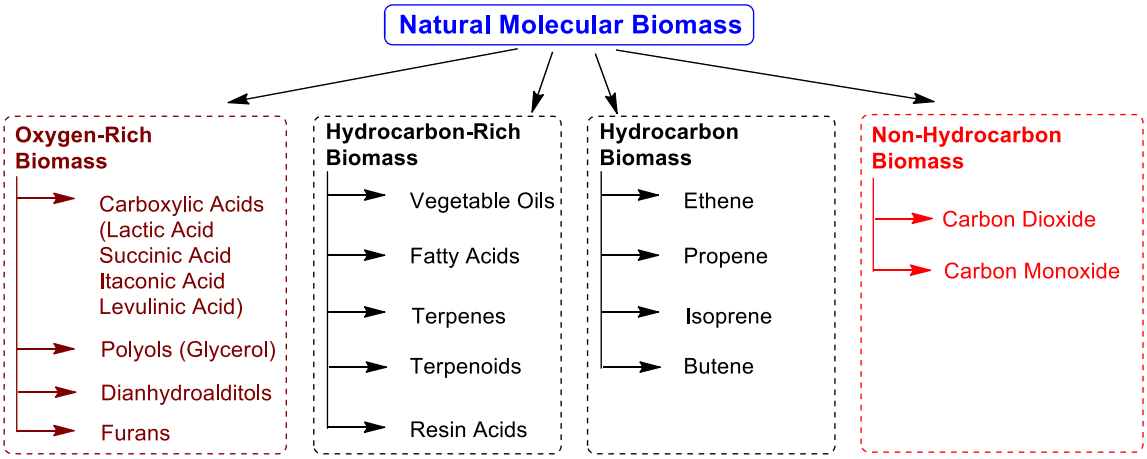

Figure 1.1 Classification of major natural molecular biomass[37]

Both the natural polymers and natural molecular biomass can be converted into monomers or precursors for renewable polymers in three major strategies. (1) Fermentation: Fermentation of carbohydrates is the most-developed pathway to transform biomass into monomers. As the most abundant renewable resources, carbohydrates can produce lactic acid and 1,3-propanediol via fermentation processes.[11, 17, 24] Each year, around 350 000 t of lactic acid are produced through fermentation worldwide. Also it should be mentioned that some well-known renewable polymers such as poly(hydroxyalkanoate)s can be prepared directly via bacterial fermentation from sugars or lipids.[38-40] (2) Chemical Transformation of Natural Polymers: Chemical degradation and transformation of natural polymers is the second method to produce renewable monomers.[11] For example, three very important basic renewable chemicals: furfural (2-furancarboxaldehyde), 5-hydroxymethylfurfural (HMF), and levulinic acid can be produced from the thermal dehydration of pentoses and hexoses in acid conditions. (3) Molecular Biomass Direct from Nature. There is a lot of molecular biomass from nature that can be directly used as monomers or precursors for renewable polymers preparation. Vegetable oils, terpenes, terpenoids, and resin acids belong to this category.[27-29, 31, 32, 35, 41]

Since natural molecular biomass has better-defined chemical structures, research on preparation of various polymers from biomass with controlled architectures and specific properties has drawn much more attention in the last several years and is a promising research area.

1.2 Renewable Rosin acids

Rosin is a renewable natural resin obtained from the exudation of pine and conifer trees.[42, 43] Produced in quantities greater than 1.2 million of tons annually, rosin is one of the most abundant renewable hydrocarbon-rich biomass, widely used as ingredients in fine chemicals such as inks, adhesives, cosmetics, vanishes, medicines and chewing gums.[27, 30] Rosin consists primarily of abietic- and pimaric-type rosin acids with characteristic hydrophobic hydrophenanthrene rings, similar in rigidity and chemical stability to petroleum based cycloaliphatic and aromatic compounds (Figure 1.2). The presence of a carboxyl group and conjugated double bond in rosin acid structures imparts them a tunable chemical reactivity. Compared with other renewable biomasses, rosin acids have three unique properties that make them good candidates for renewable polymers preparation: (1) they are hydrocarbon-rich biomass which can increase the hydrophobicity of polymers attached; (2) they have very bulky hydrophenanthrene group, which can significantly elevate thermal properties of polymers integrated; (3) rosin-derived esters are biocompatible because they are permitted to be used as food additives in chewing gum and beverages, approved by the U.S. Food and Drug Administration.[44-46]

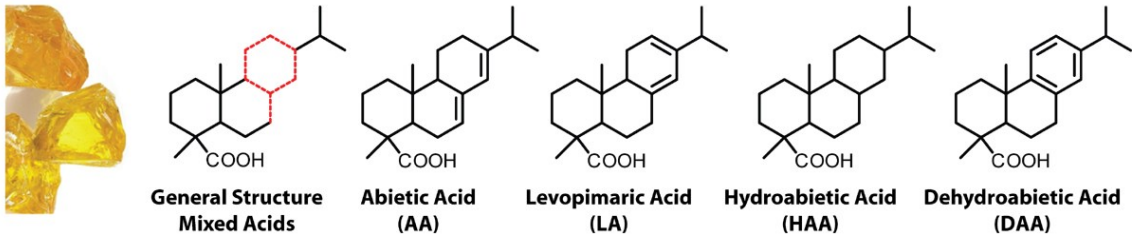

Figure 1.2 Chemical structures of representative rosin acids

Traditionally, rosin derived polymers are usually prepared by step-growth polymerization or free radical polymerization with poor controls on molecular structures and properties.[44, 47, 48] These drawbacks limit rosin polymers for broader and promising alternatives to petroleum based polymers.[49-52] In order to enhance the utilization of rosin as a renewable resource in the polymer materials area, a new synthetic strategy to incorporate rosin into polymers with controlled molecular structures, various functionality and properties is significant and needed.

1.3 Stimuli-Responsive Polymers

Stimuli-responsive polymers, which, by definition have the capability to respond to external or internal stimuli, are of great interest because of their promising applications in a variety of areas such as drug delivery, tissue engineering and sensors. [53-63] Stimuli responsive polymers are usually classified into different categories according to their response to various stimuli, including pH, temperature, redox-potential, light, etc. (Figure 1.3). Among various stimuli-responsive polymers, pH and temperature-responsive polymers are mostly investigated.[64, 65] For pH responsive polymers, polyacids (poly(acrylic acid)) and polybases (poly(2-(dimethylamino)ethyl methacrylate)) are two major classes. The polymers solubility and macromolecular conformations can be altered in aqueous media by adjusting their pH values. Also a lot of block or graft copolymers containing pH-responsive blocks have been prepared and their micellization behaviors

have been well studied for potential applications in biomedical areas.[66-69] For temperature responsive polymers, poly (*N*-isopropylacrylamide) (PNIPAM) is the most well-studied temperature responsive polymer.[70-73] PNIPAM has a lower critical solution temperature (LCST) of ~32°C. The polymer chain has significant conformational change above or below LCST, resulting in drastic abruption in solubility. Since the LCST of PNIPAM is similar to the temperature of the human body, a lot of copolymers containing PNIPAM blocks have been prepared to study their possible applications in drug delivery.[74, 75]

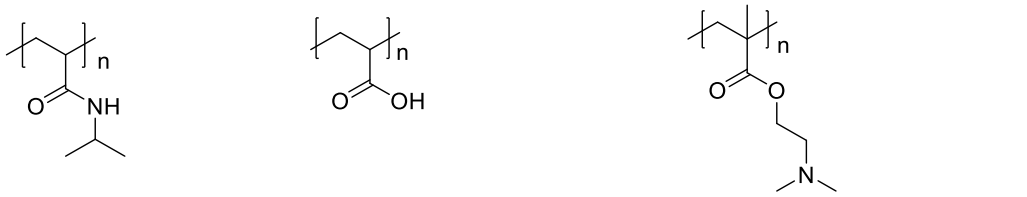

Poly(*N*-isopropylacrylamide) (PNIPAM) **Poly(acrylic acid) (PAA)** **Poly(2-(dimethylamino)ethyl methacrylate) (PDAEMA)**

Figure 1.3 Representative stimuli-responsive polymers

Besides the pH and temperature responsive polymers, novel polymer systems with responsiveness to other stimuli have drawn much more research attention in the last several years. Salt-responsive polymers are one class of novel stimuli-responsive polymers, usually containing ionic groups. They show varied solubility in aqueous solution depending on the salt concentration (or ionic strength). It should be mentioned that salt-responsive ionic polymers are considered to be appropriate as binder compositions in personal hygiene products such as wet tissues, paper towels, diapers, and so on.[76-78] The fundamental design is as follows: in wet state with higher salt concentration, the ionic charges of polymers are screened by salts and the polymer chains are insoluble in water, therefore holding the fibrous web together to provide strength.

While the salt concentration of solution decreases, the polymers become soluble due to the electrostatic repulsions and thus they can be flushed away easily.

1.4 Polymerization Techniques and "Click" Chemistry

Atom Transfer Radical Polymerization (ATRP).[79-81] ATRP is one of the most effective and widely used controlled radical polymerization (CRP) methods to prepare various polymer materials with different molecular architectures in a controlled manner. The general mechanism of ATRP is showed in Figure 1.4. The radicals (active species) P_n• are generated by a reversible redox process in the presence of a transition metal complex. Transition metal complex M_t^m/L can go through an oxidation reaction with halogen atom X, forming dormant species P_n-X. ATRP is controlled by equilibrium between propagating radicals P_n• and dormant species P_n-X. As a polymerization system containing multiple components, ATRP is influenced by many factors, including monomers, initiators, catalysts, reaction solvents and reaction temperature.

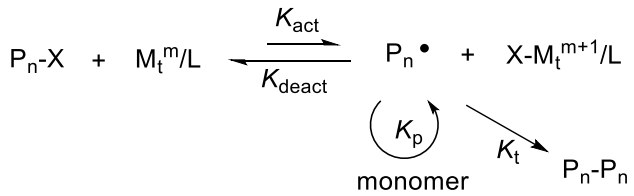

Figure 1.4 General mechanism of ATRP

Reversible Addition-Fragmentation Chain-Transfer (RAFT) Polymerization.[82-84] RAFT polymerization is another very useful controlled radical polymerization technique that has been utilized for over 30 years.[85] The term reversible addition-fragmentation transfer (RAFT) was first reported in the literature by Rizzardo et al. in 1998.[83] RAFT involves a reversible addition-fragmentation chain transfer between an active and a dormant species and is performed by adding a dithioester transfer agent, which has the

appropriate Z and R groups selected to provide an effective transfer process (Figure 1.5). In general the best RAFT agent is one that has a Z group that favors the formation of the radical intermediate. Phenyl rings are most often encountered as Z groups in RAFT agent. The best R groups are those that have steric hindrance and contain an electron withdrawing group. The stability of the radical intermediate and its capability to fragment heavily depends on the R groups. The most widely used R groups are cumyl and cyanoisopropyl groups. Currently dithiobenzoates are the most commonly used RAFT agents because of their ability to show control over various monomers and radical initiators. RAFT polymerization has been used to prepared polymers of complex architectures, including block copolymers, brush polymers and dendrimers.

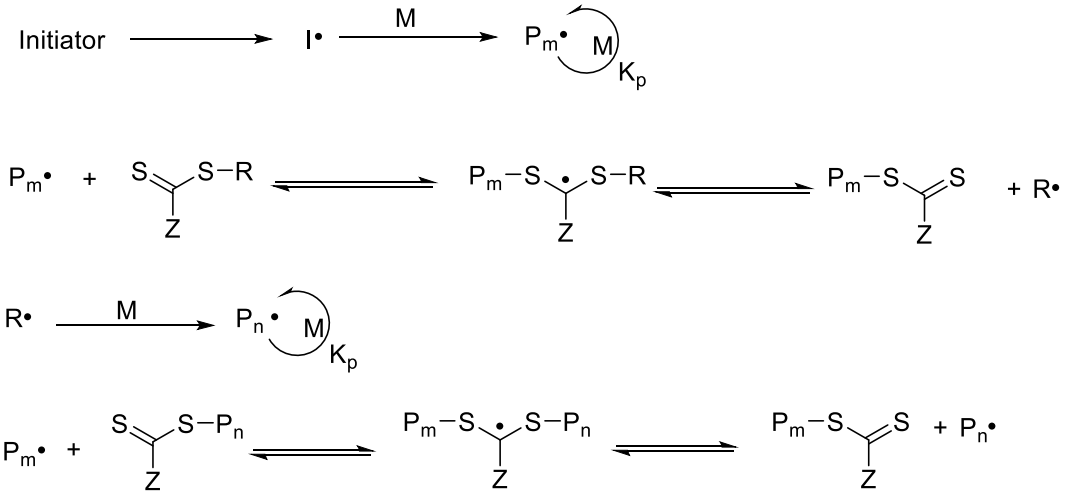

Figure 1.5 Overall mechanism of RAFT polymerization

Ring-Opening Polymeriztion (ROP).[86-88] ROP is another very important polymerization technique that has been well studied and applied in both academic and industrial areas to prepare synthetic or naturally occurring polymers. Usually cyclic monomers such as caprolactone, lactide, ethylene oxide can be polymerized by ROP in the presence of various catalysts. Usually ROP can be divided into cationic ROP and anionic ROP

depending on their different reactive center. The most common used catalysts for ROP are organometallic compounds such as tin (II) 2-ethylhexanoate ($Sn(Oct)_2$), tin (II) butoxide ($Sn(OBu)_2$), and aluminum alkoxides. Figure 1.6 exhibits a typical ROP of ε-caprolactone monomer and several representative catalysts for ROP.

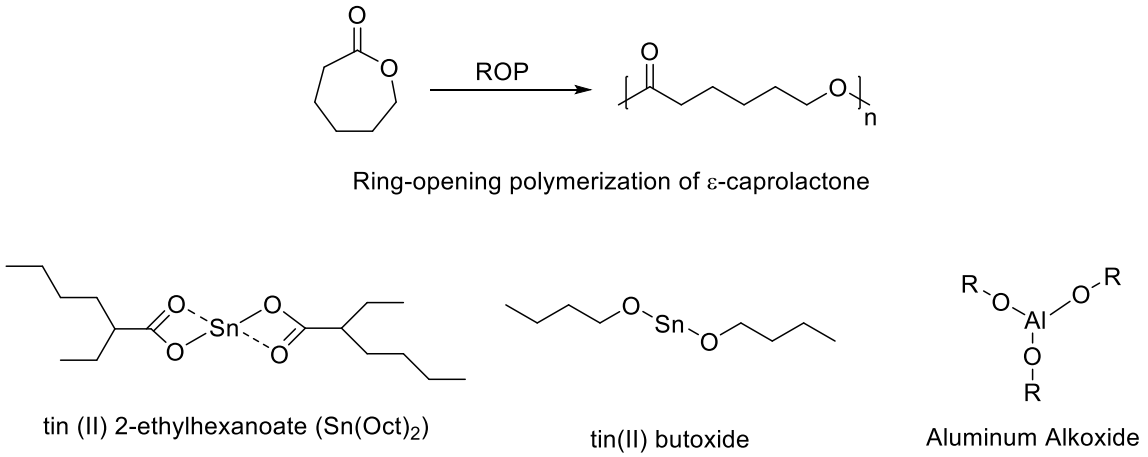

Figure 1.6 ROP of ε-caprolactone and representative ROP catalysts

Ring-Opening Metathesis Polymerization (ROMP).[89-91] ROMP is an olefin metathesis chain-growth polymerization. Compared with other traditional polymerization techniques, ROMP is a recent-developed polymerization method. However, ROMP is an attractive technique to prepare new polymers with controlled molecular architectures since it is robust, high efficient, and easy to operate. The overall mechanism of ROMP is metal-mediated carbon-carbon double bond exchange. Polymers prepared by ROMP contain unsaturated double bonds in each repeating unit. The catalysts used in ROMP includes a variety of metals and the most well-known, high efficient catalysts for ROMP are ruthenium based Grubbs' catalysts. Figure 1.7 shows the three different generations of Grubbs' catalysts.

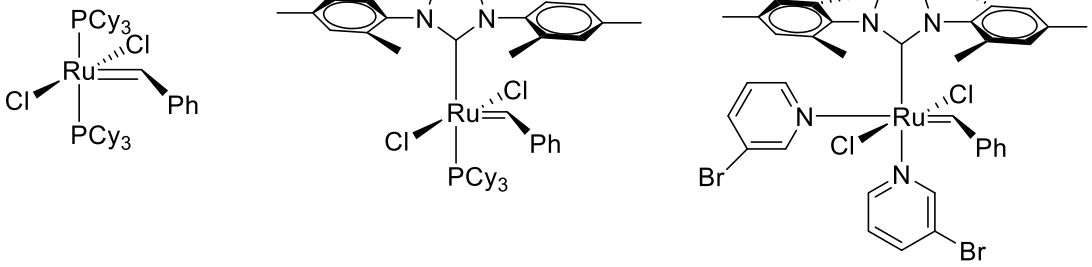

Grubbs' I catalyst Grubbs' II catalyst Grubbs' III catalyst

Figure 1.7 Grubbs' catalysts for ROMP

"Click" Chemistry.[92, 93] Click chemistry includes copper(I)-catalyzed and strain-promoted azide-alkyne cycloaddition, Diels-Alder cycloaddition, and thiol-ene reaction. Among different click chemistry, copper(I)-catalyzed azide-alkyne cycloaddition (CuAAC) is the most well-studied and widely used technique to prepare novel polymer materials with functional groups and controlled macromolecular architectures due to its high reaction efficiency, mild reaction conditions and (regio)specificity. CuAAC transforms organic azides and terminal alkynes into 1,4-disubstituted 1,2,3-triazoles (Figure 1.8). CuAAC was first reported independently by Sharpless group[94] and Meldal group[95] in 2002. Since then, CuAAC has been one of the most powerful synthesis methods in the macromolecular engineering field. It has been employed to prepare dendrimers with high efficiency.[96] Also it has been combined with controlled/living polymerization techniques including ATRP, reversible addition-fragmentation chain-transfer (RAFT) polymerization, nitroxide-mediated polymerization (NMP) to synthesize various functional polymers.[97-100]

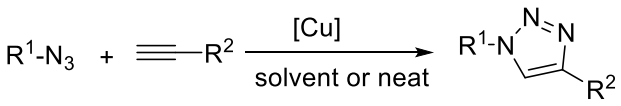

Figure 1.8 Copper catalyzed azide-alkyne cycloaddition (CuAAC)

1.5 Research Objectives

This dissertation has two main research objectives. The first objective was to develop novel polymer materials derived from renewable resources by various controlled/living polymerizations. Rosin is first derived into acrylate or methacrylate monomers for ATRP and RAFT polymerization. Also rosin-derived propargyl ester is attached to the degradable polyesters via click reaction. Finally rosin derived methacrylate monomers are combined with renewable cellulose and fatty acid-based monomers to synthesize new graft copolymers with proper glass transition temperature (T_g) for thermoplastic elastomers application. These new rosin based renewable polymer materials will have potential applications in food packaging, drug delivery, thermoplastic elastomers areas, etc.

The second goal of this research is to prepare new degradable salt-responsive polymers for application of personal care products. First, random copolymers of caprolactone (CL) and chloro-substituted CL are synthesized by ROP and then the chlorine groups are converted to azide groups, which are further reacted with quaternary ammonium salt with alkyne end groups by click reaction. Ionic random copolymers containing appropriate charged groups exhibit good salt-responsive properties in NaCl aqueous solutions. Then in order to enhance the mechanical properties of salt-responsive polymers, similar synthesis route containing ROP, ROMP, and click reaction is employed to prepare salt-responsive bottle-brush polymers with high molecular weights by "grafting-through" method. The new brush polymers containing ionic groups show not only excellent salt-responsive properties, but also improved mechanical strengths. Both the salt-responsive random copolymers and brush polymers show good degradability in

acidic media. These new degradable salt-responsive copolymers could find possible applications in many fields, especially in personal hygiene products.

CHAPTER 2

RENEWABLE POLYMERS DERIVED FROM GUM ROSIN BY ATRP AND RAFT POLYMERIZATION

2.1 Abstract

Gum rosin was used as a natural resource to prepare renewable polymers. A series of highly pure vinyl monomers were derived from dehydroabietic acid. Atom transfer radical polymerization and reversible addition-fragmentation chain-transfer polymerization of these rosin-derived monomers produced well-defined polymers with controlled molecular weight and low polydispersity. These rosin based polymers exhibited tunable thermal properties.

2.2 Introduction

Synthesis of new polymeric materials from renewable natural resources has becoming a rapidly growing research area, as these materials could potentially replace or partially replace environmentally and energy unfavorable plastics derived from petroleum chemicals.[6, 7, 9, 11, 16, 17] However, applications of renewable polymers are significantly behind petroleum-derived polymers, partially due to relative high cost and limitations in the monomer resources and therefore derived polymers. Thus, the development of novel low-cost and scalable monomers from renewable resources is essential.[2, 27, 101-104]

We have focused on developing a new class of renewable polymers using gum rosin, due to its abundance, low cost as well as its potential ability to be derivatized into polymerizable monomers. Produced at a rate of more than one million tons annually, crude rosin and gum rosin, whose major components are resin acids (primarily abietic acid) with characteristic hydrophenanthrene rings, are exudates from pine trees, and are generally used as ingredients for inks, vanishes, adhesives, cosmetics, medicines, chewing gums, etc.[42, 105, 106] However, the utilization of rosin as renewable resources for polymeric materials has been mostly focused on step-growth polymerization to prepare low molecular weight polymeric materials.[43, 44, 46, 47, 51, 107] Controlled radical

polymerization (CRP) of monomers derived from gum rosin has not been studied, partially due to the absence of polymerizable vinyl monomers with high purity.[45, 48, 52] CRP allows the preparation of well-defined polymers with controlled molecular weight, functionality as well as architectures, which can enable one to develop more advanced materials such as thermoplastic elastomers and composites.[108-110] Herein we report the synthesis of high-quality rosin-derived vinyl monomers and the first preparation of well-defined rosin-derived polymers using both atom transfer radical polymerization (ATRP) and reversible addition-fragmentation chain-transfer (RAFT) polymerization

2.3 Experimental Section

2.3.1 Materials

Dehydroabietic acid (DHAA, ~90%) was obtained from Wuzhou Chemicals, China and used as received. Tetrahydrofuran (THF, Aldrich) and anisole (Aldrich) were refluxed with sodium and distilled just before use under nitrogen atmosphere. Tris(2-(dimethylamino)ethyl)amine (Me6Tren) and cumyl dithiobenzoate (CDB) was prepared according to the literature.[111-113] 2-Hydroxyethyl acrylate (2-HEA) (stabilized, 97%, Aldrich), 2-hydroxyethyl methacrylate (2-HEMA) (stabilized, 97%, Aldrich) and 4-hydroxybutyl acrylate (4-HBA) (stabilized, 97%, Aldrich) were passed through basic alumina. Azobisisobutyronitrile (AIBN) was purified by recrystallization from methanol. Oxalyl chloride, triethylamine, sodium borohydride (NaBH4), acryloyl chloride, ethyl-2-bromoisobutyrate (EBiB) and copper(I) bromide (99.999%) were used as received (Aldrich).

2.3.2 Characterization

Gas chromatography-mass spectrometry (GC/MS) analysis of DHAA raw materials was carried out on an Agilent 6890N Network GC system and an Agilent 5973 mass selective detector. Prior to GC/MS analysis, DHAA was transformed into methyl DHAA by using TMAH (tretramethyl ammonium hydroxide) in the solution of methanol because DHAA was not gasified due to the presence of the carboxylic acid group. GC was performed on Agilent HP-5 capillary column (30m×0.25mm×0.25μm) with an oven temperature of 250 ^{o}C. Carrier gas was He at a flow-rate of 1.0 mL/min. The temperature of injection port was at 250 ^{o}C. A 0.2 μL of sample was injected into the GC system. The mass spectrometer was operated in electron ionization mode. The temperature of the ion source was 230 ^{o}C.

^{1}H NMR and ^{13}C NMR spectra were recorded on Bruker ARX 300 and ARX 400 spectrometers. The chemical shifts were recorded in ppm (δ) relative to tetramethylsilane. Mass spectra were measured on a VG S70 mass spectrometer. Gel permeation chromatography (GPC) was performed at room temperature on a Varian system equipped with a Varian 356-LC refractive index detector and a Prostar 210 pump. The columns were STYRAGEL HR1, HR2 (300×7.5 mm) from Varian. HPLC grade THF was used as eluent at a flow rate of 1 ml/min. THF and samples were filtered over microfilters with pore size of 0.2μm (Nylon, Millex-HN 13 mm Syringes Filters, Millipore, USA). The columns were calibrated using polystyrene standards. The thermal transitions of the copolymers were recorded using differential scanning calorimetry (DSC) on a TA Q200 calorimeter in a temperature range from 0 to 180 °C at a heating rate of 10 °C min^{-1} under a continuous nitrogen flow. All the data were collected during the second heating process

after cooling at 2 °C min-1 from 180 °C. The average sample mass was about 5 mg, and the nitrogen flow rate was 50 mL min^{-1}. Thermogravimetric analysis (TGA) data were collected on a TA SDT Q600 using a heating rate of 5 °C/min from 25 to 600°C under helium.

2.3.3 Synthesis

Dehydroabietic ethyl acrylate (DAEA): dehydroabietic acid (10 g, 33 mmol) was dissolved in dichloromethane (60 mL) . Oxalyl chloride (5.66 g, 36.3 mmol) was added slowly. After the solution was stirred at 0°C for 3 h, excessive oxalyl chloride was removed by distillation. Triethylamine (5.0 g, 57 mmol) and 2-HEA (4.39 g, 37 mmol) were subsequently added. The reaction mixture was stirred at 0°C overnight and then washed with 5% Na_2CO_3 solution followed by drying over anhydrous Na_2SO_4 and evaporated to dryness. The product was further purified by silica gel chromatography (ethyl acetate /hexane: 1/9 (v/v)) to afford white powder (5.0 g) in 45% yield. ^{1}H NMR (300 MHz, $CDC1_3$, δ, ppm): 7.26-7.14 (d, J = 8.21 Hz, 1H; Ar), 7.01-6.99 (d, J = 8.51 Hz, 1H; Ar), 6.91-6.87(s, 1H; Ar), 6.43-6.38 (d, J = 17.14 Hz, 1H; vinyl), 6.16-6.06(dd, J = 10.52, 10.41 Hz, 1H; vinyl), 5.85-5.82 (d, J = 10.00 Hz, 1H; vinyl), 4.36-4.27 (m, 4H; OCH_2), 2.93-2.80(m, 3H), 2.34-1.21 (m, 21H). ^{13}C NMR (400 MHz, $CDC1_3$, δ, ppm):16.49, 18.59, 21.76, 24.00, 25.19, 30.12, 33.48, 36.55, 36.95, 37.96, 44.77, 47.71, 62.01, 62.16, 123.96, 124.21, 126.91, 128.00, 131.34, 134.66, 145.76, 146.86, 165.86, 178.32. MS (ESI, m/z) for $C_{25}H_{34}O_4$: 398 (M^+).

Dehydroabietic ethyl methacrylate (DAEMA): The synthesis was similar to DAEA synthesis, using 2-HEMA instead of 2-HEA. ^{1}H NMR (300 MHz, $CDCl_3$, δ, ppm): 7.17-7.15 (d, J = 8.16 Hz, 1H; Ar), 7.00-6.98 (d, J = 7.79 Hz, 1H; Ar), 6.87-6.85(s, 1H; Ar),

6.17-6.09 (s, 1H; vinyl), 5.58-5.55 (s, 1H; vinyl), 4.38-4.26 (m, 4H; OCH_2), 2.84-2.77(m, 3H), 1.91-1.16 (m, 23H). ^{13}C NMR (400 MHz, $CDC1_3$, δ, ppm):16.49, 18.26, 18.58, 21.74, 23.99, 24.02, 25.15, 30.06, 33.48, 36.57, 36.95, 37.97, 44.77, 62.22, 62.51, 123.95, 124.17, 126.03, 126.90, 134.64, 135.94, 145.75, 146.85, 167.09, 178.31. MS (ESI, m/z) for $C_{26}H_{36}O_4$: 412 (M+).

Dehydroabietic ethyl methacrylate (**DABA**): The synthesis was similar to DAEA synthesis, using 4-HBA instead of 2-HEA. ^1H NMR (300 MHz, $CDC1_3$,*δ*, ppm): 7.12-7.09 (d, *J* = 7.83 Hz, 1H; Ar), 6.95-6.92 (d, *J* = 7.42 Hz, 1H; Ar), 6.83-6.81(s, 1H; Ar), 6.35-6.30 (d, *J* = 16.49 Hz, 1H; vinyl), 6.08-5.99 (dd, *J* = 10.31, 10.80 Hz, 1H; vinyl), 5.76-5.73 (d, *J* = 10.26 Hz, 1H; vinyl), 4.13-3.98 (m, 4H; OCH_2), 2.82-2.71(m, 3H), 1.80-1.14 (m, 25H). ^{13}C NMR (400 MHz, $CDC1_3$, *δ*, ppm):14.00, 16.81, 19.30, 22.35, 23.82, 25.30, 25.45, 26.93, 30.16, 31.62, 33.31, 36.10, 37.47, 37.97, 45.00, 47.86, 64.65, 123.66, 124.00, 124.22, 126.64, 126.95, 127.94, 145.75, 146.85, 167.09, 178.31. MS (ESI, *m*/*z*) for $C_{27}H_{38}O_4$: 426 (M^+).

Dehydroabietic acrylate (**DAA**): dehydroabietic acid (6.6 g, 22 mmol) was dissolved in diethyl ether (100 mL). $NaBH_4$ (4.54 g, 0.120 mol) in 40 mL diethyl ether were added in 30 min. After the solution was stirred at room temperature overnight, excessive $NaBH_4$ was destroyed by adding 120 mL methanol slowly. The reaction mixture was washed with 5% H_2SO_4 and the organic layer was collected and washed with 5% $NaHCO_3$ solution followed by drying over anhydrous Na_2SO_4 and evaporated to dryness, yielding dehydroabietic alcohol, which was used immediately in the next step reactions. Triethylamine (26 mL) and acrylory chloride (4 g, 44 mmol) were added slowly to the above dehydroabietic alcohol in dichloromethane (150 mL). The reaction mixture was

stirred at 0ºC overnight and the solution was washed with 5% $NaCO_3$ solution followed by drying over anhydrous Na_2SO_4 and evaporated to dryness. The product was further purified by silica gel chromatography (ethyl acetate /hexane: 1/9 (v/v)) to afford white powder (3.29g) in 46% yield. ^{1}H NMR (300 MHz, $CDC1_3$, δ, ppm): 7.20-7.17 (d, J = 8.78 Hz, 1H; Ar), 7.01-6.99 (d, J = 8.78 Hz, 1H; Ar), 6.90-6.87(s, 1H; Ar), 6.41-6.35 (d, J = 17.39 Hz, 1H; vinyl), 6.14-6.05 (dd, J = 10.30, 10.44 Hz, 1H; vinyl), 5.82-5.78 (d, J = 9.57 Hz, 1H; vinyl), 4.09-3.78 (dd, 2H; OCH_2), 2.93-2.74(m, 3H), 1.83-1.17 (m, 21H). ^{13}C NMR (400 MHz, $CDC1_3$,δ, ppm):17.54, 18.58, 19.03, 24.02, 25.45, 30.30, 33.44, 35.60, 36.97, 37.49, 37.75, 44.32, 68.00, 72.47, 123.91, 124.22, 126.91, 128.54, 130.70, 134.79, 145.62, 147.12, 166.40. MS (ESI, *m*/*z*) for $C_{23}H_{32}O_2$: 340 (M^+).

ATRP: PDAEA synthesis is used as an example. A mixture of monomer DAEA (0.5 g, 1.2 mmol), Me_6Tren (2.76mg, 0.012 mmol), EBiB (1.84 µl, 0.012 mmol) and THF (3 mL) was introduced into a polymerization tube. After three freeze-pump-thaw cycles, CuBr (1.8 mg, 0.012 mmol) was added to the flask while the contents were in the solid state and deoxygenated by vacuum followed by back-filling with nitrogen three times. The tube was heated at 90 ºC for 16 hours. The polymerization was stopped by diluting the reaction mixture with THF. The products were precipitated in methanol three times and dried to constant weight, yielding white powder. The conversion of monomers was 29% as determined from ^{1}H NMR analysis. M_n (PDAEA) = 11500 g/mol, PDI (PDAEA) = 1.20. ^{1}H NMR (300 MHz, $CDCl_3$, δ): 6.7-7.2 (broad, aromatic); 3.9-4.4 (d, O*CH2CH2O*); 2.6-2.8 (protons next to aromatic ring); 1-2.5 (broad, -*CH2CH*- and all other protons from hydrophenanthrene ring).

RAFT polymerization: PDAEMA synthesis is used as an example. A mixture of monomer DAEMA (0.5g, 1.2 mmol), AIBN (0.2mg, 0.0012 mmol), CDB (3.30mg, 0.012 mmol), and toluene (2 mL) was added to a Schlenk flask. After three freeze-pump-thaw cycles, the flask was kept at 100 ^{o}C for 24 hours. The polymerization was stopped by diluting the polymer solution with THF. The final polymer was recovered by precipitating in cold methanol three times and drying under vacuum to constant weight. M_n (PDAEMA) =10600 G/MOL, PDI (PDAEMA) =1.29 (GPC analysis). ^{1}H NMR (300MHZ, $CDCl_3$, δ): 6.7-7.0 (broad, aromatic); 3.8-4.2 (d, O*CH2CH2O*); 2.6-2.8 (protons next to aromatic ring); 1-2.5 (broad, -*CH2CH*- and all other protons from hydrophenanthrene ring).

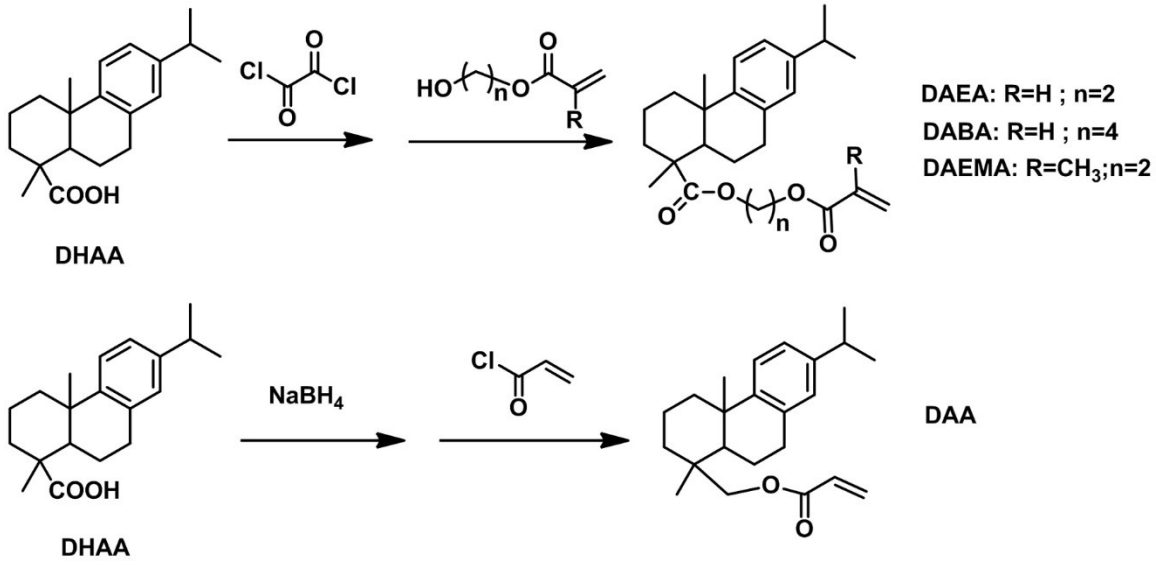

Figure 2.1 Synthesis of Vinyl Monomers from Gum Rosin

2.4 Results and Discussion[36, 114]

We selected commercial dehydroabietic acid (DHAA, a racemic mixture) as our starting rosin materials since the aromatic ring in the hydrophenanthrene make it more stable than abietic acid, while the functional carboxylic acid group allows the

derivatization of various vinyl monomers. Most DHAA from commercial sources contains ~5-10% unknown impurities, which turned out to be difficult to separate out. However, after derivatization of DHAA into vinyl monomers, we were able to remove all impurities readily through simple column chromatography. Under this scenario, four rosin-based acrylate and methacrylate monomers were synthesized (Figure 2.1). Different spacers were placed between vinyl group and dehydroabietic group in order to vary the steric effect imparted onto the vinyl group, which could have significant influence on the control of the polymerization. Moreover the thermal properties (e.g. the glass transition temperature (T_g)) of resulting polymers can be finely tuned. For dehydroabietic acrylate (DAA),[115] the dehydroabietic group is connected directly to the vinyl ester group, while dehydroabietic butyl acrylate (DABA) has the longest spacer.

DAA was prepared from acryloyl chloride and dehydroabietic alcohol, which was obtained by reduction of dehydroabietic acid with sodium borohydride. For other monomers (dehydroabietic ethyl acrylate (DAEA), DABA, dehydroabietic ethyl methacrylate (DAEMA)), dehydroabietic acid was first converted into acyl chloride under oxalyl chloride followed by in-situ esterification reaction with hydroxyl groups of corresponding (meth)acrylates. Impurities were removed by column chromatography. The structures of all monomers were confirmed by ^{1}H, ^{13}C NMR and mass spectra. Figure 2.2 shows clear evidences of the high purity of the vinyl monomers, as confirmed from chemical shifts of vinyl, aromatic, methylene protons as well as those protons next to aromatic ring. All integrations of NMR spectra matched very well. From the two-dimensional correlation spectroscopy (COSY) of ^{1}H NMR, the region between 1 and 2.5 ppm is clearly assigned to protons on the hydrophenanthrene ring. To the best of our

knowledge, this is the first report on the synthesis of highly pure vinyl monomers derived from gum rosin.

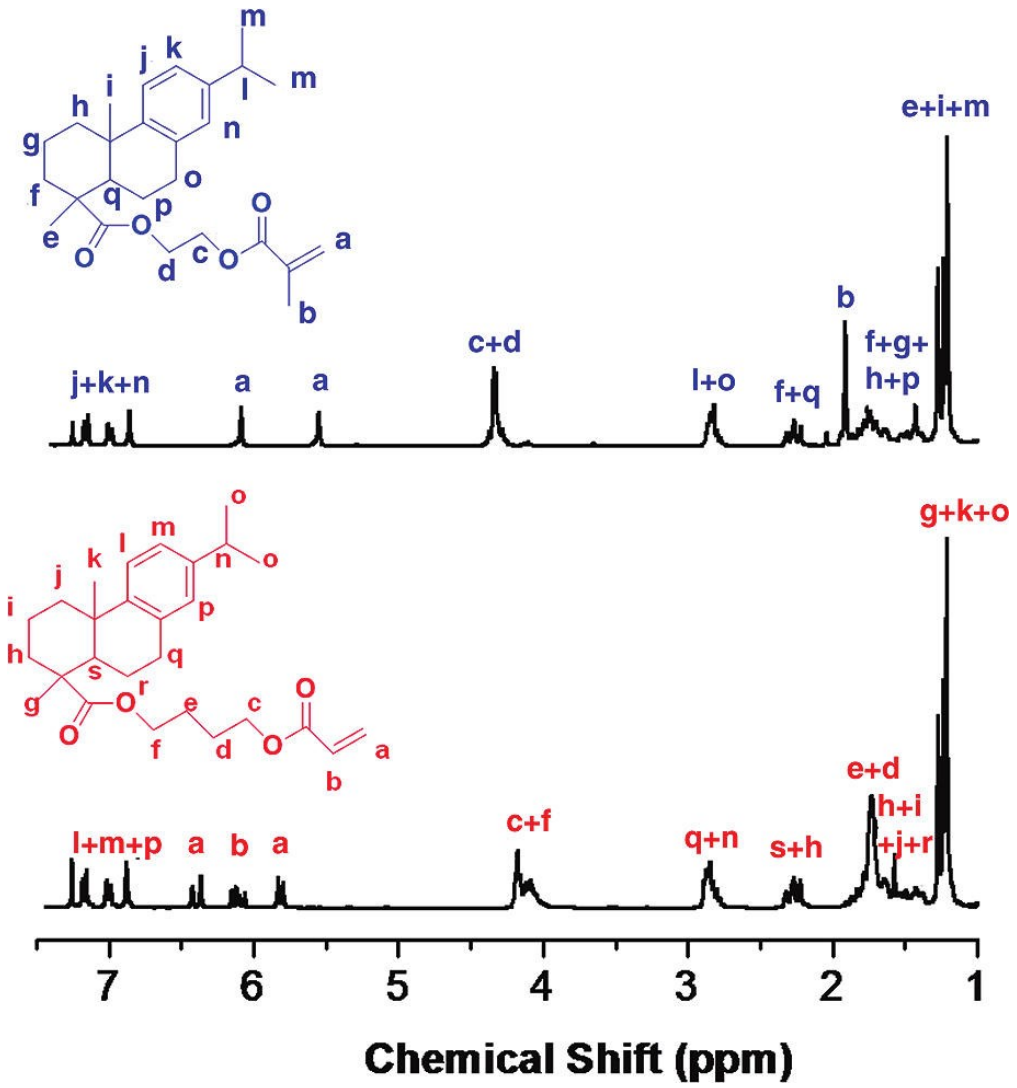

Figure 2.2 ^{1}H NMR spectra of vinyl monomers derived from rosin

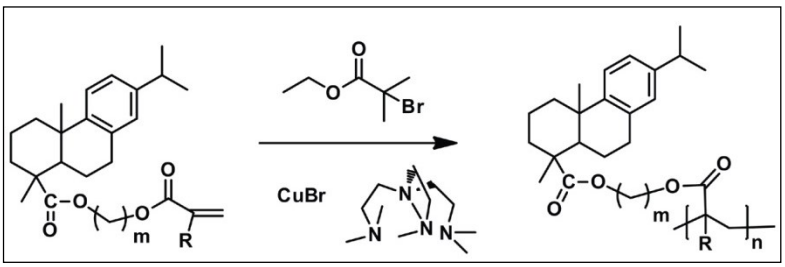

Figure 2.3 ATRP of vinyl monomers derived from DHAA

Copper-catalyzed ATRP of all vinyl monomers were carried out in various conditions and the results are summarized in Table 2.1. Gel Permeation Chromatography (GPC) traces of poly(dehydroabietic acrylate) (PDAA) were broad and multi-modal with high polydispersity index (PDI =3.65), suggesting an uncontrolled polymerization, probably due to dominating steric effect of side groups. The polymerizations of DAEA and DABA were first carried out in anisole with the use of copper (I) bromide and tris[2-(dimethylamino)ethyl]amine (Me_6Tren) as the catalyst and ligand (Figure 2.3). However both polymerizations resulted in low molecular weight (< 7000 g/mol) after 48 h (not shown). The use of more polar solvent tetrahydrofuran (THF) significantly increased the polymerization rate while maintaining PDI < 1.3. After 16 h, the molecular weight was 11500 g/mol and 21500 g/mol for poly(dehydroabietic ethyl acrylate) (PDAEA) and poly(dehydroabietic butyl acrylate) (PDABA) respectively (Runs 2 and 3 in Table 2.1). The higher molecular weight of PDABA was consistent with less hindrance due to longer spacer between the rosin moiety and the vinyl groups. The representative GPC traces are shown in Figure 2.4. The acrylate rosin polymers had a monomodal symmetric elution curve, indicating well controlled polymerization. The rate enhancement in more polar solvents could be due to improved solubility of catalysts, which has been observed in different system.[108, 116, 117]

Table 2.1 ATRP of vinyl monomers derived from gum rosin*

Run	Monomer	[M]/[I]/[C]/[L]	Solvent	Ligand	Time (h)	Conv (%)	M_n (NMR)	M_n (GPC)	M_w/M_n
1	DAA	100/1/0.5/0.5	THF	Me_6Tren	24	30	10200	5600	3.65
2	DAEA	100/1/0.5/0.5	THF	Me_6Tren	16	29	11500	4300	1.20
3	DABA	100/1/0.5/0.5	THF	Me_6Tren	16	54	21500	7700	1.25
4	DAEMA	100/1/0.5/0.5	THF	Me_6Tren	24	80	32900	36000	1.60
5	DAEMA	100/1/0.5/0.5	Anisole	Me_6Tren	20	75	31000	19000	1.33

*Initiator: ethyl-2-bromoisobutyrate; catalyst: CuBr; ligand: Me_6Tren; [M]/[I]/[C]/[L]: molar concentration ratio of monomer/initiator/catalyst/ligand; M_n(GPC): molecular weight obtained from GPC using PSt as standards; M_n(NMR): molecular weight obtained from ^{1}H NMR. Me_6Tren= tris[2-(dimethylamino) ethyl]amine; THF=tetrahydrofuran.

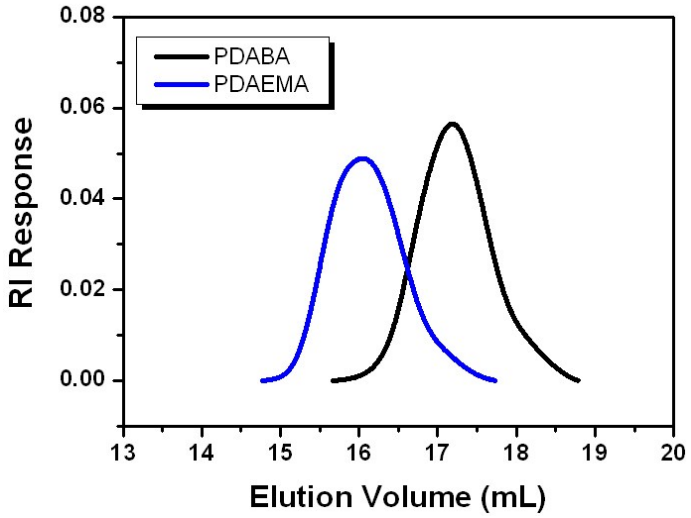

Figure 2.4 GPC traces of PDABA and PDAEMA prepared by ATRP (corresponding to runs 3 and 5 from Table 2.1 respectively)

We then carried out ATRP of methacrylate monomers (DAEMA) derived from rosin. Under the use of same solvent (THF) as used for acrylate monomers, the polymerization of DAEMA was much faster than that of acrylate. 80% conversion was achieved within 24h with a molecular weight of 32900 g/mol for poly(dehydroabietic ethyl methacrylate) (PDAEMA) (Run 4 in Table 2.1). However, the polymerization was not controlled as the PDI was as high as 1.6. Then we performed the polymerization with the use of less polar solvent: anisole. The reaction was slower but with much better control ((Run 5 in Table 2.1). The PDI was about 1.33. The GPC trace showed a symmetric single peak throughout the polymerization (Figure 2.4). Although the role of the solvent in the polymerization system is currently under investigation, some solvent-assisted side reactions such as elimination of HBr from polymethacrylic halides could occur in more polar solvents.[108, 116, 117] It is worth noting that most of the molecular weights determined by GPC were much lower than those obtained by ^{1}H NMR analysis, suggesting that rosin-derived polymers may have significantly different hydrodynamic

volumes compared to polystyrene calibration standards, probably due to large dehydroabietic side groups.

^{1}H NMR spectra (Figure 2.5) of acrylate and methacrylate polymers show that the characteristic signals of vinyl protons from monomers at 5.4－6.5 ppm disappeared, accompanied by the appearance of broad peaks at 1-2.5 ppm corresponding to –CH_2-CH- protons from the polymer backbone. All other peaks of dehydroabietic side groups were broader with nearly same chemical shifts as those of the monomers.

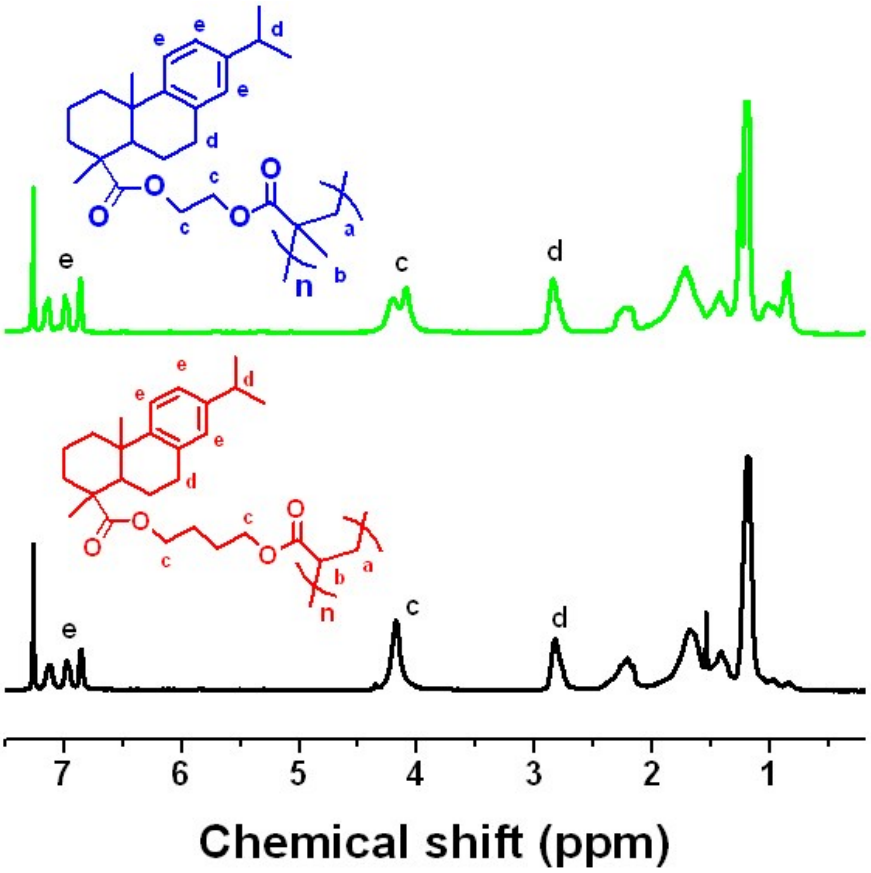

Figure 2.5 ^{1}H NMR spectra of PDABA and PDAEMA prepared by ATRP (corresponding to runs 3 and 5 from Table 2.1 respectively)

Also RAFT polymerization was carried out to polymerize two rosin-derived monomers DAEMA and DAEA (Figure 2.6). The procedure of RAFT polymerization is very close to free radical polymerization; however, the final polymer molecular weight

and PDI for these two radical polymerization techniques should differ. As previously mentioned, RAFT polymerization is a controlled radical polymerization technique. A desired molecular weight can be achieved by adjusting the molar ratio of monomer to RAFT agent. The first polymerization system consisted of monomer (DAEMA), initiator (AIBN) and RAFT agent (CDB). The solvent was toluene. The molar ratio used for these materials was: [DAEMA]:[CDB]:[AIBN] = [100]:[1]:[0.1].

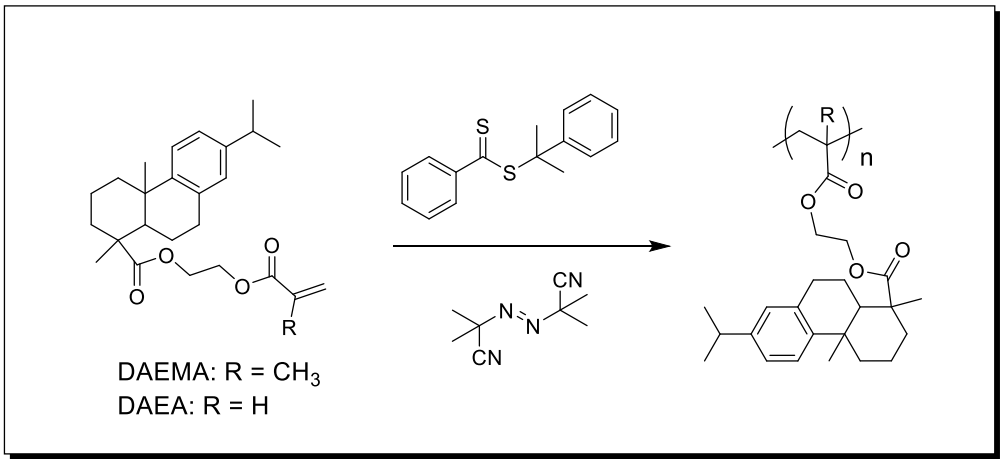

Figure 2.6 Preparation of rosin-derived acrylic polymers by RAFT polymerization

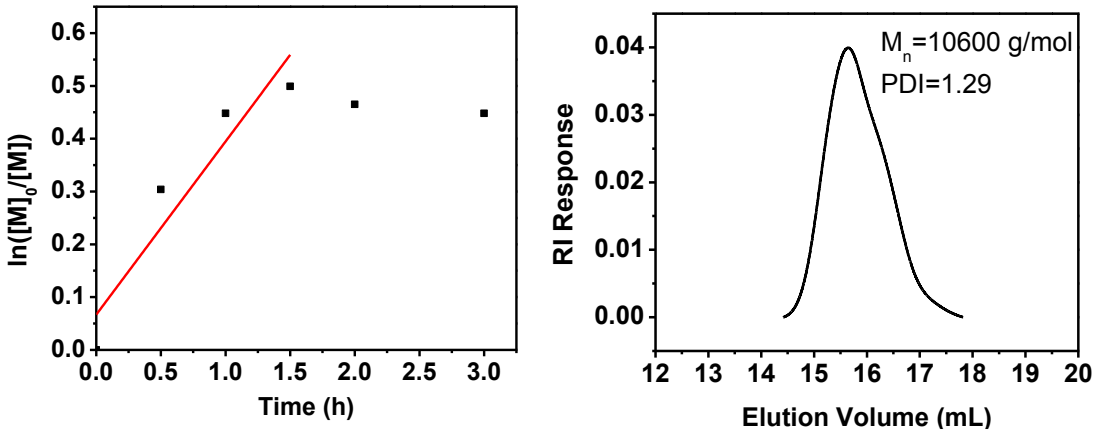

Figure 2.7 Kinetic plot and GPC trace of PDAEMA polymers prepared by RAFT in toluene at 100 ºC

As shown in Figure 2.7, the GPC trace showed the polymer has an approximate number-average molecular weight of 10,600 g/mol and a low PDI=1.29, indicating that

the polymerization was well controlled. However, the kinetic study showed that the polymerization was living only when the reaction conversion was below 35%. When the reaction conversion was higher than 35%, the conversion was nearly constant, indicating the polymerization stopped.

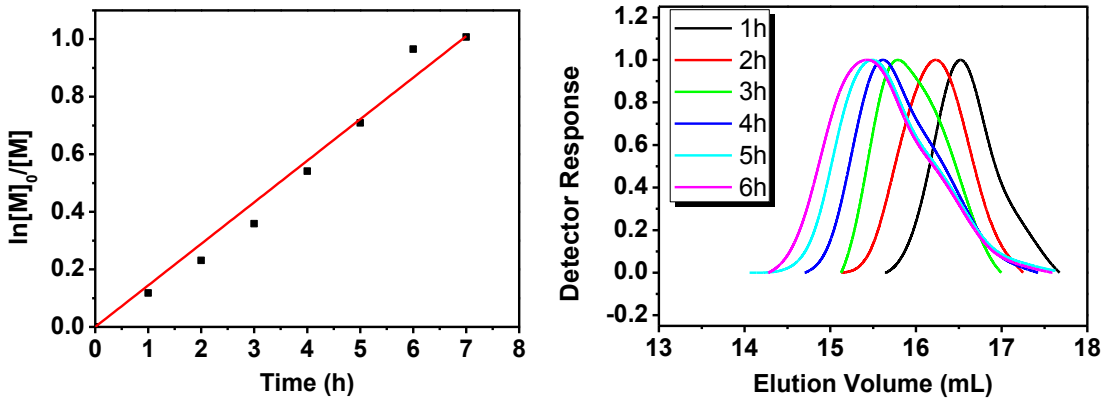

Figure 2.8 Kinetic plot and GPC traces of PDAEMA polymers prepared by RAFT in toluene at 70 °C

We then decreased the polymerization temperature to 70 °C, while keeping all other reaction conditions exactly the same. As shown in Figure 2.8, the kinetic plot showed a linear correlation, indicating a living polymerization. GPC showed very clean shifts to higher molecular weight with the increase of reaction time. The final polymer had a PDI below 1.3. Figure 2.9 shows the ^{1}H NMR spectrum of PDAEMA prepared by RAFT. Each peak would be clearly assigned to the corresponding protons. All these results demonstrated that RAFT polymerization of DAEMA monomer worked much better at a lower reaction temperature and with a relatively longer reaction time.

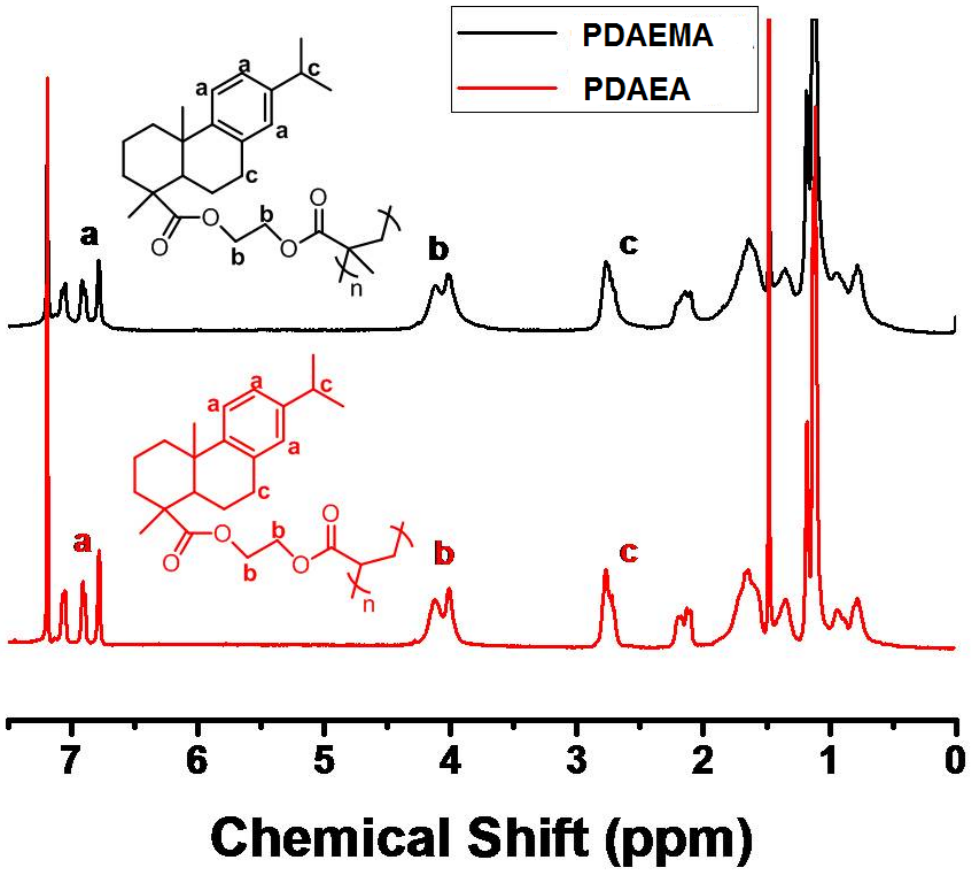

Figure 2.9 ^{1}H NMR spectra of PDAEMA polymer by RAFT polymerization in toluene at 100ºC and PDAEA polymer by RAFT polymerization in THF at 80ºC

RAFT polymerization was also used to synthesize PDAEA. Similarly, the initiator AIBN and the RAFT agent CDB were combined with the monomer DAEA in a reaction system to obtain PDAEA. Similar to the synthesis of PDAEMA, the first experiment was run with a molar ratio of [DAEA]:[CDB]:[AIBN]of [100]:[1]:[0.1] at 100°C in toluene for 24 hrs. The molecular weight (M_n), according to the GPC trace, was 21,400 g/mol with a PDI of 1.5. The next experiment was performed under the similar conditions but at 80°C for almost 2 days. Obtained polymers had a molecular weight of 11,400 g/mol and a PDI of ~2.0. Since the polymerization was very slow in toluene, a reaction was then performed using tetrahydrofuran (THF) as the solvent for 23 hrs at 80°C. Although a low

yield was obtained, a molecular weight of 29,100 g/mol and a PDI of 1.3 showed that THF was a better solvent for the controlled polymerization of DAEA (Figure 2.10). The ^{1}H NMR spectrum of the obtained polymers had all the characteristic proton peaks, which were clearly assigned (Figure 2.9).

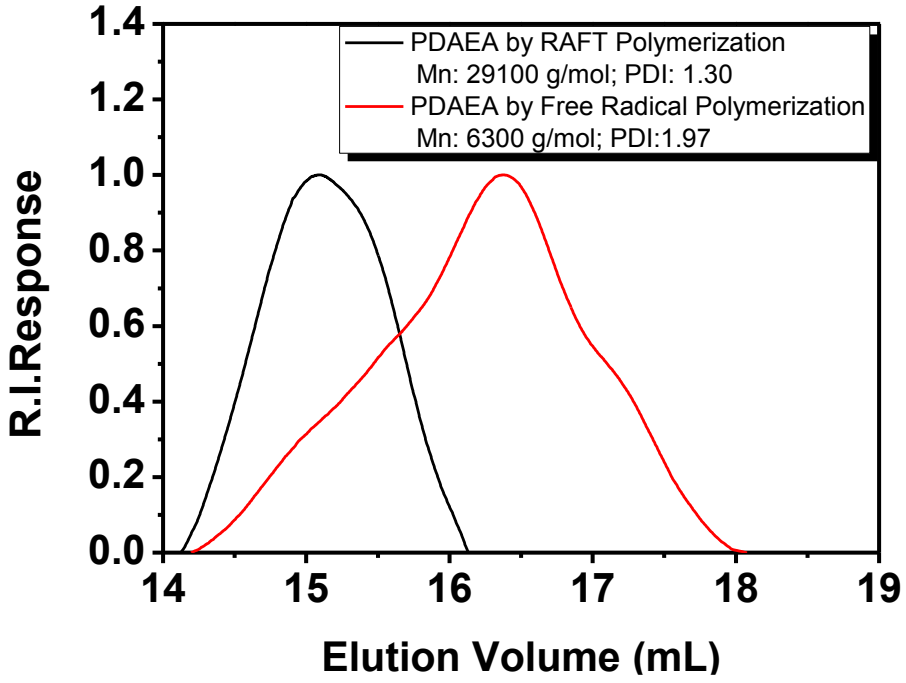

Figure 2.10 GPC traces of PDAEA prepared by RAFT polymerization in THF at 80 ^{o}C and by free radical polymerization in THF at 80 ^{o}C

To compare RAFT polymerization with free radical polymerization, a reaction was conducted without the controlling agent CDB in THF at 80°C for 21hrs. The molecular weight of the resulting polymer was 6,300 g/mol and had a PDI of 1.97 (Figure 2.10). This demonstrated that RAFT resulted in not only a higher molecular weight, but also a lower PDI. All these experiments indicated that polymerization of DAEA by RAFT was relatively slow compared to polymerization of DAEMA, but controlled if THF was used as the reaction solvent.

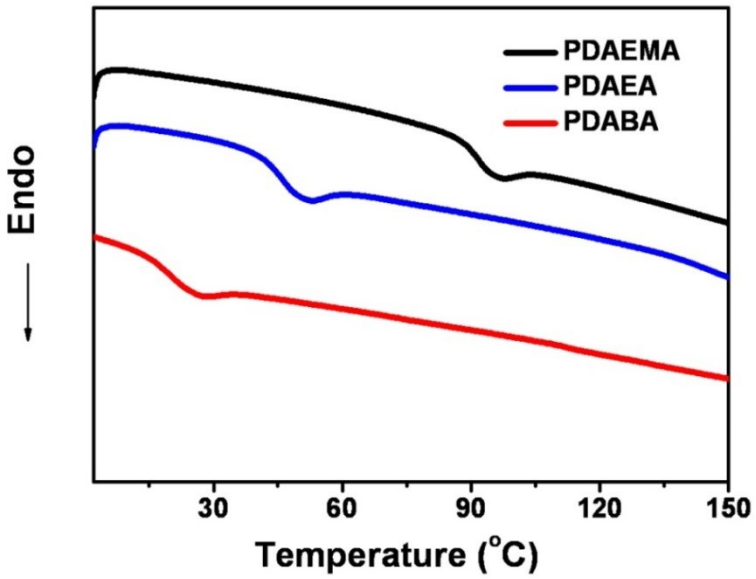

Figure 2.11 DSC traces of PDAEA, PDABA and PDAEMA prepared by ATRP (corresponding to Runs 2, 3 and 5 from Table 2.1 respectively)

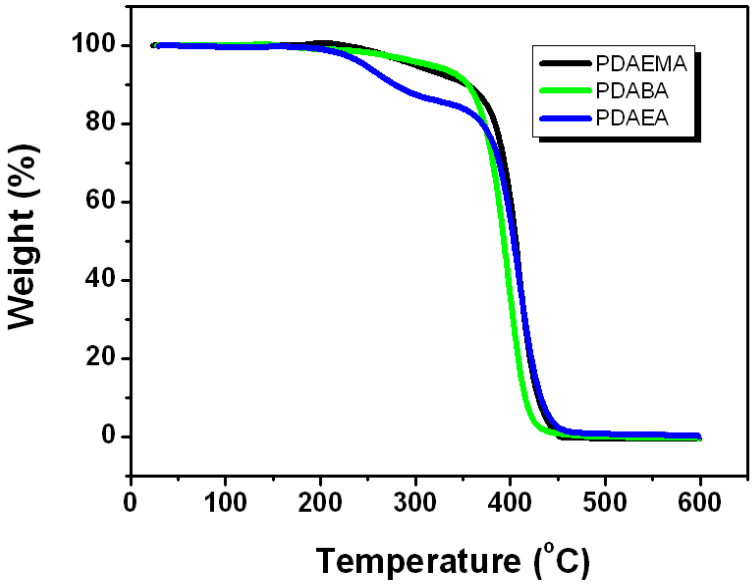

Figure 2.12 TGA traces of PDAEA, PDABA and PDAEMA polymers prepared by ATRP (Run 2, 3 and 5 from Table 2.1)

The thermal properties of PDAEA, PDABA, and PDAEMA polymers were characterized with the aid of Differential Scanning Calorimeter (DSC) (Figure 2.11). All polymers exhibited typical thermoplastic behaviors, with no melting observed. The glass transition temperatures (T_g) showed a dependence on the chemical structures of the

backbone and side groups. The methacrylate polymer (PDAEMA) showed the highest T_g ~ 90 °C, while the lowest T_g (~22 °C) was observed in acrylate polymers with the longest spacers between side groups and backbone (PDABA), about 20 °C lower than that of PDAEA. This was in agreement with the concept that the longer spacer reduced the rotation barriers of acrylate polymers and decreased the T_g. Thermogravimetric Analysis (TGA) of these different polymers was carried out under N_2 (Figure 2.12). All polymers showed two-stage weight loss behavior. The first stage exhibited a slight weight loss with similar onsets at 220 °C, although PDAEA showed noticeable higher loss (~15wt%) than that of PDABA and PDAEMA (~5wt%). TGA traces of the second stage were similar with onsets at nearly 325 °C followed by almost complete weight loss, due to full decomposition of polymer backbones.

2.5 Conclusions

In conclusion, we have developed a strategy to synthesize a new class of monomers and well-defined polymers from abundant low-cost renewable natural resources: gum rosin. Highly pure rosin-derived acrylate and methacrylate monomers were prepared through simple esterification with dehydroabietic acid. The first well-defined rosin-derived polymers with low polydispersity and controlled molecular weight were obtained using ATRP and RAFT polymerization. These polymers exhibited tunable thermal properties (e.g. glass transition temperature) by simple manipulation of monomer structures. The successful synthesis of rosin-derived monomers and well-defined polymers opens a new avenue towards development of a variety of rosin-derived renewable polymeric materials (e.g. thermoplastic elastomers, hybrids, composites) as potential competing replacement for petroleum-derived plastics.

CHAPTER 3

DEGRADABLE ROSIN ESTER-CAPROLACTONE GRAFT COPOLYMERS[2]

[2] K. Yao, J. Wang, W. Zhang, J. S. Lee, C. Wang, F. Chu, X. He, and C. Tang. *Biomacromolecules* **2011** *12* (6), 2171-2177

3.1 Abstract

We have carried out the synthesis of side-chain rosin ester-structured poly(ε-caprolactone) (PCL) through a combination of ring-opening polymerization and click chemistry. Rosin structures are shown to be effectively incorporated into each repeat unit of caprolactone. This simple and versatile methodology does not require sophisticated purification of raw renewable biomass from nature. The rosin properties have been successfully imparted to the PCL polymers. The bulky hydrophenanthrene group of rosin increases the glass transition temperature of PCL by more than 100 ^{o}C, while the hydrocarbon nature of rosin structures provides PCL excellent hydrophobicity with contact angle very similar to polystyrene and very low water uptake. The rosin-containing PCL polymers exhibit full degradability and biocompatibility (non-toxic). This study illustrates a general strategy to prepare a new class of renewable hydrocarbon-rich degradable polymers.

3.2 Introduction

The development of renewable polymers is driven by carbon footprint reductions and a strong desire to shift away from our dependence on fossil fuels as organic material feedstocks.[6, 9, 10] The small share (<5%) of renewable polymers in the commercial market is largely due to high cost and inferior performance compared with synthetic polymers produced from petroleum chemicals. While novel processing approaches and modifications of existing biorenewable polymers such as polylactide[118-120] or polyalkanoates[121, 122] can be effective, the next stage of growth in this arena will rely on the development of judicious synthetic strategies to next-generation materials that involve

the design, preparation, and controlled polymerizations of new structures from abundant biomass.[7, 11, 16-18, 27, 30]

Biodegradable polymers have attracted much attention due to their widespread biomedical applications as well as the use as environmentally benign disposable engineering plastics.[123-125] There are two major classes of biodegradable polymers. The first class of biodegradable polymers is those polymers derived from natural biomass or produced by microorganisms such as polylactide (PLA), polyhydroxyalkanoate (PHA) and chitin.[126, 127] Monomers of some of these polymers can be obtained entirely from nature. In contrast, the second class of biodegradable polymers is synthetic polymers such as polycaprolactone.[128, 129] In order to broaden the use of biodegradable polymers for new applications, it is desirable to tune the physical properties of degradable polymers through numerous approaches, including the combination of natural biomass and synthetic polymers.[130-133]

Rosin is a renewable natural resin obtained from the exudation of pine and conifer trees.[42, 43] Rosin consists primarily of abietic- and pimaric-type resin acids (or rosin acids) with characteristic hydrophobic hydrophenanthrene rings. Rosin acids have at least three unique properties which most other natural biomass lacks of: 1) they are a class of hydrocarbon rich biomass, which can render hydrophobicity to any polymers attached; 2) they have very bulky hydrophenanthrene group, which can significantly alter thermal properties of polymers integrated; 3) rosin-derived esters are biocompatible as they are permitted to be used as food additives such as those in chewing gum and beverages, approved by US Food and Drug Administration. On the other hand, functionalization of

carboxyl group of rosin acids allows to integrate rosin moiety into polymers as backbone or side chains.[44-46, 114, 134]

Figure 3.1 A general strategy toward degradable rosin ester-structured polymers

Herein we report a strategy to prepare a class of novel degradable structured polymers which combine properties of both rosin acids and degradable polymers (Figure 3.1). In this Chapter we show that we have imparted rosin properties to degradable poly(ε-caprolactone) (PCL). We demonstrate that rosin ester-integrated PCL exhibits excellent hydrophobicity, highly elevated glass transition temperature (therefore service temperature) and low water uptake while retaining its full degradability. Specifically, we prepare side-chain rosin ester-containing PCL through a combination of ring-opening polymerization (ROP) and click chemistry with high fidelity. We believe that such strategy should be generalized to prepare other types of degradable structured polymers such as PLA and PHA.

3.3 Experimental Section

3.3.1 Materials

Dehydroabietic acid (DHAA, ~90%) and hydrogenated rosin were obtained from Wuzhou Chemicals, China and used as received. Gum rosin was purchased from Acros and used as received. Toluene and tetrahydrofuran (THF) were refluxed with sodium and distilled out just before use under nitrogen atmosphere. 2-Chlorocyclohexanone, m-chloroperoxybenzoic acid (mCPBA), oxalyl chloride, triethylamine, propargyl alcohol, Sn(II) 2-ethylhexanoate ($Sn(Oct)_2$), dichloromethane (CH_2Cl_2), *N, N*-dimethylformamide

(DMF), methanol, sodium azide, copper iodine and 1,8-diazabicyclo[5.4.0]undec-7-ene (DBU) were purchased from Sigma-Aldrich and used as received. α-Chloro-ε-caprolactone (αClεCL) and 2-hydroxyethyl 2-bromoisobutyrate (HEBIB) were prepared according to the literature.[135, 136]

3.3.2 Characterization

^{1}H (300 MHz) and ^{13}C (75 MHz) NMR spectra were recorded on a Varian Mercury spectrometer with tetramethylsilane (TMS) as an internal reference. Fourier Transform Infrared Spectrometry (FTIR) spectra were recorded on a PerkinElmer spectrum 100 FTIR spectrometer. Gel permeation chromatography (GPC) was performed at 25 ºC on a Varian system equipped with a Varian 356-LC refractive index detector and a Prostar 210 pump. The columns were STYRAGEL HR1, HR2 (300×7.5 mm) from Waters. HPLC grade THF was used as eluent at a flow rate of 1 mL/min. THF and polymer solutions were filtered over microfilters with a pore size of 0.2 μm (Nylon, Millex-HN 13 mm Syringes Filters, Millipore, USA). The columns were calibrated against polystyrene standards. Differential scanning calorimetry (DSC) experiments were conducted on a DSC Q200 instrument (TA instruments). The samples were heated from –80 ºC to 180 ºC at a rate of 10 ºC/min, maintained at 180 ºC for 2 min and then cooled to –70 ºC at a rate of 10 ºC/min. The data were collected from the second heating scan. The average sample mass was about 5 mg, and the nitrogen flow rate was 50 mL/min. Thermogravimetric analysis (TGA) was operated on a SDT Q600 TGA system (TA instruments), ramping from 25 ºC to 800 ºC at a rate of 10 ºC/min, and maintaining at 800 ºC for 5 min under nitrogen gas at a flow rate of 100 mL/min. Contact angle test data were collected on a VCA-Optima goniometer (AST Products, Inc).

3.3.3 Synthesis

Synthesis of Dehydroabietic Propargyl Ester (DAPE): Dehydroabietic acid (10 g, 33 mmol) was dissolved in dichloromethane (40 mL) in a round bottom flask equipped with a magnet stirrer and a temperature control unit. Oxalyl chloride (5.12 g, 40 mmol) was added within 1 h at 0 ^{o}C and the reaction was then run at 22 ^{o}C for 3h. Excessive oxalyl chloride was excluded by distillation with dichloromethane. Then triethylamine (5.0 g, 57 mmol) and propargyl alcohol (1.96 g, 34.9 mmol) were directly added into the above flask with 100 mL dichloromethane and the reaction was run at 22 ^{o}C for 24 h. The product in dichloromethane was washed with 5 % $NaCO_3$ solution and purified through silica gel chromatography with hexane and ethyl acetate as eluent at a ratio of 9/1. The final product was a white transparent liquid. ^{1}H NMR ($CDCl_3$, δ, ppm): 7.21-7.15 (d, *J* = 8.04Hz, 1H; Ar), 7.04-6.98 (d, *J* = 8.04Hz, 1H; Ar), 6.92-6.87 (s, 1H; Ar), 4.77-4.57(m, 2H; OCH_2), 2.95-2.75(m, 3H), 2.46-2.41 (m, 1H; C≡CH), 2.35-1.16(m, 21H). ^{13}C NMR ($CDCl_3$, δ, ppm): 177.7 (C=O); 146.7, 145.7, 134.7, 127.0, 124.2, 123.9 (Aromatic C); 78.0 (-C≡*C*H); 74.5 (-*C*≡CH); 52.0 (-O*C*H_2-); 49.0(C(C)*C*HCH_2), 44.8 (CH_2(CH_3)*C*CO), 37.9, 36.9 (CH_2*C*H_2C), 35.9 (CH_2*C*H_2CH_2), 33.4 (H_3C*C*HCH3), 30.0 (CH_2*C*H_2C(CH)=C), 25.3, (*CH3*C(C=C-)), 21.7 (*C*H_3C(CO)), 18.5, 18.3 (CH*C*H_3). FTIR (cm^{-1}): 3280, 2956-2869, 1731, 1497, 1459, 1385, 1363, 1239, 1169, 1122, 1106, 1075, 1037, 991, 822.

Synthesis of Hydrogenated Rosin Propargyl Ester (HRPE) and Gum Rosin Propargyl Ester (GRPE): The synthesis was similar to the DAPE synthesis, using hydrogenated rosin and gum rosin as starting materials respectively. Both hydrogenated rosin and gum rosin are a mixture of rosin acids, with hydroabietic acid and abietic acid

as the major rosin acid respectively. A few representative rosin acids of hydrogenated rosin and gum rosin are shown in Figure 3.2.

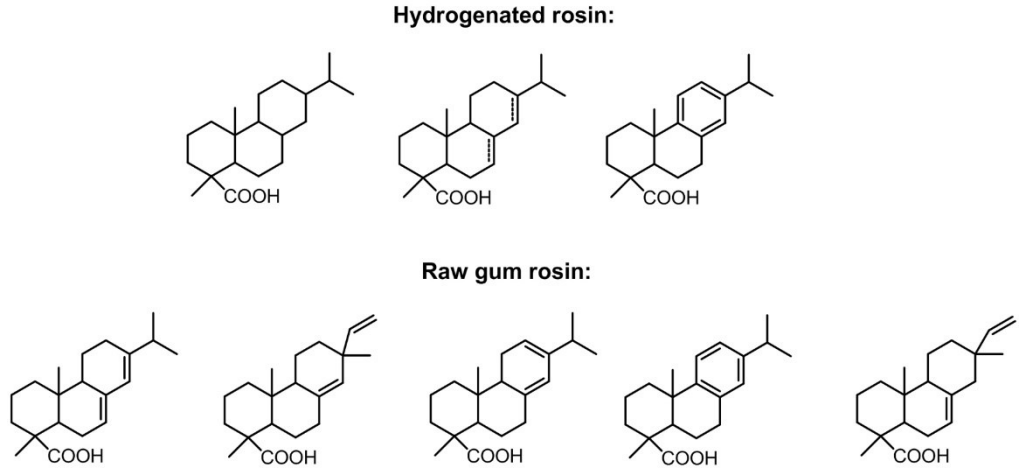

Figure 3.2 Representative chemical structures (not an exhaustive list) of hydrogenated rosin and gum rosin

Synthesis of Poly(α-chloro-ε-caprolactone) by Ring-opening Polymerization[136]: α-Chloro-ε-caprolactone (1.0 g, 6.7 mmol), HEBiB (28.4 mg, 0.134 mmol) and $Sn(Oct)_2$ (5.4 mg, 0.0134 mmol) were dissolved in dry toluene (1.0 mL) in a Schlenk flask and the flask was purged with nitrogen for 10 min. Then the polymerization was carried out in a preheated oil bath at 120 °C for 12 h under continuous stirring. After polymerization, the solution was diluted with dichloromethane and precipitated in cold methanol. The polymer was finally recovered by centrifugation (8000 rpm at 25 °C for 15 min) and dried in a vacuum oven until constant weight. The conversion of monomers was almost 100% as determined by ^{1}H NMR. M_n (poly(αClεCL), GPC) = 7200 g/mol, PDI (poly(αClεCL), GPC) = 1.34. ^{1}H NMR ($CDCl_3$, δ, ppm): 4.25–4.17 (t, –CHClCO–), 4.17-4.07 (t, $–OCH_2–$), 2.07–1.16 (broad, $–CH_2CH_2CH_2–$).

Synthesis of Poly(α-azide-ε-caprolactone)[137]: Poly(αClεCL) (1.0 g, 6.7 mmol azide units) was dissolved in DMF (10 mL) in a round-bottom flask, followed by the addition

of sodium azide (2.2 g, 33.5 mmol). The mixture was stirred at room temperature overnight. After evaporation of DMF, 10 mL toluene was added, and the insoluble salt was removed by centrifugation. The polymer was recovered by solvent evaporation. ^{1}H NMR ($CDCl_3$, δ, ppm): 4.28–4.13 (t, –OCH_2–), 3.90–3.80 (t, –CHN_3CO–), 1.95–1.23 (broad, –$CH_2CH_2CH_2$–).

Synthesis of Rosin Ester-Containing Polycaprolactone by Click Chemistry: Use dehydroabietic propargyl ester-substituted PCL (PCL-*g*-DAPE) synthesis as an example. 1 equiv. poly(αN_3εCL), 1.2 equiv of DAPE and 0.1 equiv of CuI were mixed in a Schlenk flask and purged with N_2 for 10 min. 0.1 Equiv. DBU was dissolved in deoxygenated THF and transferred to the flask. The solution was stirred at 35 °C overnight.[138, 139] After the click reaction, the polymer was passed through a neutral aluminum oxide column to remove the copper catalyst and then precipitated in water for three times. The final product was dried in a vacuum oven at room temperature. ^{1}H NMR ($CDCl_3$, δ, ppm): 7.80 (s, CH=C, triazole), 7.20–6.78 (m, aromatic, DAPE), 5.43–5.02 (s, triazole–CH–CO, O–CH_2–triazole), 4.21–3.88 (s, –OCH_2–), 2.93–2.60 (m, protons next to aromatic ring). PCL-*g*-HRPE and PCL-*g*-GRPE were synthesized using similar conditions.

3.3.4 Cell Culture and Toxicity Test

The C3H10T1/2 mesenchymal stem cells (ATCC, Manassas, VT) were cultured in high glucose DMEM (Invitorgen, Carlsbad, CA) supplemented with 10% fetal bovine serum (Hyclone, Logan, Utah), 100 U/ml penicillin (Hyclone, Logan, Utah) and 100 μg/ml streptomycin (Hyclone, Logan, Utah) at 37 ^{o}C in a humidified, 5 % CO_2 incubator.

C3H10T1/2 cells were seeded in 33 mm Petri dishes at a density of 1.25×10^5 cells/dish in 1 ml medium. After 24 hr, the cell culture medium was replaced with fresh

medium either without or with rosin ester-containing polyesters at a concentration up to 100 μg/ml. The cells were then further cultured for 2 days to monitor their proliferation by taking phase contrast images every day.

3.4 Results and Discussion

ROP and click chemistry[140, 141] were combined to prepare rosin ester-containing PCL. We first carried out a proof-of-concept study to explore whether rosin esters can be incorporated into each repeat unit of ε-caprolactone backbone using a model rosin acid, dehydroabietic acid. Then we further explored the expansion of this concept with the use of hydrogenated rosin and raw gum rosin, both containing a mixture of rosin acids with rather complicated compositions. The integration of hydrogenated rosin and raw gum rosin into degradable polymers is also coincidental with the notion toward continuous reduction of manufacturing cost in utilization of biomass. Table 3.1 summarized the results of synthesis of various rosin ester-containing PCL.

Table 3.1 Molecular weight data of rosin ester-containing PCL

	Poly(αClεCL)			Poly(αN$_3$εCL)			Rosin Ester-Containing PCL		
	M_n (g/mol) (NMR)	M_n (g/mol) (GPC)	PDI	M_n (g/mol) (NMR)	M_n (g/mol) (GPC)	PDI	M_n (g/mol) (NMR)	M_n (g/mol) (GPC)	PDI
1	7400	6900	1.45	7750	8900	1.50	24600	11000	1.41
2	7400	5900	1.38	7750	8600	1.31	24800	10400	1.57
3	7400	7200	1.34	7750	9800	1.28	22800	12200	1.34

1: PCL-*g*-DAPE; 2: PCL-*g*-HRPE; 3: PCL-*g*-GRPE

Synthesis of Dehydroabietic Propargyl Ester-Containing Polycaprolactone: As a proof-of-concept study, we prepared a model rosin ester-containing PCL. We chose

dehydroabietic acid (DHAA) as the starting rosin acid to prepare a propargyl ester derivative. DHAA was first reacted with oxalyl chloride in dry dichloromethane to yield dehydroabietic acyl chloride **1**, as shown in Figure 3.3. Propargyl alcohol was then added to the solution of **1** in the presence of triethylamine, yielding dehydroabietic propargyl ester **2** (DAPE). The structure and purity of DAPE were characterized with the aid of ^{1}H NMR analysis (Figure 3.4), with characteristic chemical shifts of aromatic protons in the range of 6.7-7.2 ppm, while alkyne protons, methylene protons next to the alkyne group and protons next to the aromatic group were located at 2.4 ppm, 4.7 ppm and 2.8 ppm respectively. In parallel, azide substituted PCL **5** was prepared in a multi-step route according to a reported procedure[137, 142] α-Chloro-ε-caprolactone **3** (αClεCL) monomers were prepared by the Baeyer-Villiger oxidation of α-chlorocyclohexanone in the presence of *m*-chloroperoxybenzoic acid. Monomer **3** underwent conventional ROP using Sn(II) 2-ethylhexanoate ($Sn(Oct)_2$) as the catalyst and 2-hydroxyethyl 2-bromoisobutyrate (HEBIB) as the initiator, yielding chlorine-substituted PCL **4** (poly(αClεCL)), which was then reacted with excess sodium azide in *N,N*-dimethylformamide (DMF) at room temperature to provide an azide-substituted PCL poly(α-azide-ε-caprolactone) **5** (poly($\alpha N_3\varepsilon$CL)). The click reaction was then carried out between **5** and **2** in DMF with the use of CuI/DBU (1,8-diazabicyclo[5.4.0]undec-7-ene) as the catalyst, yielding DAPE-substituted PCL (PCL-*g*-DAPE).

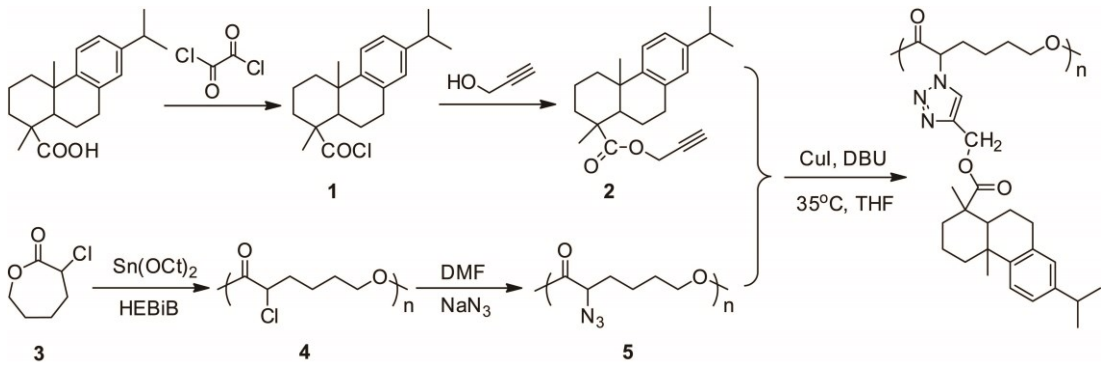

Figure 3.3 Preparation of DAPE Containing Polycaprolactone by Combining Ring-opening Polymerization and Click Chemistry

Chemical structures of poly(αClεCL), poly(αN$_3$εCL) and PCL-*g*-DAPE were characterized with the aid of ^{1}H NMR and FTIR. According to the ^{1}H NMR spectra shown in Figure 3.4, the proton next to azide group shifted from 4.2 ppm to 3.8 ppm following the azide replacement of chlorine group. The integration of NMR spectra indicated all chlorine groups were converted to the azide groups, which also showed characteristic strong absorption at ~ 2120 cm^{-1} in FTIR spectra (Figure 3.4). After the click reaction, the chemical shift at 7.8 ppm of PCL-*g*-DAPE polymers was assigned to the characteristic proton from the triazole group. Aromatic protons (6.7-7.2 ppm) and protons next to the aromatic group (2.8 ppm) were clearly present in the spectra. Integration of these characteristic protons demonstrated the quantitative reaction between alkyne-containing rosin esters and azide-substituted PCL, indicating high fidelity of the click reaction. FTIR spectra further confirmed the 100% efficiency of the click reaction. The peak at ~2120 cm^{-1}, corresponding to the azide absorption, disappeared completely after the click reaction and a new absorption band at ~1650 cm^{-1} emerged, corresponding to absorption of the triazole group. No degradation of the PCL backbone was observed during the click reaction.

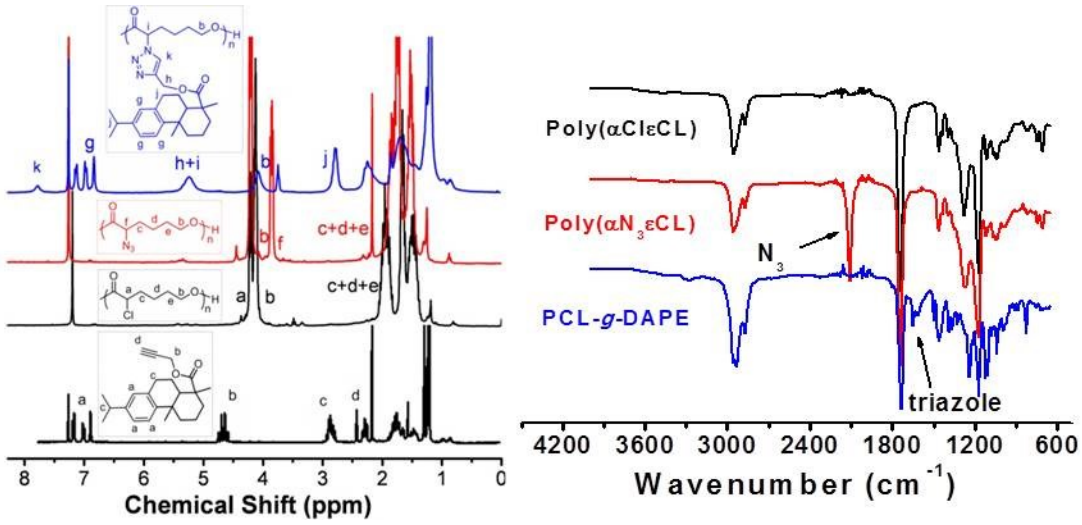

Figure 3.4 ^{1}H NMR and FT-IR spectra of poly(αClεCL), poly(αN$_3$εCL) and PCL-*g*-DAPE

The PCL-*g*-DAPE polymers were then characterized by gel permeation chromatography (GPC). As shown in Figure 3.5, the GPC traces showed that after click reaction, the molecular weight of DAPE-substituted PCL increased appreciably, compared to that of poly(αClεCL) polymers. Meanwhile the polydispersity index (PDI) of the substituted PCL did not show dramatic change (Table 3.1), indicating that the polymer main chain was not degraded during the click reaction. The higher molecular weight of poly(αN$_3$εCL) may be due to the more polar nature of the azide group and their stronger interaction with the GPC column. It should be pointed out that the molecular weights of rosin ester-containing PCLs determined by GPC were much lower than that obtained by ^{1}H NMR analysis. The possible reason is that the rosin ester-containing polycaprolactone may have significantly different hydrodynamic volume compared to polystyrene calibration standards, very similar to our early report.[134]

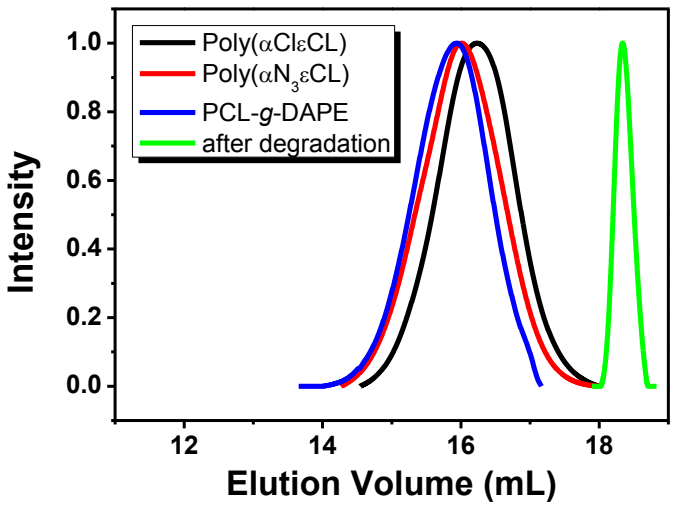

Figure 3.5 GPC traces of poly(αClεCL), poly(αN3εCL), PCL-*g*-DAPE and acid-degraded PCL

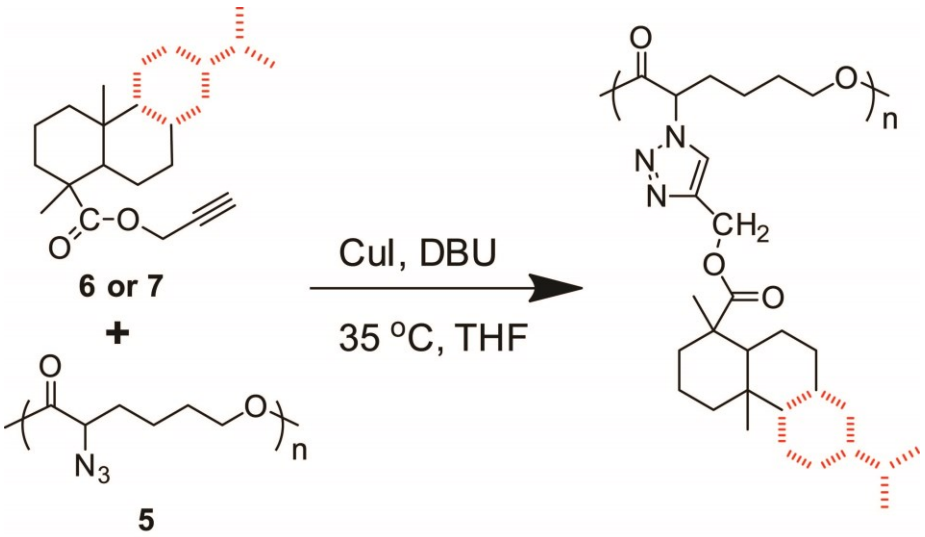

Figure 3.6 Preparation of side-chain hydrogenated rosin propargyl ester (HRPE, **6**) and gum rosin propargyl ester (GRPE, **7**)-containing polycaprolactone by combining ring-opening polymerization and click chemistry

Synthesis of Hydrogenated Rosin Propargyl Ester and Gum Rosin Propargyl Ester-Containing Polycaprolactone: The successful synthesis of model rosin ester-containing PCL polymers through a mild click reaction motivated us to carry out a one-pot preparation of multiple rosin esters substituted PCL from raw gum rosin or hydrogenated rosin (obtained by hydrogenation of raw gum rosin with aid of transition metal catalysts.

It consists mainly of hydroabietic acid which tends to provide better chemical stability) (Figure 3.6). Both resources are much more affordable compared with model rosin acids. The hypothesis was based on the presence of carboxyl group for all rosin resources, regardless of how complicated an isomerization occurs between different rosin acids (see representative rosin acids in Figure 3.2). First, hydrogenated rosin propargyl ester **6** (HRPE) and gum rosin propargyl ester **7** (GRPE) were synthesized from hydrogenated rosin and raw gum rosin respectively using the similar procedure to the synthesis of DAPE. ^{1}H NMR analysis of HRPE and GRPE clearly indicated all carboxyl groups were converted to the propargyl group. Then similar click reaction conditions were used to prepare HRPE and GRPE-substituted PCLs. The ^{1}H NMR spectra (Figure 3.7) showed the presence of all characteristic signals such as triazole protons, methylene protons next to the triazole group as well as protons from the PCL backbone. FT-IT spectra also clearly showed the disappearance of the azide group and the appearance of the triazole group after the click reactions (Figure 3.8). GPC traces of both PCL-*g*-HRPE and PCL-*g*-GRPE showed the progressive increase of molecular weight after the click reactions, while PDIs remained nearly same, similar to the synthesis of PCL-*g*-DAPE (Figure 3.9).

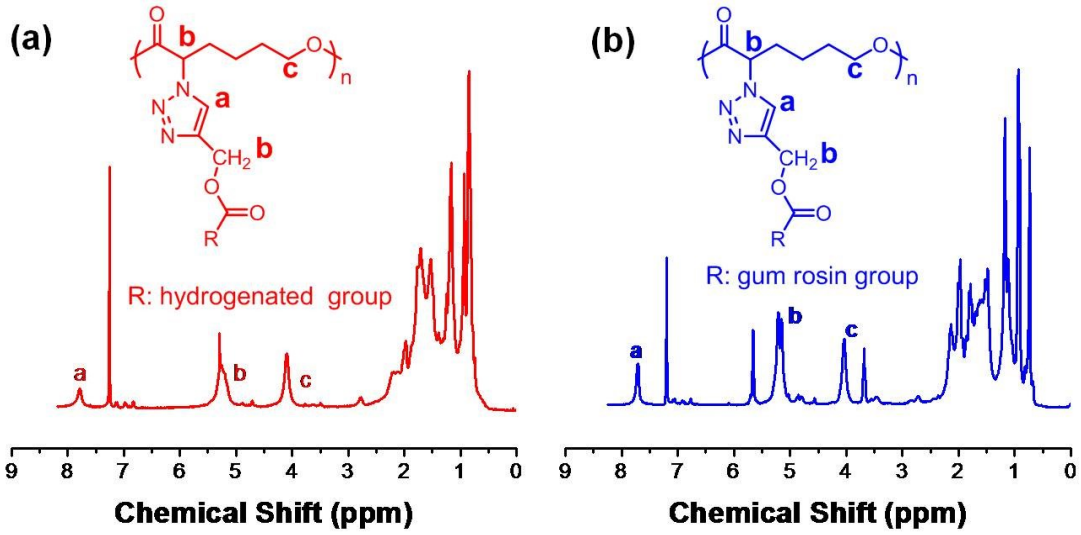

Figure 3.7 ^{1}H NMR spectra of (a) PCL-*g*-HRPE and (b) PCL-*g*-GRPE in $CDCl_3$

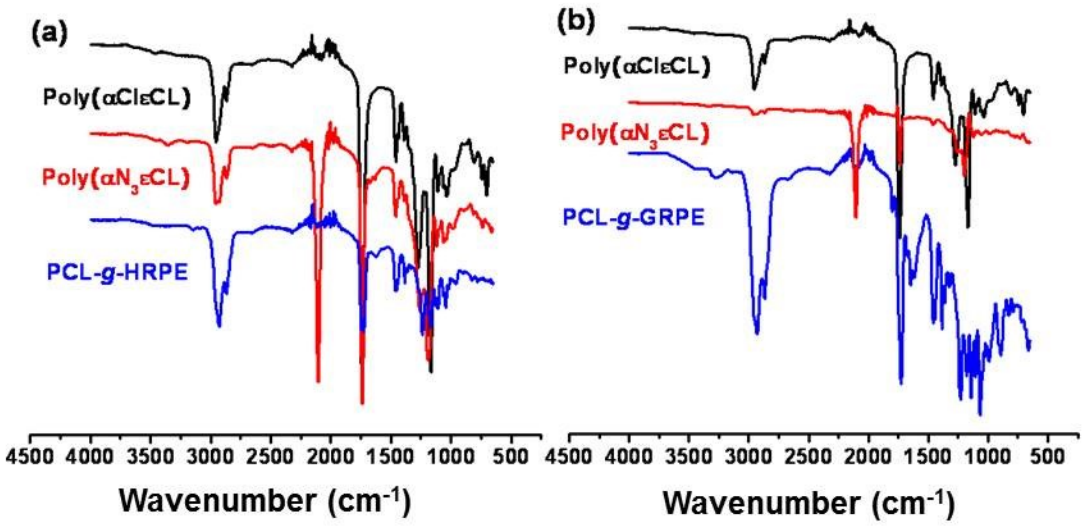

Figure 3.8 FTIR Spectra of (a) hydrogenated rosin propargyl ester-substituted PCL (PCL-*g*-HRPE) and (b) gum rosin propargyl ester-substituted PCL (PCL-*g*-GRPE)

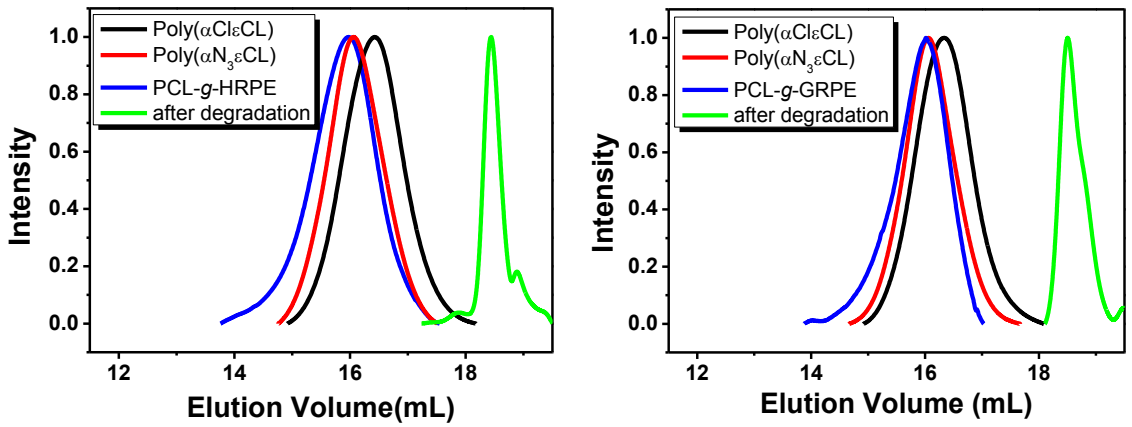

Figure 3.9 GPC traces of PCL-*g*-HRPE, PCL-*g*-GRPE and their acid-degraded PCL

Thermal Properties of Rosin Ester-Containing Polycaprolactone: The notion that the bulky hydrophenanthrene rings would play a significant role in dictating thermal properties of rosin ester-containing PCL was verified by Differential Scanning Calorimetry (DSC). Compared to the very low glass transition temperature (T_g) (~ –50 °C - –60 °C) of unsubstituted, chlorine or azide-substituted PCL (Figure 3.10A), the T_g of rosin acid-substituted PCL changed to ~ 55 - 85 °C, more than a 100 °C increase (Figure 3.10B). This is a substantial change, potentially broadening the utility of substituted PCL, e.g. use as engineering biodegradable thermoplastics. Furthermore, the increase of T_g was consistent with the size of substituted rosin moiety. The DAPE has characteristic aromatic structures which make it more rigid, therefore increasing the rotation barrier of PCL backbone and appearing to have the highest T_g (~ 85 °C) for PCL-*g*-DAPE. The HAPE has dominant saturated cycloaliphatic rings with the least fraction of aromatic ring structures, thus exhibiting the lowest T_g (~ 55 °C) for PCL-*g*-HRPE. The GRPE has structures in between, with both significant aromatic and cycloaliphatic ring structures, which result in a T_g (~ 64 °C) between those of DAPE and HAPE for PCL-*g*-GRPE.

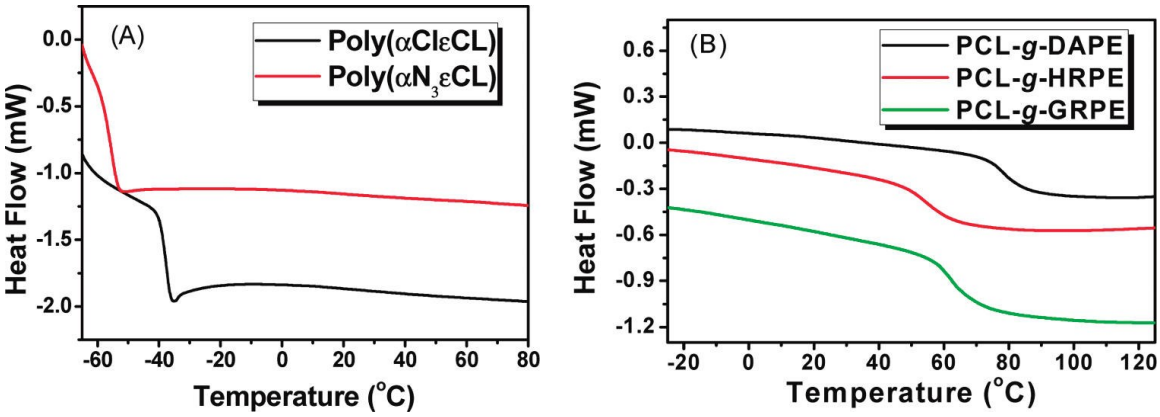

Figure 3.10 DSC curves of (A) poly(αClεCL) and poly(αN_3εCL), and (B) rosin ester-containing PCLs. The curves were collected from the second heating scans

Degradability and Hydrophobicity of Rosin Ester-Containing Polycaprolactone: The degradability of rosin ester-containing PCLs was tested according to two different methods: acid-catalyzed degradation and hydrolytic degradation. The acidic degradation was carried out in a diluted HCl/tetrahydrofuran (THF) solution (~ 0.15 M HCl). According to the GPC characterization (Figures 3.5 and 3.9), all rosin ester-containing PCLs (including PCL-*g*-DAPE, PCL-*g*-HRPE and PCL-*g*-GRPE) degraded completely within 1 hour, with only molecular rosin moieties left, indicating the preservation of degradability of PCLs with the presence of bulky rosin moieties. It is worthy to mention that these molecular rosin moieties could be further digested and degraded by microbials in nature, as reported in the literature.[143]

Preliminary hydrolytic degradation tests of rosin ester-containing PCLs were carried out in phosphate buffered saline (PBS) solution at 37 °C for several weeks. As an example, Figure 3.11 shows the mass loss profile and molecular weight change of PCL-*g*-HRPE as a function of degradation time. In the PBS solution, hydrogenated rosin propargyl ester-substituted PCL degraded gradually. After 60 days, the polymers lost about 10% of their initial mass. Meanwhile the molecular weight monitored by GPC

showed a decrease of about 20% compared to the initial molecular weight, as shown by normalized number-average molecular weight ratio ($(M_n)_t/(M_n)_0$) as a function of degradation time in Figure 3.11. Longer degradation testing (e.g. 6 months to 1 year) is currently in progress.

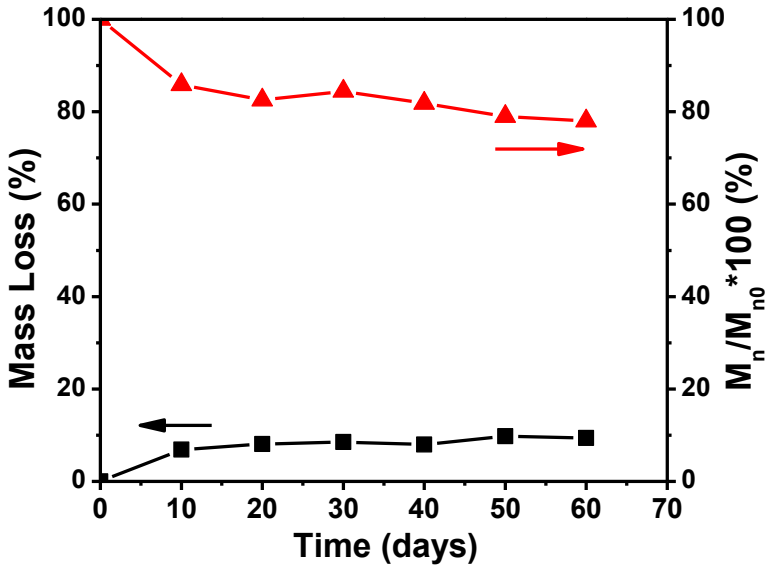

Figure 3.11 Mass loss and molecular weight (GPC data) profiles of PCL-*g*-HRPE during hydrolytic degradation

The introduction of hydrocarbon-based hydrophenanthrene ring in each repeat unit of PCL polymers should render the rosin ester-containing PCL more hydrophobic. We examined the contact angles of the rosin substituted PCLs and compared them with unsubstituted PCL and polystyrene (a hydrocarbon-based polymer derived from petroleum chemicals). Thin and smooth polymer films for contact angle measurement were prepared by spin-casting THF solutions of polymers onto glass substrates. Figure 3.12 shows the images of contact angle measurement. They clearly showed that the rosin ester-containing PCLs had much higher contact angles than that of unsubstituted PCL, indicating the successful impartation of rosin hydrophobicity to PCL polymers.

Significantly, the contact angles of rosin-substituted PCLs (~ 83 – 91°) were very close to that of hydrocarbon-based polystyrene with comparable molecular weight (~ 87°), suggesting that the hydrophenanthrene rosin moieties prefer to locate on the surface of polymer films with ester groups embedded inside the films. The excellent hydrophobicity is desirable for many applications such as encapsulation of hydrophobic drugs for drug delivery.

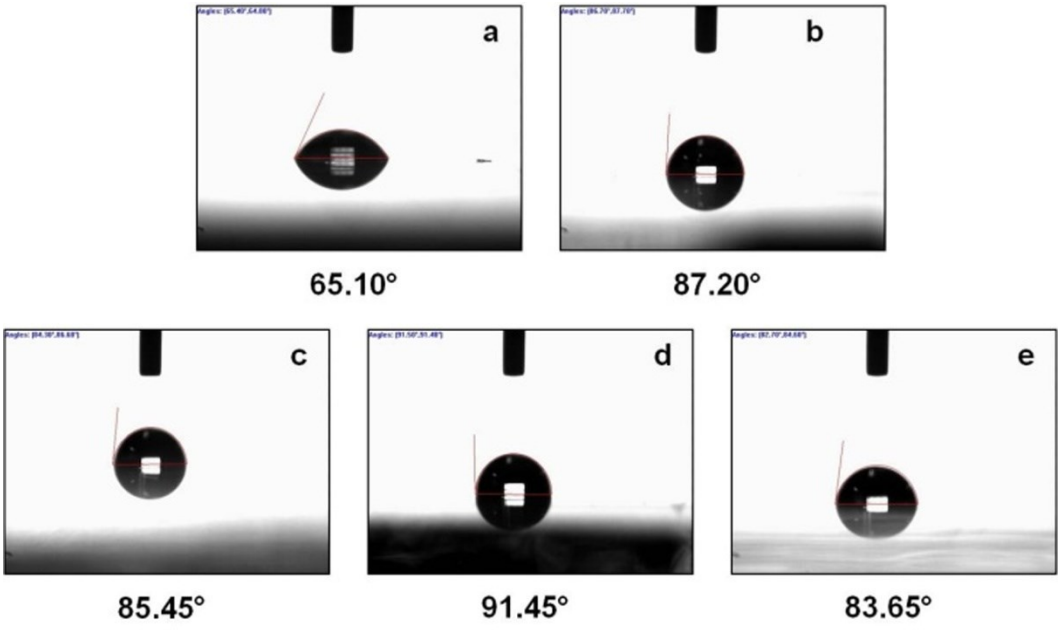

Figure 3.12 Contact angle images of (a) unsubstituted PCL, (b) polystyrene (M_n = 17,400 g/mol), (c) PCL-*g*-DAPE, (d) PCL-*g*-HRPE and (e) PCL-*g*-GRPE

One of the most important properties of degradable polymers is their water uptake property. For many applications, it requires minimal water uptake to ensure longer shelf-life during the use of these materials, while it would be ideal to have fast degradation under composting or biodegradation conditions.[103, 144-146] We tested the water uptake property of rosin ester-containing PCLs using the following method. A series of PCL-*g*-HRPE thick films on glass slides were prepared by drop-casting polymer solution on

clean glass slides and dried until constant weight. The glass slides were then submerged in excess deionized-water. The slides were then removed from water at prescribed intervals and the mass was weighted to calculate the water uptake. Figure 3.13 shows the water uptake profile of the PCL-*g*-HRPE polymer films. It is clear that the water absorbed by the polymers remained less than 1.7 wt% of the initial mass in about 15 days, suggesting the excellent resistance of rosin-substituted polymers to water, mostly due to the hydrophobic nature of the side hydrophenanthrene group.

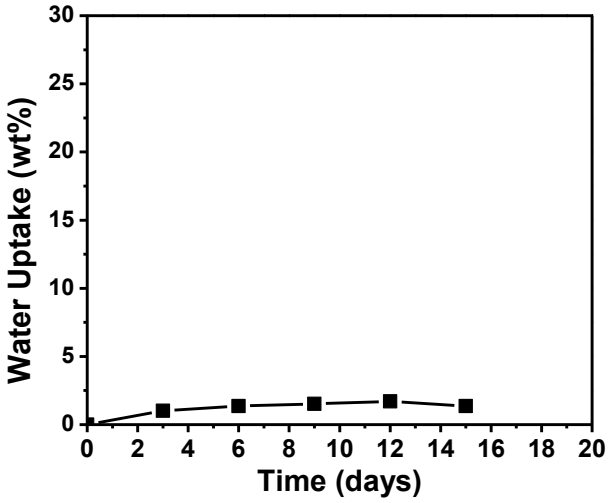

Figure 3.13 Water uptake profile of PCL-*g*-HRPE polymers

Biocompatibility of Rosin Ester-Containing Polycaprolactone: As shown in Figure 3.14, the cells incubated with the various rosin ester-containing PCL retained the same phenotypical (spindlelike) morphology as the control cells (cultured in normal medium without the polymers). Moreover, cells cultured with PCL-*g*-HRPE at concentrations as high as 100 μg/ml proliferated to confluence in 2 days similarly to the control cells, although the cell proliferation was slightly inhibited by PCL-*g*-DAPE and PCL-*g*-GRPE at 100 μg/ml. Taken together, toxicity of all the rosin ester-containing PCL was

considered to be negligible, at least when their concentration was not higher than 100 μg/ml.

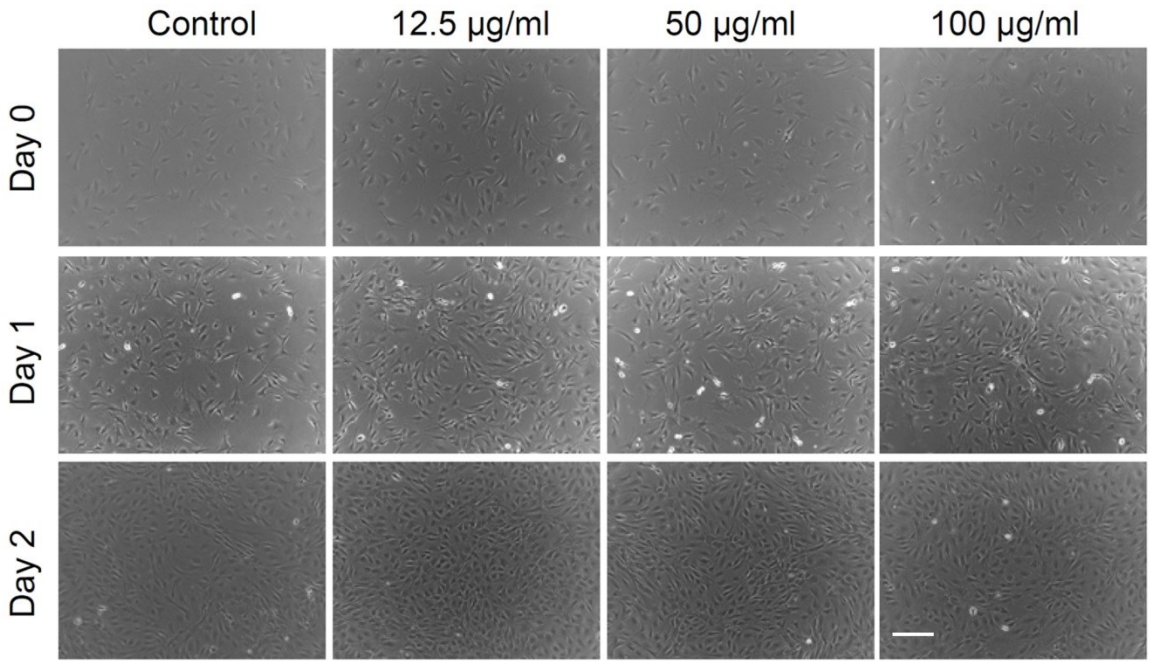

Figure 3.14 Typical images showing proliferation of C3H10T1/2 Mesenchymal stem cells cultured either without (control) or with 12.5-100 μg/ml PCL-g-HRPE in two days. Scale bar: 200 μm that applies to all images in the same panel

3.5 Conclusions

In conclusion, we have developed a strategy to prepare rosin ester structured polycaprolactone through a combination of ring-opening polymerization and "click chemistry". Each repeat unit of polymers contained bulky hydrophobic hydrocarbon-based hydrophenanthrene ring as side groups. It was demonstrated that the integration of rosin moieties rendered excellent hydrophobicity and significantly altered glass transition temperature while retaining full degradability of polycaprolactone. Preliminary biocompatibility test indicated that rosin ester-containing caprolactone graft copolymers are non-toxic. Our strategy paves a way to prepare other degradable rosin-structured

polymers such as polylactide and polyhydroxyalkanoate. Given their compatibility of breakdown by-products (rosin esters) to the environments after degradation, degradable rosin ester-structured polymers may present a new class of environmentally benign green plastics for applications such as food-packaging materials, drug delivery, etc.

CHAPTER 4

SUSTAINABLE THERMOPLASTIC ELASTOMERS DERIVED FROM RENEWABLE CELLULOSE, ROSIN AND FATTY ACIDS[3]

[3] Y. Liu†, K. Yao†, X Chen, H. Ploehn, Z. Wang, C. Wang, F. Chu and C. Tang. Submitted to *Polymer Chemistry*, 09/11/2013
† These authors equally contributed.

4.1 Abstract

Two series of graft copolymers, cellulose-*g*-poly(*n*-butyl acrylate-*co*-dehydroabietic ethyl methacrylate) (Cell-*g*-P(BA-*co*-DAEMA)) and cellulose-*g*-poly(lauryl methacrylate-*co*-dehydroabietic ethyl methacrylate) (Cell-*g*-P(LMA-*co*-DAEMA)), were prepared by "grafting from" atom transfer radical polymerization (ATRP). In these novel graft copolymers, cellulose, DAEMA (derived from rosin), and LMA (derived from fatty acids) are all sourced from renewable natural resources. The "grafting from" ATRP strategy allows the preparation of high molecular weight graft copolymers consisting of a cellulose main chain with acrylate copolymer side chains. By manipulating the monomer ratios in the P(BA-*co*-DAEMA) and P(LMA-*co*-DAEMA) side chains, graft copolymers with varying glass transition temperatures (-50 ^{o}C ~ 60 ^{o}C) were obtained. Tensile stress-strain and creep compliance testing were employed to characterize mechanical properties. These novel graft copolymers did not exhibit linear elastic properties above about 1% strain, but they did manifest remarkable elasticity at strains of 500% or more. These results suggest that these cellulose-based, acrylate side-chain polymers are potential candidates for service as thermoplastic elastomers materials in applications requiring high elasticity without rupture at high strains.

4.2 Introduction

Recently, extensive research has focused on the preparation of novel polymeric materials from renewable resources due to their potential as alternatives to petroleum-based plastics.[6, 9, 10, 14, 35, 37, 147, 148] Considering the environmental impacts of polymers sourced from petroleum resources, incentives are increasing to design and prepare new "green" polymers derived from renewable, sustainable resources. The main challenge is

in preparing "green" polymers having physicochemical properties comparable or superior to their counterparts prepared from petroleum resources.[7, 11, 16-18, 27, 30]

Thermoplastic elastomers (TPEs) are an important class of engineering polymers having both thermoplastic and elastomeric properties. TPEs can be melt-processed at high temperatures, but at lower temperatures they function as elastomers, manifesting significant elastic recovery from large deformations without fracture.[149] Consequently TPEs have applications in many fields, including automotive parts, sporting goods, and medical devices. First generation TPEs consist of ABA triblock copolymers in which hard minority domains of block A are microphase-separated within a soft matrix of block B. Triblock copolymers, including polystyrene-*b*-polybutadiene-*b*-polystyrene (SBS) and polystyrene-*b*-polyisoprene-*b*-polystyrene (SIS) synthesized by anionic polymerization, have been used as commercial TPE materials for several decades.[150-152] Also (meth)acrylic based ABA triblock copolymers such as poly(methyl methacrylate)-*b*-poly(*n*-butyl acrylate)-*b*-poly(methyl methacrylate) (PMMA-*b*-PBA-*b*-PMMA) prepared by atom transfer radical polymerization (ATRP) have been reported as TPE materials.[79, 108, 153-156] All of these TPE materials based on ABA triblock copolymers are derived from fossil fuel sources.

Recently, triblock copolymer-based TPEs sourced from renewable natural resources have drawn attention. Matyjaszewski and co-workers prepared poly(α-methylene-γ-butyrolactone)-*b*-poly(*n*-butyl acrylate)-*b*-poly(α-methylene-γ-butyrolactone) (PMBL-*b*-PBA-*b*-PMBL) triblock copolymers as TPEs by ATRP, in which MBL (Tulipalin A) is a renewable natural resource isolated from tulips.[157-159] The Hillmyer group reported a series of triblock copolymers with biobased poly(lactic acid)

as end blocks.[160-163] Although various renewable resources have been employed to prepare TPEs, these partially renewable ABA triblock copolymers usually require multi-step polymerizations and have inferior mechanical properties compared with their petroleum-based counterparts (SBS/SIS).

Going beyond the first-generation ABA triblock TPEs, next-generation TPE materials based on graft copolymers have been developed in the past several years. These graft copolymers consist of either soft backbone and hard side chains, or rigid backbone and rubbery side chains, which can be prepared by various grafting chemistry strategies.[164-167] For instance, polyisoprene-*g*-polystyrene (PI-*g*-PS) has been synthesized via anionic polymerization as graft copolymer-based TPE.[165, 166] The Kramer and Bazan groups developed a graft copolymer by grafting soft *n*-butyl acrylate from rigid polyethylene copolymer backbone through ATRP.[168] Recently, we used activator-regenerated electron transfer (ARGET) ATRP[169] to prepare a series of cellulose-based graft copolymers, cellulose-*g*-poly(*n*-butyl acrylate-*co*-methyl methacrylate), as new candidate TPE materials. To the best of our knowledge, all graft copolymer TPEs prepared to date have been derived from petroleum-based resources. Graft copolymer TPEs sourced from renewable resources have not been reported in the literature.

In this work, we report the synthesis and characterization of cellulose-based graft copolymers derived from natural rosin, fatty acids, or both (Figure4.1), including cellulose-*g*-poly(*n*-butyl acrylate-*co*-dehydroabietic ethyl methacrylate) (Cell-*g*-P(BA-*co*-DAEMA)) and cellulose-*g*-poly(lauryl methacrylate-*co*-dehydroabietic ethyl methacrylate) (Cell-*g*-P(LMA-*co*-DAEMA)). Cellulose is an abundant renewable biopolymer.[170-173] DAEMA is a methacrylate-based monomer containing renewable resin

acid from rosin,[42, 44, 51, 174-178] and LMA is derived from a renewable fatty acid. In our related previous work, we reported the polymerization of DAEMA monomer by ATRP to produce homopolymers and block copolymers with controlled molecular weight and low polydispersity index.[134, 179] Now, in this work, DAEMA and BA monomers are copolymerized from a cellulose backbone by "grafting from" ATRP. Due to the different glass transition temperatures of PDAEMA (high T_g) and PBA (low T_g), graft copolymers with controlled T_g are achieved by manipulating the monomer ratios in P(BA-*co*-DAEMA) side chains. In parallel, we replace the BA with another soft monomer, LMA,[180, 181] aiming to obtain a graft copolymer Cell-*g*-P(LMA-*co*-DAEMA) based completely on renewable feedstocks. The thermal and mechanical properties of both Cell-*g*-P(BA-*co*-DAEMA)) and Cell-*g*-P(LMA-*co*-DAEMA) were characterized to evaluate their potential utility as TPEs.

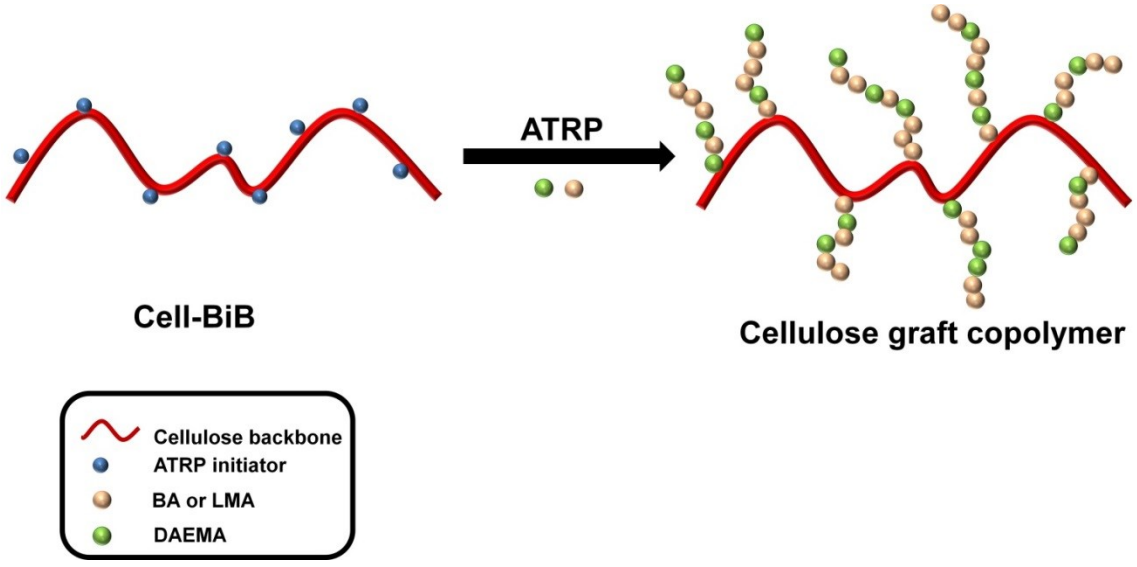

Figure 4.1 Cellulose based graft copolymers by "grafting from" ATRP

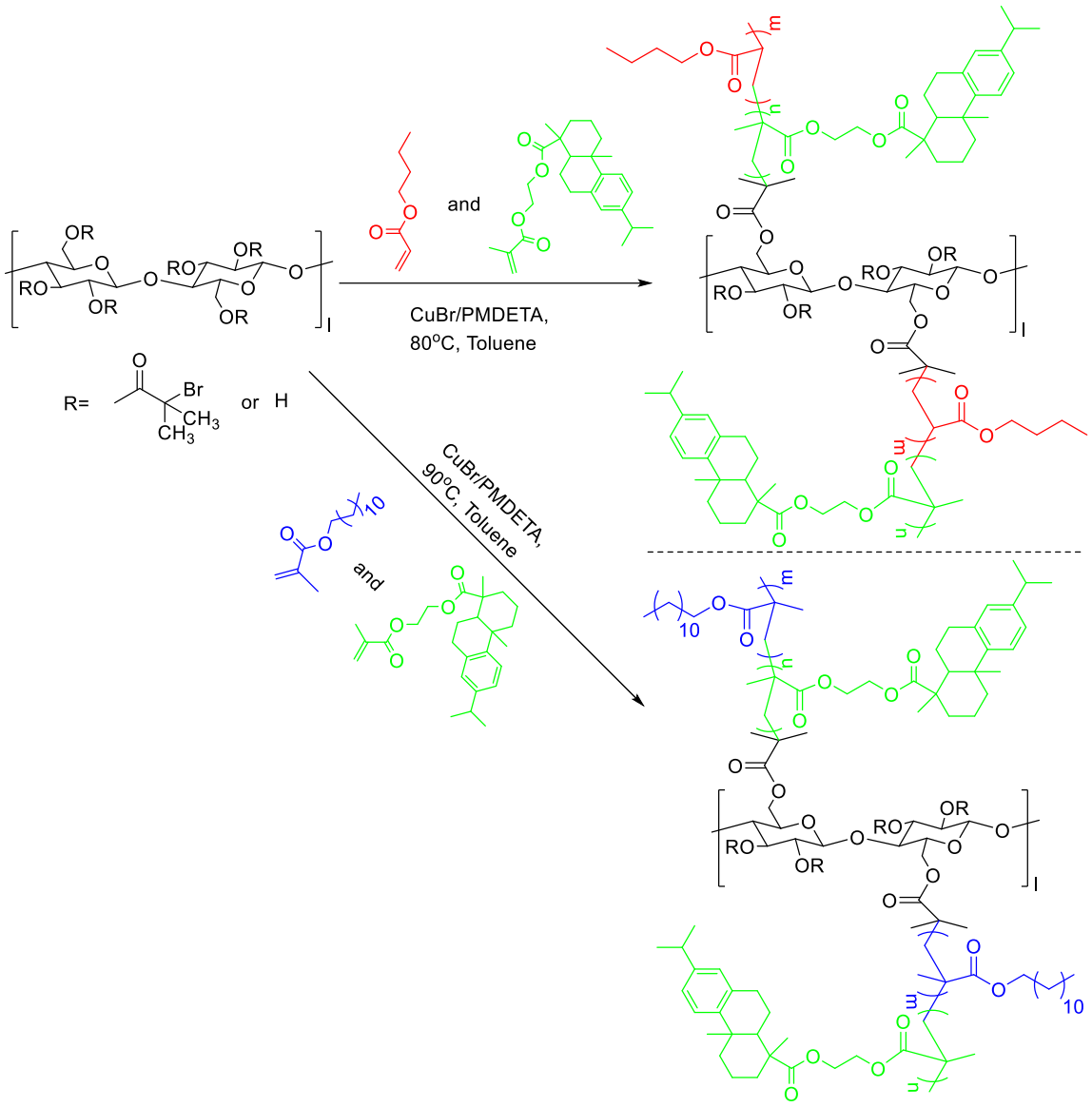

Figure 4.2 Synthesis of renewable graft copolymers Cell-*g*-P(BA-*co*-DAEMA) and Cell-*g*-P(LMA-*co*-DAEMA) by "grafting from" ATRP

4.3 Experimental Section

4.3.1 Materials

n-Butyl acrylate (BA), lauryl methacrylate (LMA), *N,N*-dimethylformamide (DMF), tetrahydrofuran (THF), toluene, methanol, Cu(I)Br, and *N,N,N',N'',N''*-pentamethyldiethylenetriamine (PMDETA) were purchased from Sigma-Aldrich. Dehydroabietic ethyl methacrylate (DAEMA) and cellulose 2-bromoisobutyrylate (Cell-BiB) were synthesized according to procedures reported in early work.[134, 169] BA and LMA were passed through a basic alumina column before polymerization. Toluene was refluxed with sodium and distilled under a nitrogen atmosphere before use. All other reagents were used as received.

4.3.2 Characterization

^{1}H (400 MHz) NMR spectra were recorded on a Varian Mercury spectrometer with tetramethylsilane (TMS) as an internal reference. Gel Permeation Chromatography (GPC) was performed using a Waters system equipped with a 515 HPLC pump, a 2410 refractive index detector, and three Styragel columns (HR1, HR3, HR4 in the effective molecular weight range of 100~5000, 500~30,000, and 5000~500,000, respectively) with HPLC grade THF as the eluent at 30 ^{o}C and a flow rate of 1.0 mL/min. THF and polymer solutions were filtered over microfilters with a pore size of 0.2 μm (Nylon, Millex-HN 13 mm Syringes Filters, Millipore, USA). The columns were calibrated against polystyrene standards. Differential scanning calorimetry (DSC) experiments were conducted on a DSC Q2000 instrument (TA instruments). The samples were heated from –70 ^{o}C to 200 ^{o}C at a rate of 10 ^{o}C/min, maintained at 200 ^{o}C for 2 min and then cooled to –70 ^{o}C at a rate of 10 ^{o}C/min. The data were collected from the second heating scan. The average

sample mass was about 5 mg, and the nitrogen flow rate was 50 mL/min. Thermogravimetric analysis (TGA) was operated on a Q5000 TGA system (TA instruments), ramping from 25 ^{o}C to 1000 ^{o}C at a rate of 10 ^{o}C/min, and maintaining at 1000 ^{o}C for 5 min under nitrogen gas at a flow rate of 20 mL/min. Contact angle test data were collected on a VCA-Optima goniometer (AST Products, Inc). Taping mode atomic force microscopy (AFM) experiments were conducted using a Multimode Nanoscope V system (Veeco, Santa Barbara, CA). The measurements were performed using Si cantilevers with a nominal spring constant and resonance frequency at 20-80 N/m and 230-410 kHz, respectively (TESP, Bruker AFM probes, Santa Barbara, CA). The height and phase images were acquired simultaneously at the set-point ratio A/A_0 = 0.9-0.95, where A and A_0 means the "tapping" and "free" cantilever amplitudes, respectively. The polymer thin films were prepared by spin-coating in DMF and thermally annealed at 150 ^{o}C under vacuum for 48 h.

Tensile stress-strain testing was performed in an Instron 5543A testing machine. The film samples were prepared by casting THF solutions of polymers on polytetrafluoroethylene substrate followed by removal of solvent at room temperature for 48 h. The films were further dried at 40^{o}C under vacuum to constant weight. Dumbbell samples with a length of 17.9 mm and width of 4.7 mm were cut from the cast films and tested at room temperature with the crosshead speed of 25 mm/min.

Tensile creep and creep recovery experiments were performed using a dynamic mechanical analyzer (TA Instruments RSAIII). The test specimens were prepared in the shape of rectangular film strips, typically ~6 mm wide and over 25 mm long. Their thickness varied from sample to sample, ranging between 0.3 mm to 1.2 mm, and the

gauge length for the testing was 15 mm. In a tensile creep and recovery test, a film specimen is subjected to a constant stress level of 0.02 MPa for 10 minutes, and the strain in response to the stress was recorded during this period. After 10 minutes, the tensile stress was released, and the strain recovery was recorded for at least another 100 minutes.

From the tensile creep and creep recovery experiments, several properties of interest can be obtained, namely the elastic creep compliance J_s^0, the extensional viscosity η_0, the relaxation time τ, and the percentage of elastic strain recovery χ. To obtain these properties, first a strain-time curve is converted into a compliance-time curve by normalizing the strain ε with the constantly applied stress level σ_0. Then the steady-state part of the compliance curve is fitted with a linear function of time. The y-intercept of fitted line gives J_s^0, while the inverse of the slope gives η_0. The relaxation time τ is calculated as the product of J_s^0 and η_0, to the first order of approximation. The recoverable compliance, J_r, is the difference between the maximum compliance (J_{max}) measured when the stress is removed, and the plateau (residual) compliance value (J_{nr}) measured at the end of the test. The percentage of elastic strain recovery is calculated as

$$\chi = [(J_{max} - J_{nr})/J_{max}] \times 100\% \qquad (1)$$

4.3.3 Synthesis

Cellulose-*g*-poly(*n*-butyl acrylate-*co*-dehydroabietic ethyl methacrylate) (Cell-*g*-P(BA-*co*-DAEMA)): Take sample BA80DAEMA20 as an example, A mixture of Cell-BiB (3.2 mg, 0.01 mmol of Br), Cu(I)Br (1.4 mg, 0.01 mmol), and dry toluene (1 mL) was introduced into a Schlenk flask and purged with nitrogen for 15 min. BA (1.03 g, 8 mmol), DAEMA (0.83 g, 2 mmol), and PMDETA (1.8 mg, 0.01 mmol) were dissolved in

2 mL dry toluene in a round bottom flask and purged with nitrogen for 15 min. Then the solution of monomers and PMDETA ligand were transferred to the Schlenk flask under nitrogen atmosphere by syringe. The reaction flask was placed into an oil bath preheated at 80 ºC for 24 hours under continuous stirring. The polymerization was stopped by diluting the reaction mixture with THF. The products were passed through a neutral alumina column and precipitated in cold methanol three times and dried to constant weight. ^{1}H NMR ($CDCl_3$, δ): 6.7-7.2 (m, aromatic protons); 3.7-4.4 (m, O*CH$_2$CH$_2$O* in PDAEMA and OC*H$_2$* in PBA); 2.6-2.8 (protons next to aromatic ring).

Cellulose-*g*-poly(lauryl methacrylate-*co*-dehydroabietic ethyl methacrylate) (Cell-*g*-P(LMA-*co*-DAEMA)): Cell-*g*-P(LMA-*co*-DAEMA) was polymerized in a similar procedure to the synthesis of Cell-*g*-P(BA-*co*-DAEMA). The polymerization temperature was set at 90 ºC. Take sample LMA70DAEMA30 as an example, Cell-BiB (3.2 mg, 0.01 mmol of Br), Cu(I)Br (1.4 mg, 0.01 mmol) were dissolved in dry toluene (1 mL) in a Schlenk flask and purged with nitrogen for 15 min. LMA (1.78 g, 7 mmol), DAEMA (1.24 g, 3 mmol), and PMDETA (1.8 mg, 0.01 mmol) were dissolved in a small rounded bottom flask by 2 mL of dry toluene and purged with nitrogen for 15 min. Then the solution of monomers and PMDETA ligand were added into the Schlenk flask under nitrogen atmosphere by syringe. After polymerization, the reaction mixture was also diluted with THF, passed through an alumina column and precipitated in cold methanol three times. The final product was dried under vacuum to constant weight. ^{1}H NMR ($CDCl_3$, δ): 6.7-7.2 (m, aromatic protons); 3.7-4.3 (m, O*CH$_2$CH$_2$O* in PDAEMA and OC*H$_2$* in PLMA); 2.6-2.8 (protons next to aromatic ring).

4.4 Results and Discussion

Synthesis of Graft Copolymers Cell-*g*-P(BA-*co*-DAEMA) and Cell-*g*-P(LMA-*co*-DAEMA): As shown in Figure 4.2, cellulose-based graft copolymers were prepared by "grafting from" ATRP using cellulose 2-bromoisobutyrylate (Cell-BiB) as macroinitiator, copper(I) bromide (CuBr) as catalyst and *N,N,N′,N′,N″*-pentamethyldiethylenetriamine (PMDETA) as ligand. Cell-BiB macroinitiator was synthesized according to previous reports (Br content: 3.17 mmol/g).[169, 182] Utilizing the Cell-BiB macroinitiator, DAEMA and BA were copolymerized in toluene with the molar ratio of [M]:[Cell-BiB]:[CuBr]:[PMDETA]=1000:1:1:1. By manipulating the feed ratio of DAEMA and BA, a series of Cell-*g*-P(BA-*co*-DAEMA) graft copolymers with various compositions were prepared (Table 4.1).

Table 4.1 Characteristics of Cell-*g*-P(BA-*co*-DAEMA) graft copolymers

Sample name[a]	[M]/[I]	PBA content (mol%)[b]	PBA content (wt%)	M_n (g/mol)[c]	PDI	T_g (°C)[d]
BA90DAEMA10	1000	88.1	69.7	54800	2.40	-15.64
BA80DAEMA20	1000	85.1	64.0	40700	3.95	0.57
BA75DAEMA25	1000	77.7	52.0	49300	1.90	14.12
BA70DAEMA30	1000	68.9	40.8	31700	3.95	16.36
BA60DAEMA40	1000	66.9	38.6	28000	3.17	41.17
BA50DAEMA50	1000	54.9	27.4	27000	3.92	59.22

[a]Sample names are defined by the feed ratio of BA/DAEMA with the numbers following BA and DAEMA representing the feed molar percentages of monomers. [b]Calculated from ^{1}H NMR spectra. [c]Measured by GPC (THF solvent). [d]Measured by DSC.

In the ^{1}H NMR spectra of Cell-*g*-P(BA-*co*-DAEMA) graft copolymers (Figure 4.3), the peaks between 5.5 and 6.5 ppm, corresponding to the vinyl protons in both

DAEMA and BA monomers, disappeared completely, indicating the success of ATRP of DAEMA and BA from the cellulose macroinitiator. The peaks at 6.8-7.2 ppm were assigned to the aromatic protons in DAEMA. The peaks in the range of 3.7 to 4.3 ppm corresponded to the methylene protons next to the ester groups in both DAEMA and BA units. The molar ratio of DAEMA/BA can be calculated using

$$\frac{Mole\ (DAEMA)}{Mole(BA)} = \frac{\frac{I_a}{3}}{\frac{I_{bc} - \frac{4}{3}I_a}{2}} \qquad (2)$$

where I_a is the integration area of aromatic protons in DAEMA moiety, and I_{bc} is the integration area of methylene protons next to the ester groups from both DAEMA and BA units. As summarized in Table 4.1, the molar ratios of DAEMA/BA in Cell-*g*-P(BA-*co*-DAEMA) are quite close to the molar feed ratios of the two monomers, indicating the similar reactivity of DAEMA and BA monomers during the polymerization.

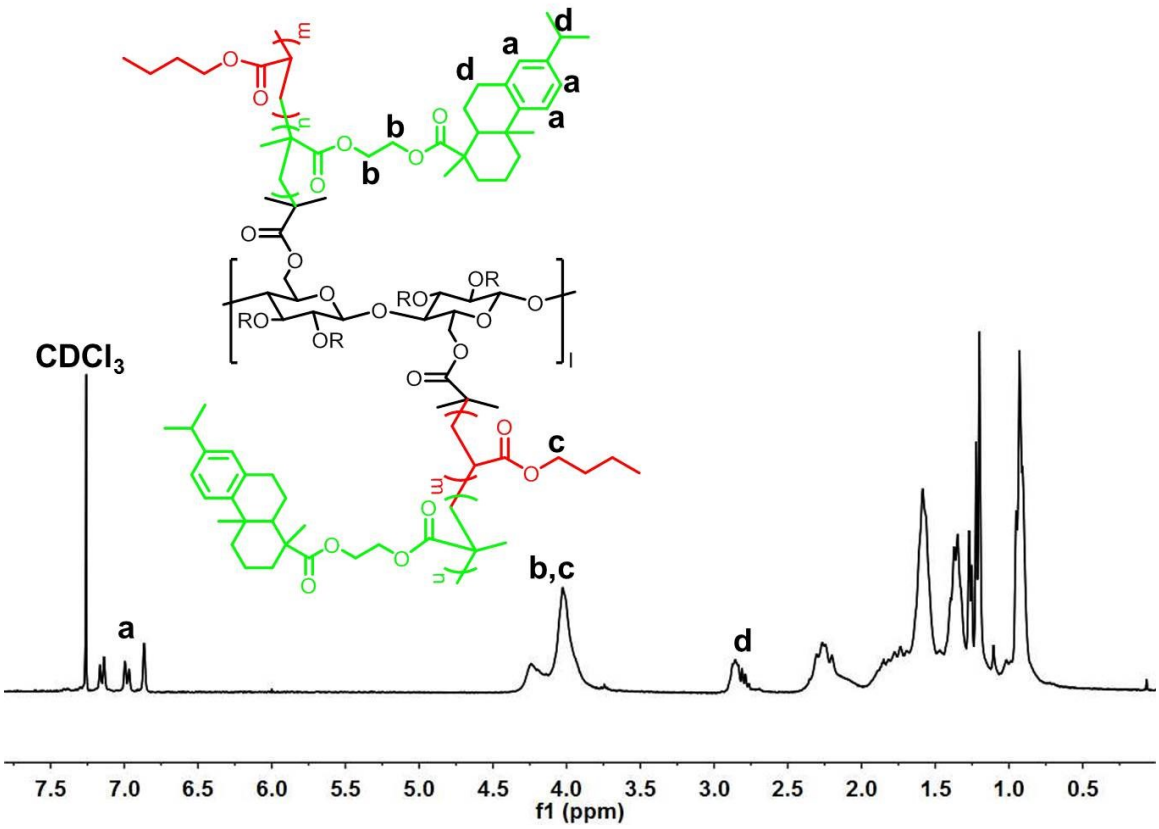

Figure 4.3 Typical ^{1}H NMR spectrum of Cell-*g*-P(BA-*co*-DAEMA), sample BA70DAEMA30

The successful synthesis of Cell-*g*-P(BA-*co*-DAEMA) by ATRP motivated us to prepare a novel, fully renewable graft copolymer, Cell-*g*-P(LMA-*co*-DAEMA), replacing the petroleum-based butyl acrylate (BA) with lauryl methacrylate (LMA) derived from natural fatty acids. Similar to the synthesis of Cell-*g*-P(BA-*co*-DAEMA), LMA and DAEMA were copolymerized using Cell-BiB as macroinitiator and CuBr/PMDETA as catalyst/ligand system. Cell-*g*-P(LMA-*co*-DAEMA) with different LMA/DAEMA compositions were prepared by controlling the feed ratio of LMA and DAEMA monomers.

Table 4.2 summarizes the characteristics of Cell-*g*-P(LMA-*co*-DAEMA).Table 4.2 Results of graft copolymers Cell-*g*-P(LMA-*co*-DAEMA)

Sample name[a]	[M]/[I]	PLMA content (mol%)[b]	PLMA content (wt%)	M_n (g/mol)[c]	PDI	T_g (°C)[d]
LMA90DAEMA10	1000	91.2	86.5	242600	2.67	-48.03
LMA80DAEMA20	1000	81.1	72.6	101100	4.35	-27.34
LMA70DAEMA30	1000	73.0	62.5	142800	3.84	-4.83
LMA65DAEMA35	1000	68.1	56.8	129900	3.71	8.60
LMA60DAEMA40	1000	61.5	49.6	83300	3.52	10.55
LMA50DAEMA50	1000	56.9	44.9	200100	4.62	27.50

[a]Sample names are defined by the feed ratio of LMA/DAEMA, the numbers behind LMA and DAEMA represent the feed molar percentages of monomers. [b]Calculated from ^{1}H NMR spectra. [c]Measured by GPC (THF solvent). [d]Measured by DSC.

Figure 4.4 shows a representative ^{1}H NMR spectrum of Cell-*g*-P(LMA-*co*-DAEMA). The disappearance of vinyl proton peaks between 5.5 and 6.5 ppm suggested the successful ATRP of LMA and DAEMA from the cellulose backbone. Comparing the spectrum in Figure 4.4 with the ^{1}H NMR spectrum of Cell-*g*-P(BA-*co*-DAEMA) in Figure 4.3, the characteristic proton peaks (aromatic protons **a** and methylene protons **b, c**) have almost same chemical shift, indicating the similar chemical structures of two graft copolymers. Due to the similar chemical structures of LMA and BA (both have methylene protons next to ester groups), the LMA molar content was also determined by equation 1. Once again, the molar content of LMA and DAEMA determined from ^{1}H NMR correlates closely with the monomers' molar feed ratio.

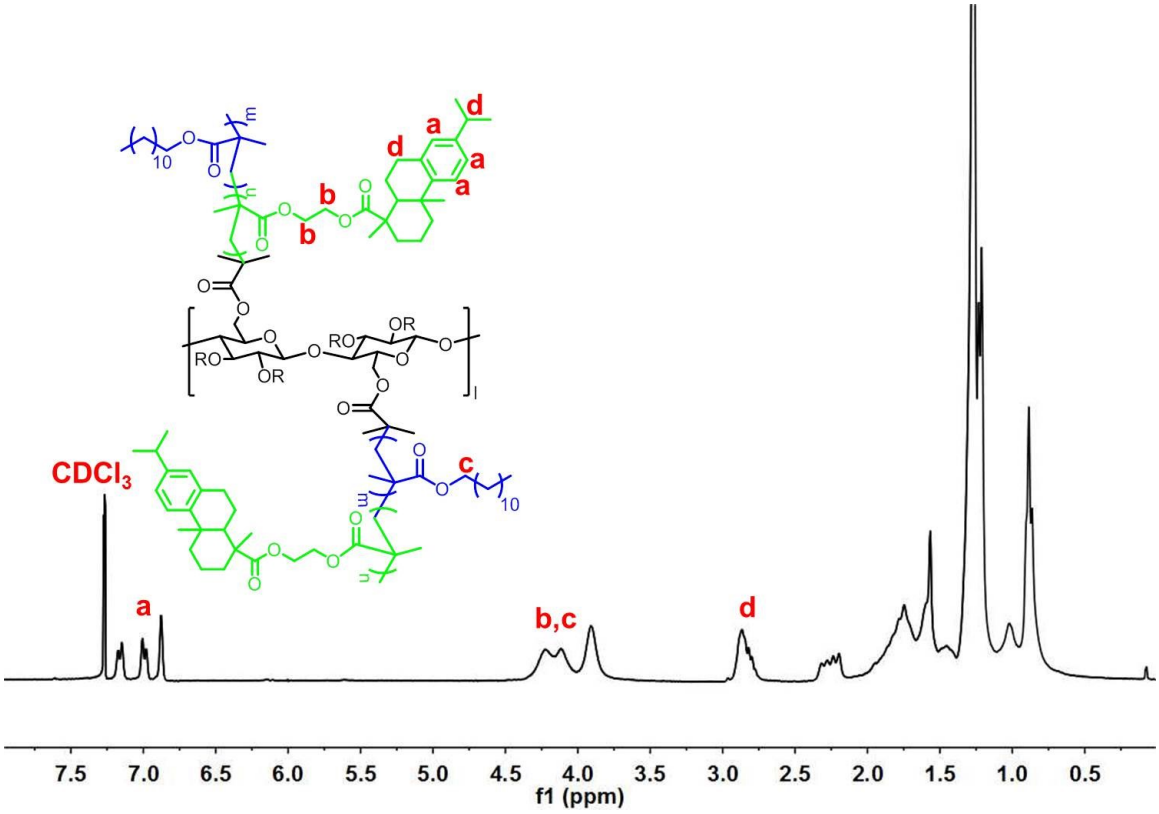

Figure 4.4 Typical ^{1}H NMR spectrum of Cell-*g*-P(LMA-*co*-DAEMA), sample LMA60DAEMA40

The molecular weights of Cell-*g*-P(BA-*co*-DAEMA) and Cell-*g*-P(LMA-*co*-DAEMA) graft copolymers were measured by GPC using THF as eluent solvent. As shown in Figure 4.5, the GPC traces of the two graft copolymers are shifted to higher molecular weight compared to the Cell-BiB macroinitiator (black curve, M_n=15500 g/mol, PDI=1.86). The molecular weight (M_n) and polydispersity index (PDI) values of the two graft copolymers are listed in Tables 4.1 and 4.2, respectively. Considering the high PDI value of cellulose macroinitiator (PDI=1.86), the high PDI values (2~4) of the graft copolymers are not surprising. Also, some of the GPC traces for the Cell-*g*-P(LMA-*co*-DAEMA) graft copolymers show bimodal shapes, indicating that ATRP of

LMA/DAEMA was less controlled compared with that of BA/DAMEA system, in which all the GPC traces showed monomodal curves.

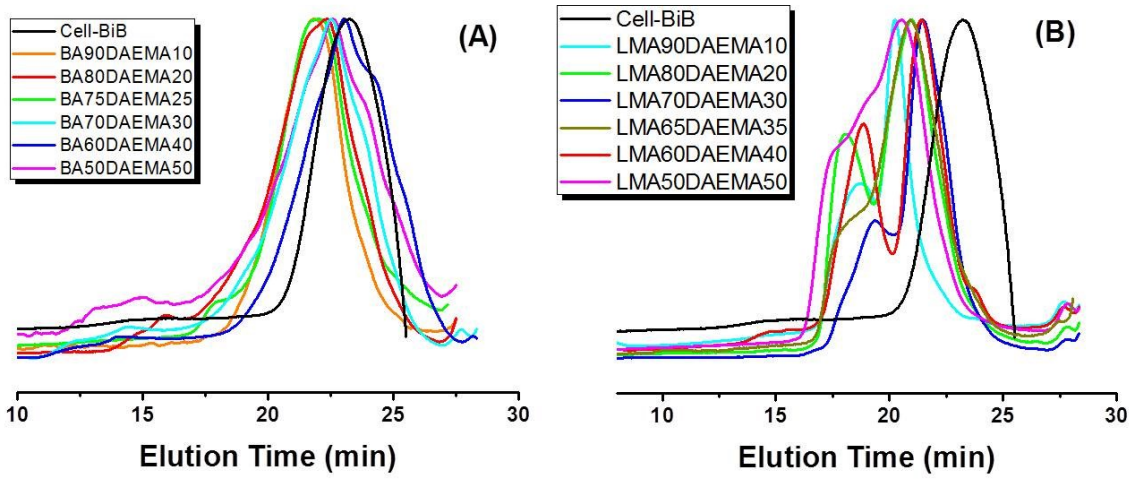

Figure 4.5 GPC traces of **(A)** Cell-*g*-P(BA-*co*-DAEMA) and **(B)** Cell-*g*-P(LMA-*co*-DAEMA) graft copolymers

Thermal Properties: Glass transition temperatures (T_g) of all graft copolymers were characterizing using differential scanning calorimetry (DSC). As shown in Figure 4.6, all DSC traces of cellulose-based graft copolymers yielded a single T_g value. The T_g values for both Cell-*g*-P(BA-*co*-DAEMA) and Cell-*g*-P(LMA-*co*-DAEMA) increased with the feed molar percentage of DAEMA. The T_g values for Cell-*g*-P(BA-*co*-DAEMA) increase from -15 ºC to 60 ºC as DAEMA feed percentage increases from 10% to 50% (Figure 4.6 (A)). The T_g values of Cell-*g*-P(LMA-*co*-DAEMA) increase from -48 ºC to 27 ºC as DAEMA feed percentage increases from 10% to 50% (Figure 4.6 (B)). The DAMEA has bulky hydrophenanthrene ring, and DAMEA homopolymer has a high T_g (~90 ºC).[134] Therefore, we expect that increasing DAEMA content in the graft copolymers leads to lower chain mobility and thus higher T_g values. Comparing the two kinds of graft

copolymers with similar DAMEA molar content, Cell-*g*-P(LMA-*co*-DAEMA) copolymers always have lower T_g values than the corresponding Cell-*g*-P(BA-*co*-DAEMA) copolymers, probably due to the longer flexible alkyl chains of LMA compared to the more compact BA monomers.

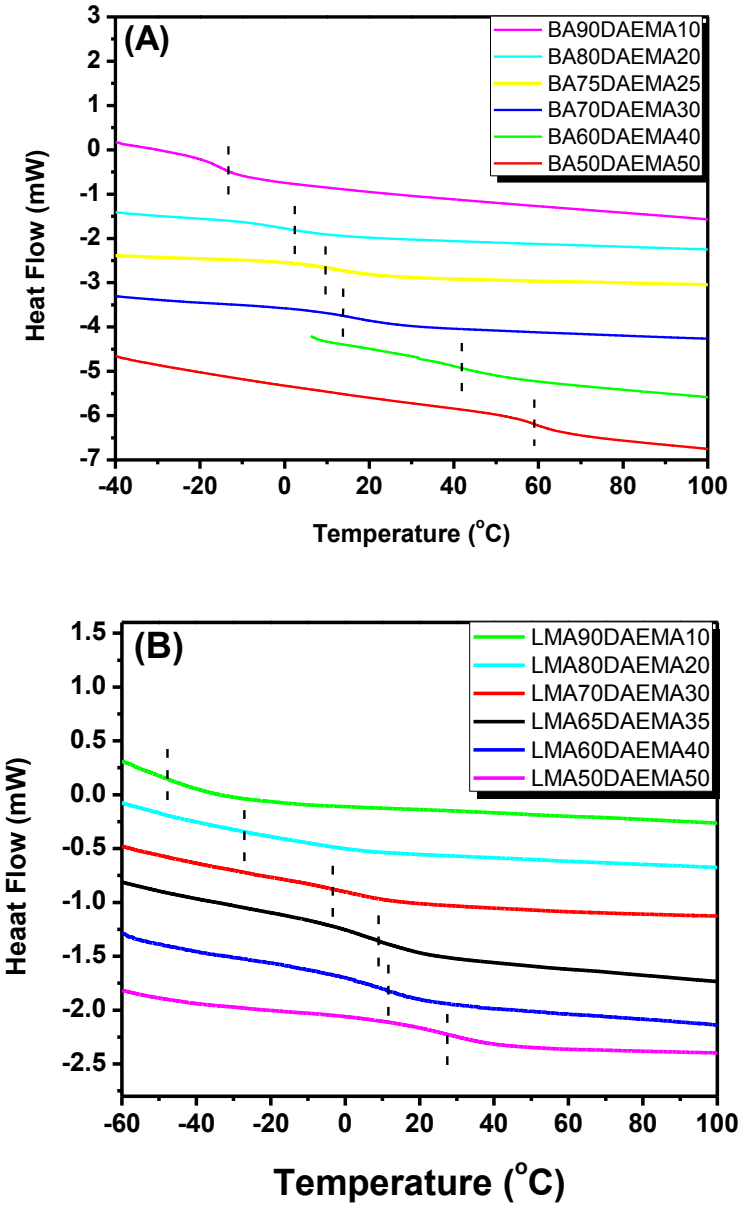

Figure 4.6 DSC curves of **(A)** Cell-*g*-P(BA-*co*-DAEMA) and **(B)** Cell-*g*-P(LMA-*co*-DAEMA)**.** In each plot, the DAEMA mole percent values increase for curves ordered from top to bottom

The thermal stability of Cell-*g*-P(BA-*co*-DAEMA) and Cell-*g*-P(LMA-*co*-DAEMA) graft copolymers was studied by thermal gravimetric analysis (TGA). The cellulose macroinitiator exhibited a weight loss with onset temperature at ~250°C. After incorporating P(BA-*co*-DAEMA) side chains, all of the TGA curves for Cell-*g*-P(BA-*co*-DAEMA) showed increased onset decomposition temperatures of ~370°C, independent of the DAEMA molar content. For Cell-*g*-P(LMA-*co*-DAEMA) graft copolymers, the onset decomposition temperatures are all greater than that of Cell-BiB and generally increase (from ~250 to ~325°C) with DAEMA molar content. The increasing thermal stability of Cell-*g*-P(LMA-*co*-DAEMA) with increasing DAEMA content can be explained by the higher thermal stability of DAEMA's hydrophenanthrene moiety, which compensates for the lower thermal stability of LMA. However, the graft copolymers containing LMA are less thermally stable than the corresponding copolymers containing BA.

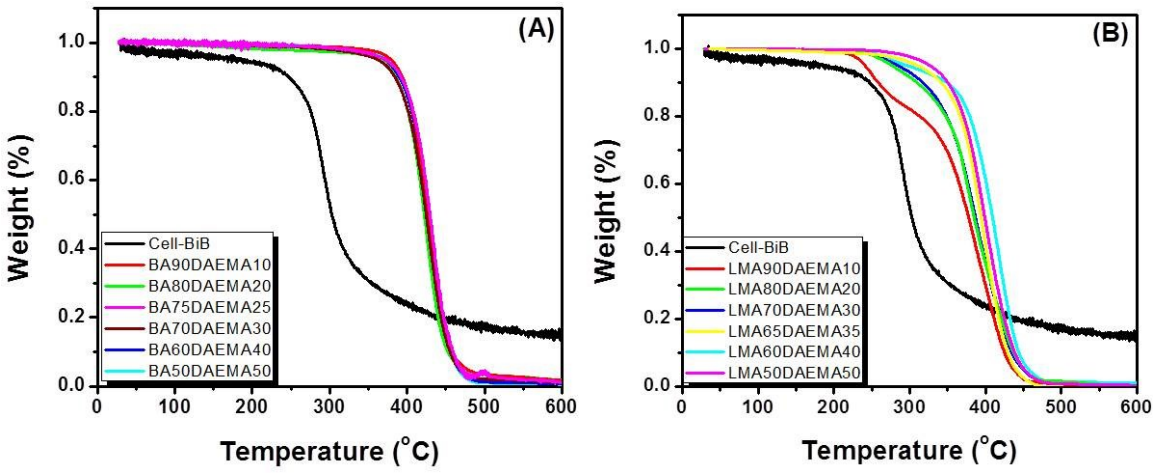

Figure 4.7 TGA curves of **(A)** Cell-*g*-P(BA-*co*-DAEMA) and **(B)** Cell-*g*-P(LMA-*co*-DAEMA) graft copolymers

Mechanical Properties: Mechanical properties of Cell-*g*-P(BA-*co*-DAEMA) and Cell-*g*-P(LMA-*co*-DAEMA) graft copolymers were characterized by tensile stress-strain and creep compliance testing. Considering the Cell-*g*-P(BA-*co*-DAEMA) graft copolymers, sample BA90DAEMA10 forms tacky films at room temperature that are more liquid-like than elastic due to the high BA content and low T_g, making them unsuitable for tensile testing. Samples BA60DAEMA40 and BA50DAEMA50 are too brittle to form films for tensile testing: the relatively high T_g of graft copolymers with high DAEMA content makes these materials glassy at room temperature and prone to fracture when handled.

Figure 4.8(A) shows tensile stress-strain curves for Cell-*g*-P(BA-*co*-DAEMA) copolymers with intermediate DAEMA content. All three samples show failure strains greater than 500%. Sample BA80DAEMA20 did not fail, but underwent continuous elongation to a strain of 2500%, with the tensile stress never exceeding 0.5 MPa. Cell-*g*-P(BA-*co*-DAEMA) copolymers with 25 and 30% DAEMA content behaved differently, showing sharp increases in stress at low strain followed by ductile yielding and elasto-plastic deformation up to failure. The yield stresses in these copolymers are greater than 1.5 MPa. The T_g values for these samples (Figure 4.6(A)) are about 10-20°C below ambient temperature. These observations suggest an optimal DAEMA content between 25 and 40 mol% leads to graft copolymers with a suitable balance between side-chain attraction (imparting elastic character and ability to support tensile stress) and chain disentanglement (enabling large strain deformation and postponing failure to higher strains). These properties can be tuned by varying the DAEMA content.

Figure 4.8(B) shows tensile stress-strain results for Cell-*g*-P(LMA-*co*-DAEMA) graft copolymers. The copolymers with the lowest and highest DAEMA contents (10-

20% and 50%, respectively) gave films that were too liquid-like or too brittle to form good films for tensile testing. Again, the optimal DAEMA content seems to be in the 25-45% range, yielding copolymers with T_g values 10-30°C below ambient temperature. The three samples with intermediate DAEMA content (30, 35, and 40%) all showed steep stress increases at low strain, ductile yielding, and elasto-plastic deformation to large failure strains (>500%). As DAEMA content increases, the failure strain decreases, but the failure tensile stress increases. The tensile strengths of the Cell-*g*-P(LMA-*co*-DAEMA) graft copolymers were generally less than those of the Cell-*g*-P(BA-*co*-DAEMA) copolymers. This suggests that the long-chain LMA monomers disrupt the side chain attraction of the DAEMA monomers, thus reducing the ability of the LMA-containing copolymers to sustain tensile stress.

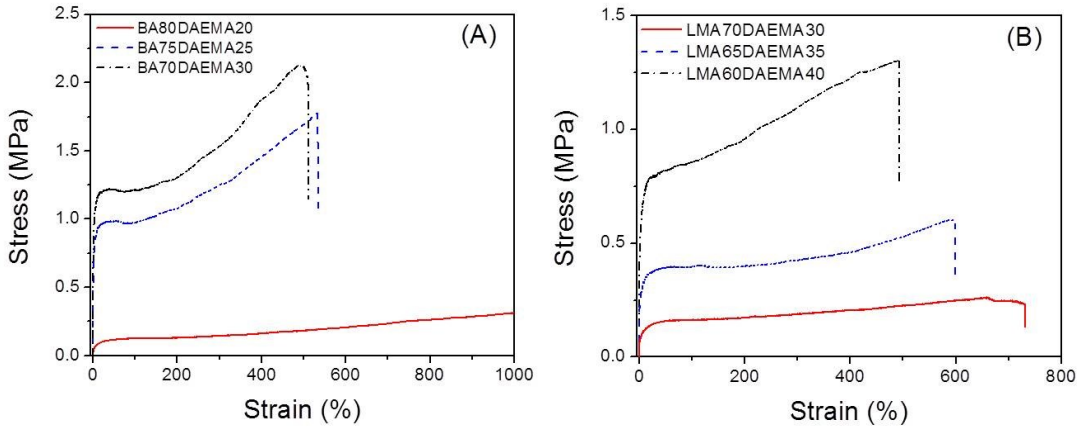

Figure 4.8 Stress-strain curves for (A) Cell-*g*-P(BA-*co*-DAEMA) and (B) Cell-*g*-P(LMA-*co*-DAEMA) graft copolymers with different monomer feed ratios

Considering the tensile stress-strain data at small strains (not shown here), none of the graft copolymers show linear elastic behavior above about 1% strain. Recognizing the limited range of linear elasticity in these materials, we still equate the initial stress-strain slope with the Young's modulus. For Cell-*g*-P(BA-*co*-DAEMA) copolymers

containing 20, 25, and 30 mol% DAEMA (Figure 4.9(A)), the corresponding Young's modulus values are 8.9, 71, and 99 MPa. For Cell-*g*-P(LMA-*co*-DAEMA), the Young's modulus values are 20, 56, and 58 MPA for copolymers with 30, 40, and 45 mol% DAEMA, respectively. The apparent Young's moduli of these graft copolymers definitely increase with DAEMA content. However, the elastic properties of these cellulose-based graft copolymers differ from those of first-generation ABA triblock copolymers, which manifest linear elasticity up to significantly larger strains.[183]

Creep compliance equals the time-dependent strain divided by the constant applied stress.[184] Figure 4.9 shows the results for creep compliance under applied tensile stress (left-hand plots with increasing compliance) as well as creep recovery after stress removal (right-hand plots with decreasing compliance), both plotted as compliance vs. time curves. The linearity of the creep compliance data between t = 5 and 10 min indicates that steady-state creep was attained in all of the samples. The y-intercept and slope of the steady state creep compliance vs. time yields the elastic compliance J_s^0, the extensional viscosity η_0, and their product, the relaxation time τ. Upon removal of the tensile stresses, all of the creep recovery curves reached plateau compliance values by the end of the recovery period. The Experimental section describes the computation of the elastic strain recovery from the maximum and plateau residual compliances. The values of J_s^0, η_0, τ, and χ for all samples are summarized in Table 4.3.

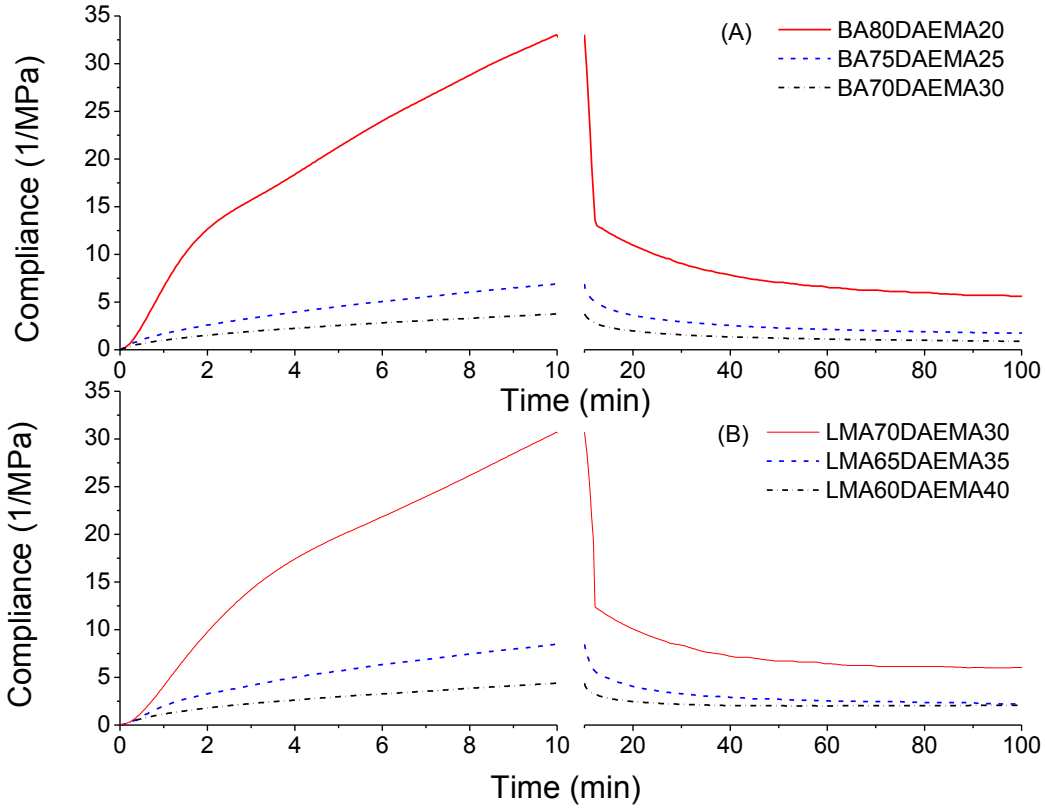

Figure 4.9 (A) Creep compliance and recovery curves for (A) Cell-*g*-P(BA-*co*-DAEMA) and (B) Cell-*g*-P(LMA-*co*-DAEMA) graft copolymers with different monomers feed ratios

Table 4.3 Copolymer properties obtained from creep recovery tests

Sample	J_s^0 (MPa^{-1})	η_0 (MPa·s)	τ (min)	χ(%)
BA80DAEMA20	9.892	25.7	4.23	83.4
BA75DAEMA25	2.201	126.3	4.63	73.9
BA70DAEMA30	1.376	250.4	5.74	78.9
LMA70DAEMA30	8.621	27.2	3.90	80.5
LMA65DAEMA35	2.988	108.3	5.40	71.8
LMA60DAEMA40	1.554	210.2	5.44	53.6

These results show that for both sets of graft copolymers, J_s^0 decreases and η_0 increases with increasing DAEMA content. Values of $1/J_s^0$ (units of MPa), representing the materials' elastic character, increase with DAEMA content. Thus as DAEMA molar

fraction increases, the copolymer has increasing elastic character as well as higher extensional viscosity, or resistance to creep. Although the relaxation time increases slightly with DAEMA content, the value of τ is between 4 and 6 min for all of the copolymers. The magnitude of the relaxation time may be controlled by the dynamics of the long-range deformation of the Cell-BiB main chain during creep, with a secondary effect of increasing side-chain attraction as DAEMA molar content increases.

The samples deformed substantially during the creep testing, with some samples showing tensile strains as large as 65%. Upon removal of the tensile stresses, all of the graft copolymers showed elastic strain recovery values between 50% and 85% (see Table 4.3), indicative of rubber-like elasticity. For Cell-*g*-P(LMA-*co*-DAEMA) graft copolymers, the elastic recovery clearly increased with LMA content, perhaps due to the increased molecular mobility of the monomer's long alkyl chains. For Cell-*g*-P(BA-*co*-DAEMA) graft copolymers, the dependence of χ on BA content is not clear, but all of these copolymers have relatively high values of elastic recovery.

Overall, the mechanical property results demonstrate that by changing the DAEMA content, the room temperature viscoelastic behavior of these graft copolymers can be changed significantly. Increasing DAEMA content may increase the strength of side-chain attraction, resulting in greater tensile strength, toughness, extensional viscosity, and resistance to creep. All of the graft copolymers undergo elasto-plastic deformation to large strain deformation (500% or more) before experiencing failure. Creep recovery tests show that all of these graft copolymers have large elastic strain recovery after undergoing large tensile strains.

Hydrophobicity and Morphology: DAEMA monomer has hydrocarbon-based hydrophenanthrene structure, which can increase the hydrophobicity of attached polymers, as demonstrated in prior reports.[185] Thus Cell-*g*-P(BA-*co*-DAEMA) and Cell-*g*-P(LMA-*co*-DAEMA) graft copolymers with DAEMA units in the side chains are expected to be more hydrophobic than the starting Cell-BiB macroinitiator. Contact angle measurements were employed to characterize the hydrophobicity of cellulose-based graft copolymers and the Cell-BIB macroinitiator. The polymers in THF solution were spin-cast on glass substrates to give polymer thin films for contact angle measurement. Five different spots on each film sample were tested and an average contact angle was obtained. Figure 4.10(A) shows the contact angle values of water drops on graft copolymer films versus the DAEMA molar content. Figure 4.10(B) shows images of water droplet on the films of Cell-BiB, Cell-*g*-P(BA-*co*-DAEMA) and Cell-*g*-P(LMA-*co*-DAEMA). Compared with Cell-BiB macroinitiator (contact angle: ~77^{o}), both Cell-*g*-P(BA-*co*-DAEMA) and Cell-*g*-P(LMA-*co*-DAEMA) graft copolymers have higher contact angles, ranging from 89^{o} to 105^{o}, indicating that DAEMA increases the hydrophobicity of the graft copolymers. The DAEMA content in the graft copolymers appears to have little effect on the contact angle. A possible reason may be that the hydrophobic hydrophenanthrene moieties prefer to stay on the surface of films, a result seen in earlier studies of lignin-rosin composites.[186]

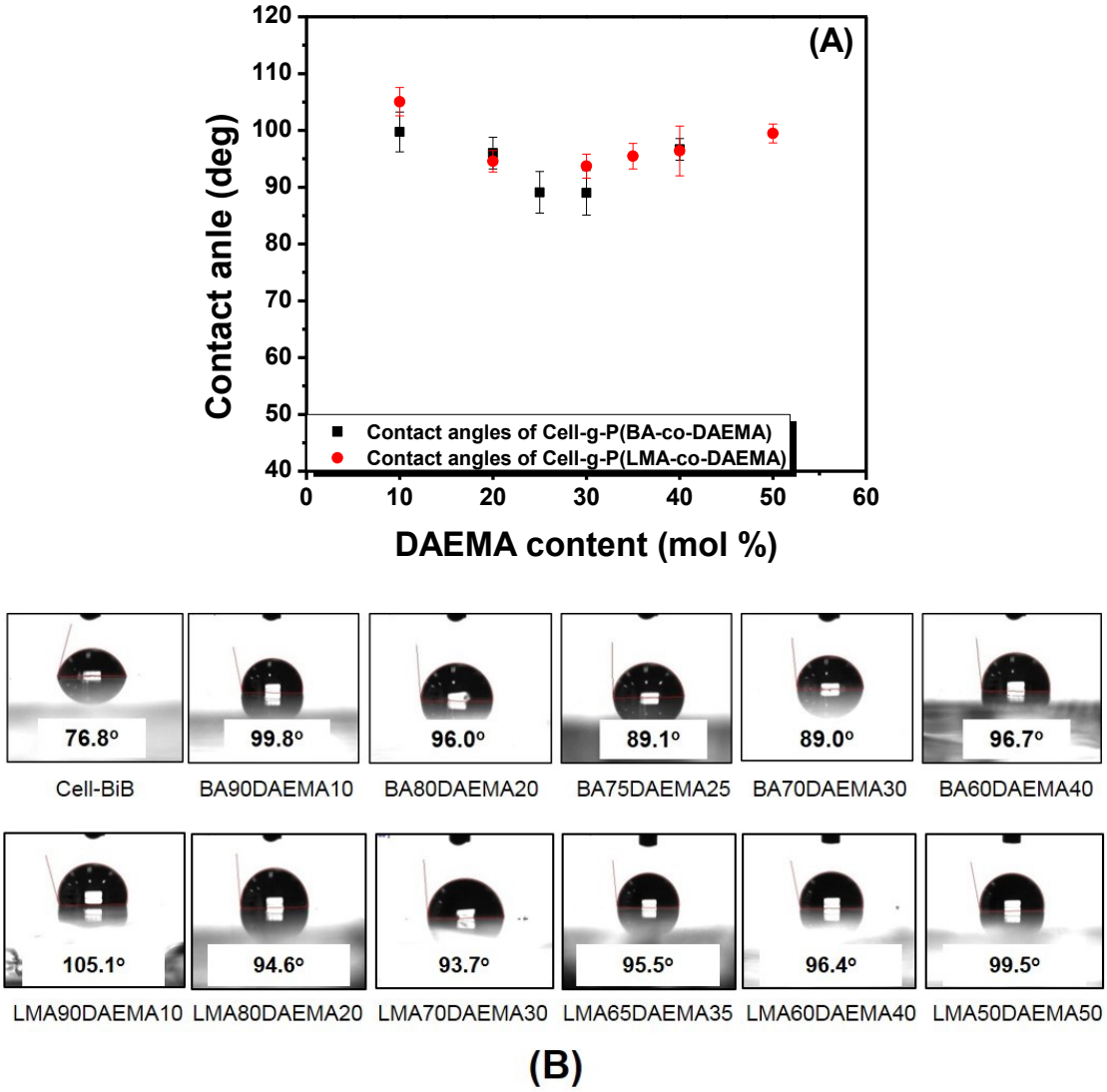

Figure 4.10 (A) Plot of contact angles of Cell-*g*-P(BA-*co*-DAEMA) and Cell-*g*-P(LMA-*co*-DAEMA) against DAEMA content. (B) Images of water droplets on the films of Cell-BiB, Cell-*g*-P(BA-*co*-DAEMA) and Cell-*g*-P(LMA-*co*-DAEMA)

Atomic force microscopy (AFM) was employed to image the surface morphologies of Cell-*g*-P(BA-*co*-DAEMA) and Cell-*g*-P(LMA-*co*-DAEMA) copolymers. As shown in Figure 4.11, the phase images of both Cell-*g*-P(BA-*co*-DAEMA) and Cell-*g*-P(LMA-*co*-DAEMA) copolymers exhibited homogeneous morphologies with no observed microphase separation. There are two possible scenarios

here. First, the graft copolymers may be a truly homogeneous system. Second, given the rigidity of cellulose and PDAEMA chains, if phase-separated, may be embedded in a rubbery matrix of PBA or PLMA, with only the homogeneous matrix observed on the surface.

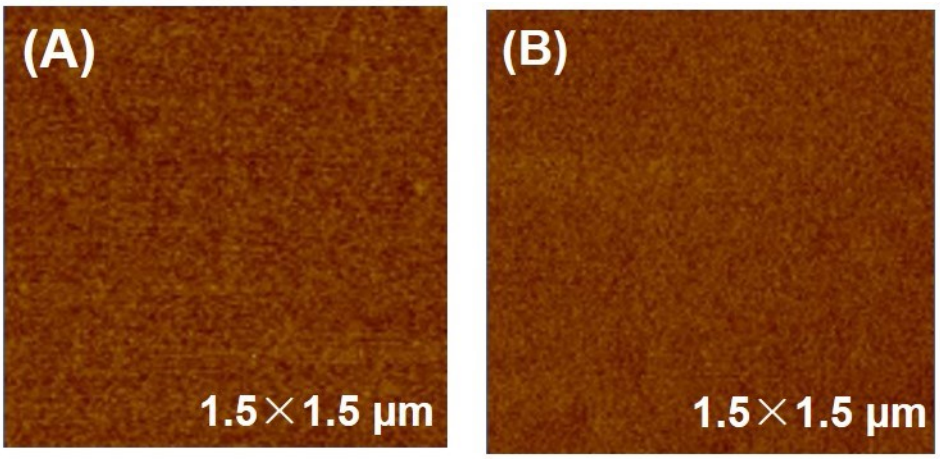

Figure 4.11 (A) AFM phase image of Cell-*g*-P(BA-*co*-DAEMA) film annealed at 150 ºC (sample: BA80DAEMA20). (B) AFM phase image of Cell-*g*-P(LMA-*co*-DAEMA) film annealed at 150 ºC (sample: LMA70DAEMA30)

In the classic TPE triblock copolymer system, the soft polymer chains should form a matrix with the rigid segments dispersed as well-ordered minority domains.[163, 183] However in our case, the rigid cellulose backbone is less than 1 wt % of the entire graft copolymer. The soft PBA or PLMA segment is a majority component with another rigid PDAEMA as a minority component. This particular system could be very similar to our early report on the Cell-*g*-P(BA-*co*-MMA).[169] The mechanical properties are largely dictated by the DAEMA content in the graft copolymers. Physical cross-links are mostly likely originated from both DAEMA and cellulose, which could form separated glassy domains of DAEMA and aggregated cellulose domains. When the sample is stretched, the initial deformation is attributed to soft BA or LMA chain in the side chains. When the stretching increases, the physical cross-linked DAEMA and cellulose chains start to take

the higher stress transmitted from soft matrix. Particularly in the graft architecture, the cellulose chains are stretched for taking higher stress.

4.5 Conclusions

In conclusion, we prepared two graft copolymers Cell-*g*-P(BA-*co*-DAEMA) and Cell-*g*-P(LMA-*co*-DAEMA) with cellulose as backbone and rosin derivative as side chains via "grafting from" ATRP. By adjusting the DAEMA content, high molecular weight graft copolymers with various T_g were obtained. These graft copolymers exhibited good elastomeric properties, excellent hydrophobicity, and good thermal stability, which were confirmed by mechanical property tests, contact angle measurements, and TGA, respectively. Given the fact that cellulose, DAEMA, and LMA are all sourced from renewable natural resources, we anticipate that these renewable polymeric materials with graft copolymer architecture may be attractive as potential candidates for use as next-generation thermoplastic elastomer materials. These materials may be able to replace TPEs in some applications which can tolerate some amount of creep, as long as the elastic properties and tensile strength at large deformation can be further improved.

CHAPTER 5

DEGRADABLE AND SALT-RESPONSIVE RANDOM COPOLYMERS[4]

[4] K. Yao, C. Tang, J. Zhang, and C. Bunyard. *Polymer Chemistry* **2013,** *4* (3), 528-535. Reproduced by permission of the Royal Society of Chemistry

5.1 ABSTRACT

We report a new class of degradable stimuli-responsive random copolymers that exhibit high sensitivity to salt concentrations. Cationic random copolymers, poly(ε-caprolactone)-*co*-poly(ε-caprolactone-*graft*-quaternary ammonium) (PCL-*co*-P(CL-*g*-QA)), were synthesized by a combination of ring-opening polymerization and copper-catalyzed click chemistry. Random copolymers with various compositions of QA were prepared by adjusting the ratio of CL and substituted CL. Due to the presence of cationic QA groups at the polymer side chain, these random copolymers showed salt concentration (or ionic strength)-dependent solubility. In salt-free water or water with low salt (NaCl, $CaCl_2$) concentrations, random copolymers were soluble due to the overwhelming domination of electrostatic repulsion interactions between cationic QA species over attractive hydrophobic interactions between CL segments. The solubility of copolymers decreased with the increase of salt concentrations due to the screening effect of salts to shield the repulsion interactions QA species and thus significant change of macromolecular conformations. It was found that the salt responsiveness of synthesized random copolymers was maximized when the CL-*g*-QA fraction was ~ 15% in the copolymers. These random copolymers were readily degradable in diluted acidic conditions.

5.2 Introduction

Stimuli-responsive polymers, which, by definition, have capability to respond to external or internal stimuli, have drawn much attention due to their potential applications in a variety of areas such as drug delivery, tissue engineering and sensors.[53-63] Stimuli-responsive polymers can be classified into different categories according to their response

to pH, temperature, redox-potential, light, etc.[187-196] Among various stimuli-responsive polymers, pH and temperature-responsive polymers are mostly studied. Polyacids (i.e. poly(acrylic acid)) and polybases (i.e. poly(2-(dimethylamino)ethyl methacrylate)) are two major classes of pH-responsive polymers.[64, 65] Solubility and macromolecular conformations of these polymers can be altered in aqueous solution by adjusting pH values. A rich array of block or graft copolymers containing pH-responsive segments have been synthesized and their micellization behaviours have been well studied for potential applications in biomedical fields.[66-69, 185] Temperature-responsive polymers, on the other hand, require fundamentally different chemical structures and compositions of macromolecular skeleton or pendant group.[197, 198] The most well-studied temperature-responsive polymer is poly(*N*-isopropylacrylamide) (PNIPAM).[70-73] PNIPAM has a lower critical solution temperature (LCST) at ~ 32 ^{o}C, above or below which the polymer chain has a significant conformational change, resulting in drastic abruption in solubility. Since the LCST of PNIPAM is close to the temperature of human body, a lot of copolymer systems containing PNIPAM blocks have been prepared to investigate their possible applications in drug delivery.[74, 75, 199]

In order to broaden the applications of stimuli-responsive polymers, there are enormous efforts to design and synthesize novel stimuli-responsive polymers, which can respond to other stimuli. Salt-responsive polymers are usually ionic polymers containing charged groups. They exhibit varied solubility in aqueous solution depending on the salt concentration (or ionic strength). Liu *et al.* reported salt-responsive micellization behaviour based on a double hydrophilic sulfobetaine block copolymer.[200] They observed purely salt-induced formation/dissociation of core/shell micelles and the structural

inversion. Pedersen and co-workers synthesized an ionic triblock copolymer composed of methoxy poly(ethylene glycol)), PNIPAM, and poly((3-acrylamidopropyl) trimethyl ammonium chloride) and studied its temperature/salt-responsive property.[201] The repulsive interchain interactions originating from the charged quaternary ammonium block were observed in salt-free aqueous solution, and then vanished when the salt concentration of solution increased. McCormick *et al*. reported pH/salt-responsive property of block copolymer of poly(sodium 2-acrylamido-2-methyl-1-propanesulfonate-block-*N*-acryloyl-L-alanine) with the formation of shell crosslinked micelles.[202] Overall, most early reports of salt-responsive polymers were focused on the synthesis and micellization of block copolymers. Salt-responsive polymers with other molecular architectures were much less explored.

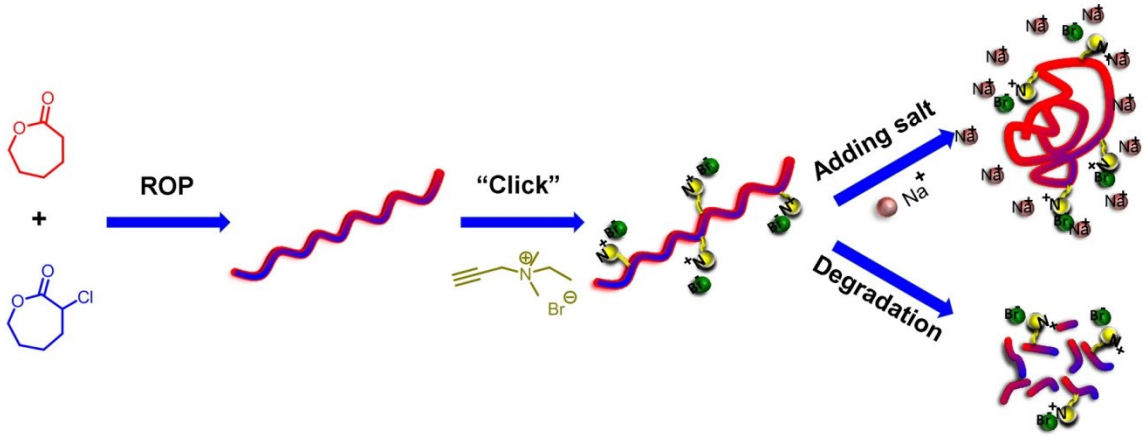

Figure 5.1 Degradable salt-responsive cationic random copolymers

Herein we report a new class of salt-responsive cationic random copolymers that are based on poly(ε-caprolactone)-*co*-poly(ε-caprolactone-*graft*-quaternary ammonium) (PCL-*co*-P(CL-*g*-QA)). These random copolymers were prepared by a combination of ring-opening polymerization (ROP) and click chemistry.[92, 136, 137] Compared to other salt-responsive polymers, PCL-*co*-P(CL-*g*-QA) copolymers have two distinct advantages. First, the salt-responsive unit is randomly distributed along the polymer chain instead of

an entire segment, thus providing different molecular conformation when interacting with salts. Second, the presence of PCL skeleton renders its degradability, while most other salt-responsive polymers are non-degradable. The biodegradability of PCL enables it for many applications especially in the biomedical field.[134, 203-206] These novel degradable salt-responsive random copolymers showed distinctive salt-responsive property and degradability. In aqueous solutions with low salt concentrations, these cationic random copolymers are soluble, while they become much less soluble when more salts are added to the solution. Our preliminary results showed that these random copolymers exhibited excellent degradation in diluted acidic media (Figure 5. 1).[207, 208]

It is worth mentioning that one of our particular motivations on the study of these random copolymers is their potential applications in personal hygiene products such as wet tissues, which usually consist of a coherent fibrous web and a binder composition.[76-78] Salt-responsive ionic polymers are considered to be appropriate as binder compositions, with most work reported in patents lacking of sufficient detail.[209, 210] The fundamental design is as follows: In the wet state with higher salt concentration, the ionic charges of polymers are screened by salts and consequently the polymer chains are insoluble in water, therefore holding the fibrous web together to provide strength. On the other hand, due to electrostatic repulsions, these polymers become soluble in water with lower salt concentration, thus can be flushed away. The addition of degradability into these compositions would make them environmentally friendly.

5.3 Experimental Section

5.3.1 Materials

Toluene and tetrahydrofuran (THF) were refluxed with sodium and distilled under a nitrogen atmosphere just before use. 2-Chlorocyclohexanone, *m*-chloroperoxybenzoic acid (mCPBA), Sn(II) 2-ethylhexanoate ($Sn(Oct)_2$), 4-*tert*-butylbenzyl alcohol, dichloromethane (CH_2Cl_2), *N,N*-dimethylformamide (DMF), methanol, diethyl ether, sodium azide, copper iodine, 1-bromoethane, 3-dimethylamion-1-propyne, and 1,8-diazabicyclo [5.4.0]undec-7-ene (DBU) were purchased from Sigma-Aldrich and used as received. ε-Caprolactone was dried over calcium hydride and purified by vacuum distillation before polymerization. α-Chloro-ε-caprolactone (αClεCL) were prepared according to early work.[136, 185]

5.3.2 Characterization

^1H (300 MHz) NMR spectra were recorded on a Varian Mercury spectrometer with tetramethylsilane (TMS) as an internal reference. Fourier Transform Infrared Spectrometry (FTIR) spectra were recorded on a PerkinElmer spectrum 100 FTIR spectrometer. Gel Permeation Chromatography (GPC) was performed at 50 ^oC on a Varian system equipped with a Varian 356-LC refractive index detector and a Prostar 210 pump. The columns were STYRAGEL HR1, HR2 (300×7.5 mm) from Waters. HPLC grade DMF was used as eluent at a flow rate of 1 mL/min. DMF and polymer solutions were filtered over microfilters with a pore size of 0.2 μm (Nylon, Millex-HN 13 mm Syringes Filters, Millipore, USA). The columns were calibrated against polystyrene standards. Optical turbidity (at 818 nm) of random copolymers in aqueous solution was measured using a UV-visible spectrophotometer (UV-2450, SHIMADZU) at room

temperature. The samples were placed in 1 cm path length quartz cells, and de-ionized water was used as control.

5.3.3 Synthesis

Synthesis of propargyl quaternary ammonium salt: 3-Dimethylamino-1-propyne (5.00 g, 60.1 mmol) was added in a round bottom flask containing 20 mL THF, followed by the addition of 1-bromoethane (7.90 g, 72.2 mmol). The reaction mixture was stirred at 35 ºC for 2 days.[138] Then the solvent and excess bromoethane were evaporated. The mixture was washed with diethyl ether three times to remove unreacted 3-dimethylamion-1-propyne. The quaternary ammonium salt was finally dried in vacuum. ^{1}H NMR (methanol-d_4) δ: 4.35 (m, 2H, CH_2N$^+$); 3.55 (q, 2H, N$^+$CH_2CH$_3$); 3.30 (m, 1H, CH≡C); 3.15 (s, 6H, N$^+$CH_3); 1.40 (t, 3H, N$^+$CH$_2$CH_3).

Synthesis of random copolymer of ε-caprolactone and α-chloro-ε-caprolactone (PCL-*co*-P(αClεCL)): αClεCL and εCL were dried by azeotropic distillation of toluene before polymerization. *α*-Chloro-*ε*-caprolactone (0.59 g, 4.0 mmol), ε-caprolactone (1.82 g, 16.0 mmol), 4-*tert*-butylbenzyl alcohol (0.033 g, 0.2 mmol) were added into a Schlenk flask followed by the addition of 1.0 mL dry toluene. The flask was tightly sealed and purged with nitrogen for 10 min. Then Sn(Oct)$_2$ (0.008 g, 0.02 mmol) was added into the flask under nitrogen atmosphere. The reaction flask was placed into an oil bath preheated at 120 ºC for 24 hours under continuous stirring. After the polymerization, the solution was diluted with dichloromethane and then precipitated in excess cold methanol. The final copolymer was recovered by centrifuge and dried at room temperature in a vacuum oven. The copolymer was characterized by ^{1}H NMR and GPC. The conversion of monomers was nearly 100% according to ^{1}H NMR analysis. ^{1}H NMR ($CDCl_3$) δ: 4.3-

4.21 (m, -C*H*ClCO-); 4.21-4.13 (m, -OCH_2- in P(αClεCL)); 4.12-4.0 (m, -OCH_2- in PCL); 2.40-2.20 (m, -CH_2CO-); 1.80-1.30 (broad, -CH_2CH_2CH_2-).

Synthesis of PCL-*co*-P(αN3εCL): PCL-*co*-P(αClεCL) (1.50 g, 2.3 mmol of αClεCL) was dissolved in 10 mL dry DMF in a round bottom flask. NaN_3 (0.75 g, 11.5 mmol) was then added and the mixture was stirred at room temperature overnight. After the reaction, DMF was evaporated under reduced pressure and then 10 mL toluene was added. The insoluble salt was removed by centrifuge. Finally the copolymer was recovered by evaporation of the solvent. ^{1}H NMR ($CDCl_3$) δ: 4.21-4.13 (m, -OCH_2- in P(αN_3εCL)); 4.12-4.0 (m, -OCH_2- in PCL); 3.85-3.78 (m, -C*H*N_3CO-); 2.40-2.20 (m, -CH_2CO-); 1.80-1.30 (broad, -CH_2CH_2CH_2-).

Synthesis of PCL-*co*-P(CL-*g*-QA) by click reaction: PCL-*co*-P(αN_3εCL) (1.00 g, 1.6 mmol of αN_3εCL), propargyl quaternary ammonium salt (0.35 g, 1.8 mmol), and CuI (0.031 g, 0.16 mmol) were dissolved in mixed DMF/THF (*v/v*:50/50) in a Schlenk flask and purged with nitrogen for 10 min. DBU (0.025 g, 0.16 mmol) was dissolved in deoxygenated THF and transferred to the flask. The solution was stirred at 35 ºC overnight. After the reaction, the mixture solution was diluted with THF and passed through a neutral aluminum oxide column to remove the copper catalyst and then precipitated in cold diethyl ether. The crude product was then dissolved in water and dialyzed against deionized water for 6 hours. The copolymer was finally recovered by freeze-drying. ^{1}H NMR (DMSO-d_6) δ: 8.60 (s, C*H*=C, triazole); 5.70-5.45 (m, triazole-C*H*-CO); 4.75-4.70 (s, triazole-CH_2-N^+); 4.15-4.05 (m, -OCH_2- in triazole-containing unit); 4.05-3.95 (m, -OCH_2- in PCL); 3.05-2.95 (m, N^+CH_3); 2.40-2.20 (m, -CH_2CO-); 1.75-1.20 (m, -CH_2CH_2CH_2-, N^+CH_2CH_3).

5.3.4 Degradation test of random copolymers

Random copolymer was first dissolved in THF to give a polymer solution with 10 mg/mL concentration. Then 0.15 M $HCl_{(aq)}$ was added to the polymer solution and the mixture was stirred at room temperature overnight. Then the solvent was evaporated and degradation product was dried in vacuum.

Table 5.1 Molecular weight information of PCL-*co*-P(αClεCL)

Entry	$f_{\alpha Cl\varepsilon CL}(\%)^a$	$F_{\alpha Cl\varepsilon CL}(\%)^b$	$M_{n,NMR}$(g/mol)	$M_{n,GPC}$(g/mol)	M_w/M_n (GPC)
1	10	8.9	11700	9400	1.41
2	15	15.3	11900	8900	1.32
3	20	19.2	12100	10800	1.37
4	30	28.2	12400	8500	1.35
5	50	47.6	13000	5400	1.53

[a] molar composition of monomer feed ratio. [b] molar composition of copolymers determined by ^{1}H NMR.

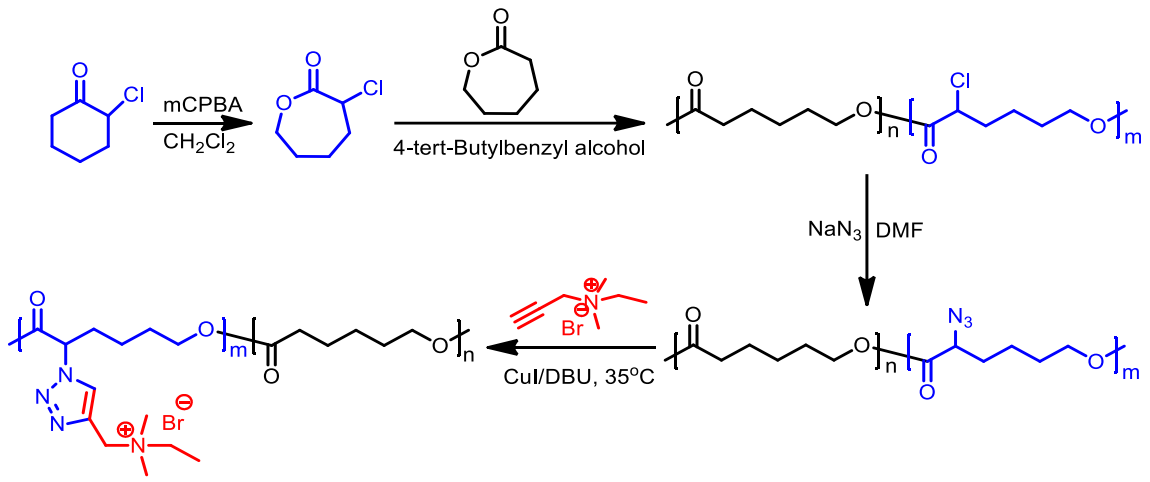

Figure 5.2 Preparation of random copolymers of caprolactone and quaternary ammonium substituted caprolactone

5.4 Results and Discussion

Preparation of cationic random copolymers PCL-*co*-P(CL-*g*-QA): "Click" type copper-catalyzed Huisgen cycloaddition reaction was used to prepare cationic random copolymers by mixing two precursors, random copolymer PCL-*co*-P(αN$_3$εCL) and propargyl quaternary ammonium in the presence of DBU and CuI, similar to the work carried out by Jerome and his coworkers.[136, 137, 142] The random copolymer of PCL and azide-substituted PCL was synthesized according to a multistep process.[137, 185]As shown in Scheme 2, α-chloro-ε-caprolactone (αClεCL) monomers were prepared with the aid of α-chlorocyclohexanone and mCPBA via Baeyer-Villiger oxidation. Ring-opening polymerization of αClεCL and εCL was then carried out using Sn(Oct)$_2$ as catalyst and 4-*tert*-butylbenzyl alcohol as initiator, yielding PCL-*co*-P(αClεCL) copolymers. The chlorine group was further converted to azide group through a typical nucelophilic substitution reaction in the presence of sodium azide, yielding PCL-*co*-P(αN$_3$εCL) copolymers. On the other hand, we carried out a quaternization reaction between 3-dimethylamino-1-propyne and bromoethane under a mild condition to prepare propargyl quaternary ammonium.[139, 185] Five PCL-*co*-P(αClεCL) copolymers with 10, 15, 20, 30 and 50 mol% of PCL-*g*-QA unit were prepared. Table 5.1 summarized the results of the random copolymers of *ε*-caprolactone and *α*-chloro-*ε*-caprolactone.

The molecular weights of random copolymers were characterized by GPC. As shown in Figure 5.3, both the chlorine-substituted and azide-substituted PCL had monomodal symmetric distribution with reasonably low PDI, indicating that the ring-opening polymerization was controlled. GPC was not used to characterize the final cationic copolymers because these ionic copolymers appeared to have complicated interactions with GPC columns.

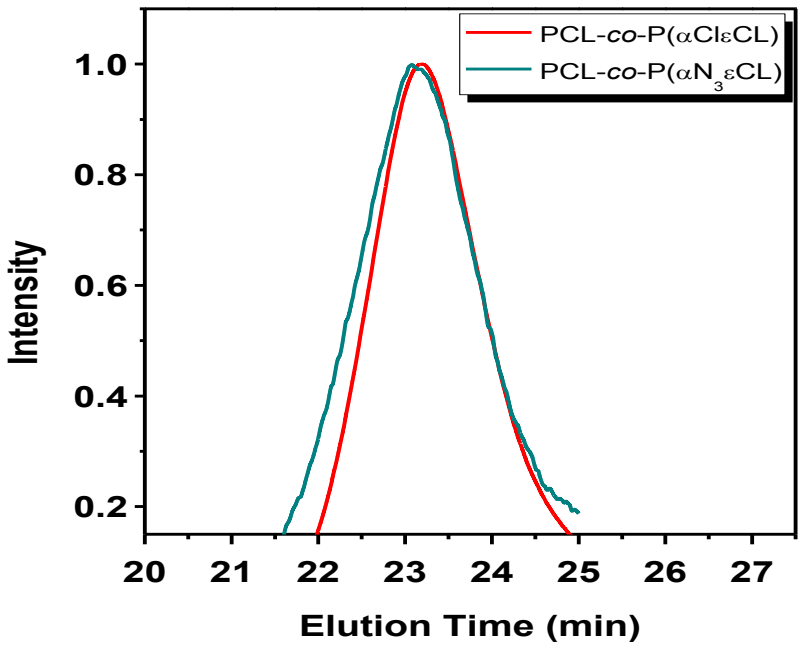

Figure 5.3 Representative GPC traces of PCL-*co*-P(αClεCL) and PCL-*co*-P(αN$_3$εCL) copolymers (15% mol of αClεCL)

Chemical structures of the random copolymers, PCL-*co*-P(αClεCL), PCL-*co*-P(αN$_3$εCL), and PCL-*co*-(PCL-*g*-QA), were characterized by both ^{1}H NMR and FT-IR. After converting the chlorine group to azide group, the peak at 4.25 ppm for the C*H*Cl proton shifted to 3.8 ppm, corresponding to the C*H*N$_3$ proton (Figure 5.4). Integration of the NMR spectra indicated the 100% conversion of the chlorine groups. The chlorine to azide conversion was also confirmed by FT-IR. (Figure 5.5) a sharp absorption peak at 2100 cm^{-1} emerged, a characteristic absorption of azide group. After the click reaction, the peak at 3.8 ppm in NMR spectra disappeared completely and a new peak at about 8.6 ppm corresponded to the proton from the triazole group. A new peak at 3.0 ppm was assigned to the methyl groups next to the triazole group. FT-IR spectra also showed that the peak at 2100 cm^{-1} disappeared compeletly after click reaction, indicating the complete reaction of azide group. A new absorption at 1660 cm^{-1}, arose, which originated from the traizole absorption.

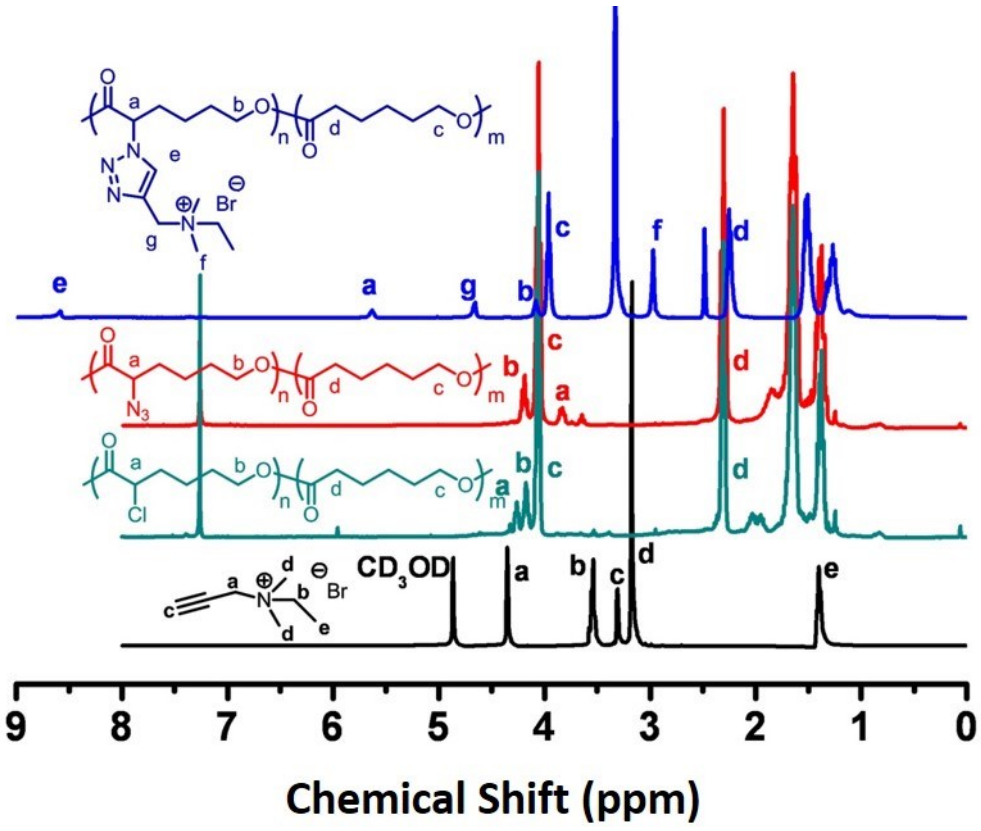

Figure 5.4 ^{1}H NMR spectra of PCL-*co*-P(αClεCL),PCL-*co*-P(αN_3εCL), and PCL-*co*-PCCL-*g*-QA) copolymers (15% mol of αClεCL)

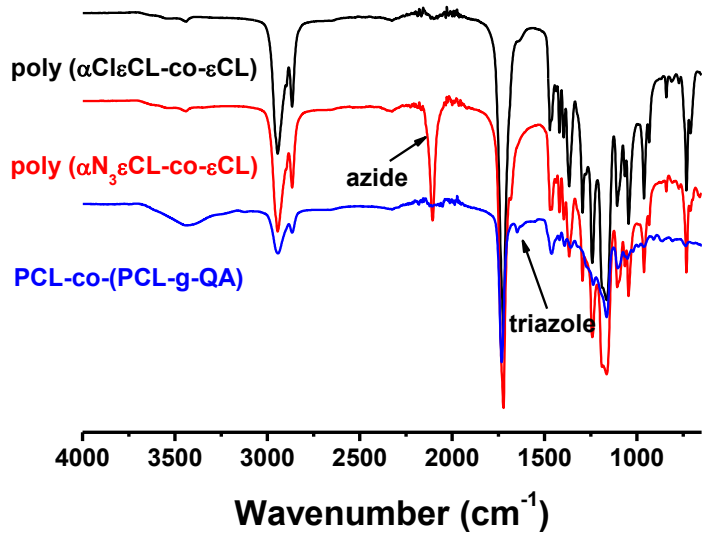

Figure 5.5 FT-IR spectra of PCL-*co*-P(αClεCL), PCL-*co*-P(αN_3εCL), and PCL-*co*-P(CL-*g*-QA) copolymers (15% mol of αClεCL)

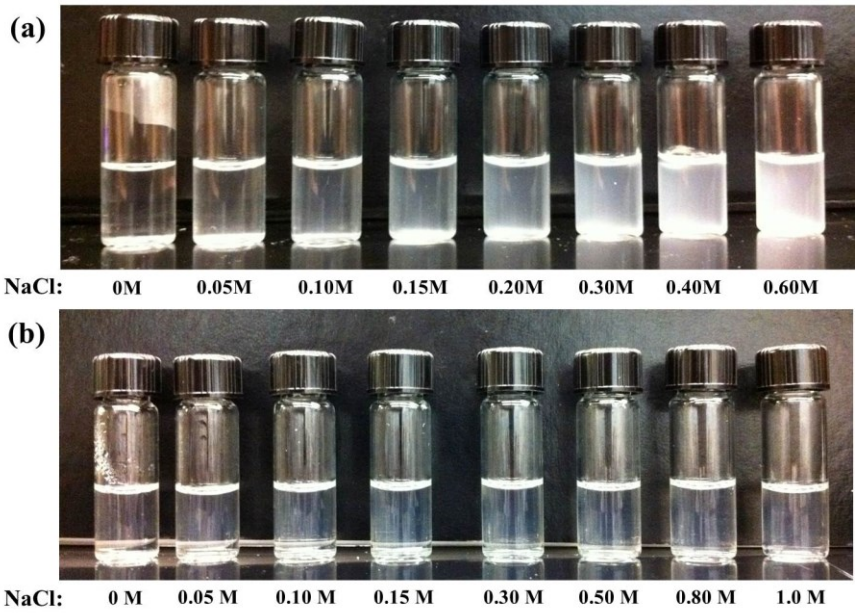

Figure 5.6 Visual appearance of PCL-*co*-P(CL-*g*-QA) aqueous solutions containing different NaCl concentrations: (a) PCL-*co*-P(CL-*g*-QA) (15mol % of P(CL-*g*-QA)); (b) PCL-*co*-P(CL-*g*-QA) (30mol % of P(CL-*g*-QA))

Salt-responsive property of PCL-*co*-P(CL-*g*-QA): Salt-responsive property of the random copolymers was characterized.[211] The copolymers were first dissolved in salt-free water to produce aqueous solutions with 1 wt% concentration. Then a series of copolymer solutions with different salt concentrations were prepared by adding varying amount of inorganic salt (NaCl) into the solutions. Figure 5.6 showed the visual appearance of the random copolymers in aqueous solutions.

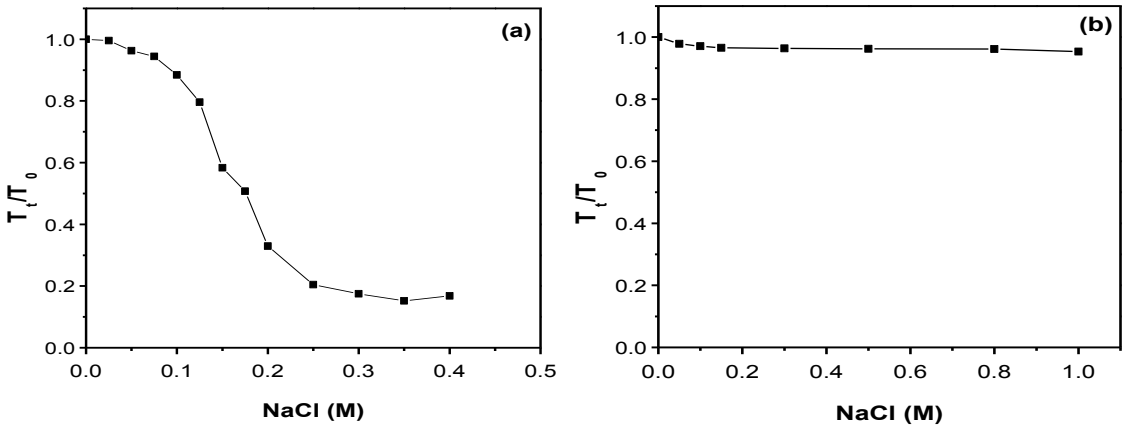

Figure 5.7 Dependence of turbidity of copolymer solutions (at 818 nm) on NaCl concentration: (a) PCL-*co*-P(CL-*g*-QA) with 15 mol% P(CL-*g*-QA); (b) PCL-*co*-P(CL-*g*-QA) with 30 mol% P(CL-*g*-QA)

PCL-*co*-P(CL-*g*-QA) with 15%mol P(CL-*g*-QA) was well dissolved in salt-free water to form a transparent solution. With the increase of NaCl concentration in solutions, the solution turned light milky and turbid. When the NaCl concentration reached 0.6 M (ionic strength also equals to 0.6M), the solution formed opaque suspension with some precipitates observed at the bottom of vials. 20%mol P(CL-*g*-QA)-containing copolymers showed similar behaviors (not shown). However, for the copolymer with more quaternary ammonium substituted PCL (i.e. ~30% mol), the solution initially showed slightly milky. However, further increase of salt concentration up to 1.0M did not result in suspension-like solution. Copolymers with higher than 30%mol P(CL-*g*-QA) were too hydrophilic to show any salt-responsive property. It should be pointed out that the random copolymer with 10% mol P(CL-*g*-QA) (sample 1 in Table 5.1) did not dissolve well in salt-free water, probably due to the high fraction of hydrophobic PCL.

The optical turbidity (at 818nm) of PCL-*co*-P(CL-*g*-QA) copolymers was then measured by a UV-Visible spectrophotometer at room temperature. We tested the

transmittance of the solutions (T_t) and compared with that of pure deionized water (T_0), as shown by solution transmittance ratio (T_t/T_0) as a function of NaCl concentration in Figure 5.7 For the copolymer with 15 mol% P(CL-*g*-QA) (Fig. 5 (a)), the transmittance ratio showed significant decrease at ~ 0.1M NaCl (ionic strength 0.1M), which corresponded to the formation of slightly turbid solution. The sharpest decrease of the transmittance ratio (~ 0.6) was observed in the range of 0.1M-0.2M of the NaCl solution ((ionic strength from 0.1M to 0.2M). The T_t/T_0 value dropped to 0.2 at NaCl concentration equal to 0.4M, corresponding to the opaque suspension solution in Figure 5.6 For the copolymer with 30 mol% P(CL-*g*-QA), the transmittance ratio showed a slight decrease when the salt concentration increased up to 0.2M. Further increasing the salt concentration did not lead to the decrease of transmittance ratio, indicating this copolymer composition did not have appreciable salt-responsive property.

Figure 5.8 Visual appearance of PCL-*co*-P(CL-*g*-QA) (15mol % of P(CL-*g*-QA)) aqueous solutions containing various NaCl concentrations

To compare different salt effects on the polymer solubility, divalent $CaCl_2$ was used to determine the salt-responsive property of PCL-*co*-P(CL-*g*-QA) copolymers. Figure 5.8 showed the concentration of $CaCl_2$ on the solubility of the copolymer (15

mol% P(CL-*g*-QA)). Compared with NaCl solution, $CaCl_2$ solution showed much higher sensitivity to the copolymers, with the formation of turbid solution as low as 0.05M $CaCl_2$, indicating a stronger "screening" effect of $CaCl_2$ to the cationic polymer chains.

UV-Visible tests further confirmed high salt-responsive property of copolymers in the presence of $CaCl_2$. Figure 5.9 showed the transmittance ratio profiles of PCL-*co*-P(CL-*g*-QA) containing 15 mol% P(CL-*g*-QA). The largest decrease of transmittance ratio of the polymer solution was in the range of 0.05M and 0.15M of salt concentration (ionic strength from 0.15M to 0.45M). With the concentration of $CaCl_2$ at 0.15M, most polymers precipitated.

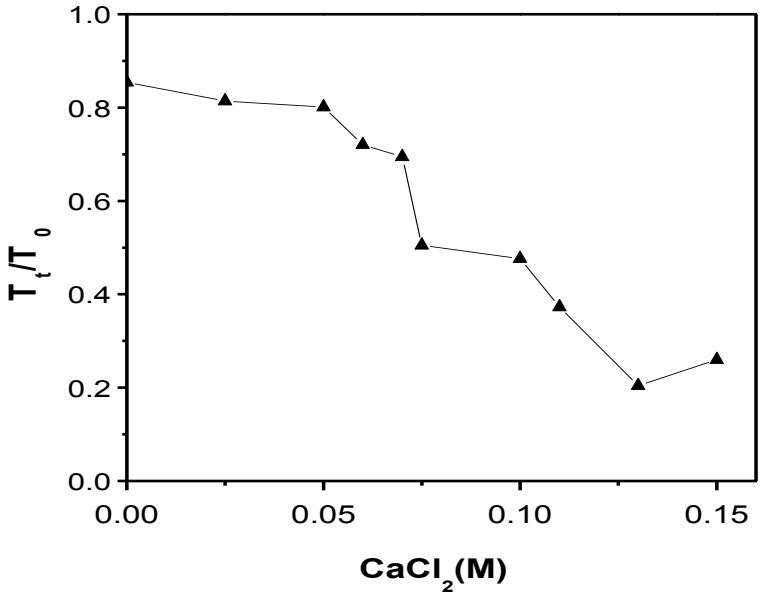

Figure 5.9 Dependence of turbidity of copolymer solutions (at 818 nm) on $CaCl_2$ concentration: PCL-*co*-P(CL-*g*-QA) (15mol % of P(CL-*g*-QA))

Compared these results with the salt-responsive tests in the presence of NaCl, we noted that as low as 0.05 M $CaCl_2$ can induce the salt-responsive behavior while 0.1 M

NaCl was required to initiate the salt-responsive behavior of polymer solution. The different salt-responsive property between NaCl and $CaCl_2$ can be explained by the different charge screening effect. One divalent Ca^{2+} can screen quaternary ammonium twice as monovalent Na^{+}. Therefore, at the same concentration in aqueous solution, Ca^{2+} can "screen" more quaternary ammonium charges, leading to easier collapse of polymer chains. On the other hand, based on ionic strength, NaCl appeared to be more effective.

Thick films (300μm) of PCL-*co*-P(CL-*g*-QA) copolymers with 15mol % of P(CL-*g*-QA) were prepared and tested solubility against water with different salt concentration. At salt free water, the entire film first cracked into many small pieces and became completely soluble and transparent within hours (Figure 5.10). However, in a 0.15M NaCl solution, the film well maintained its shape even after a few days, indicating its hydrophobic nature in salted water.

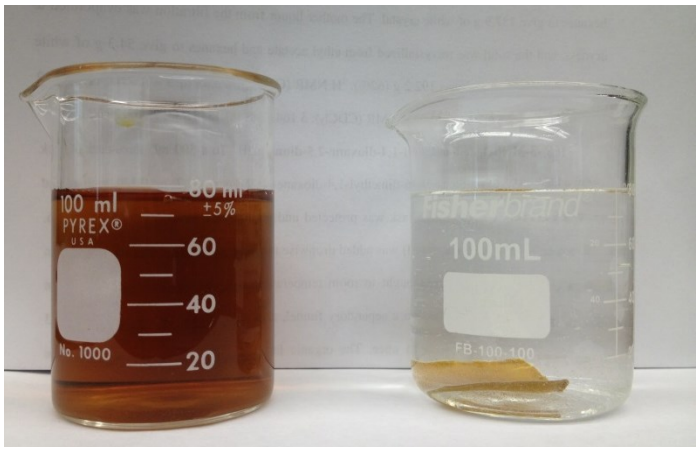

Figure 5.10 Responsiveness of thick films of PCL-*co*-P(CL-*g*-QA) (15mol % of P(CL-*g*-QA)) in different water: left) in salt-free water; right) in 0.15 M NaCl solution (note: the color appears after the chlorination of PCL)

In salt-free water or diluted solution with low salt concentration, the random copolymers are well dissolved due to electrostatic repulsion interactions between cationic

quaternary ammonium charges. With the addition of salt (NaCl or $CaCl_2$) into the aqueous solution of copolymers, the ionic screening effect started to take effect to shield the above electrostatic repulsion interactions. The copolymers gradually become insoluble with the increase of salt concentrations, resulting in the increase of turbidity of the solution observed. Our results suggested that the screening effect can play a major role in the solubility of polymers only when there is an optimal composition range of quaternary ammonium moiety in the copolymers, mostly due to the balance of hydrophilic and hydrophobic components in the copolymer chain.[201, 212, 213]

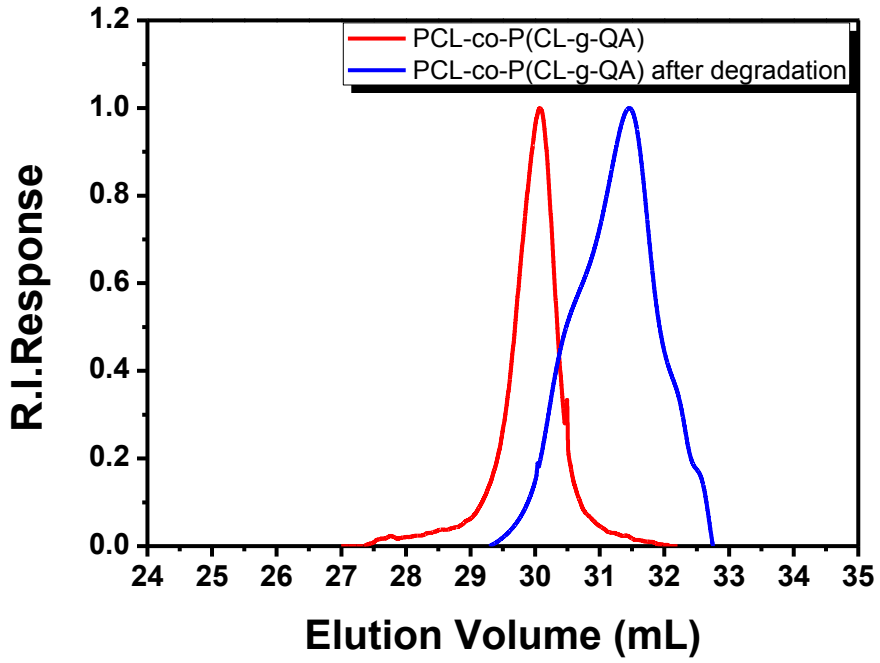

Figure 5.11 GPC traces of PCL-*co*-P(CL-*g*-QA) and its acid-degraded product from PCL-*co*-P(CL-*g*-QA)

Degradability of PCL-*co*-P(CL-*g*-QA): The degradability of cationic random copolymers was tested by acid-catalyzed degradation method. 10 mg/mL polymer

solution (1mL) was added with 0.15M HCl (0.2mL) to give a final solution with 0.025M HCl and 8.3 mg/mL random copolymers. After the degradation in acidic condition, the GPC traces (Figure 5.11) showed that the degraded species shifted to a much lower molecular weight in the range of monomeric units, indicating the preservation of excellent PCL degradability, even after the incorporation of quaternary ammonium groups, consistent with earlier reports.[136, 134, 185]

5.5 Conclusions

In conclusion, we have developed a novel strategy to prepare degradable salt-responsive cationic random copolymers PCL-*co*-P(CL-*g*-QA) by combing ROP and click reaction. The high efficiency of click reaction allowed us to manipulate the compositions of salt-responsive groups in the cationic copolymers. The turbidity and solubility tests indicated that PCL-*co*-P(CL-*g*-QA) with 15mol% PCL-*g*-QA showed the best salt responsive property. This new class of degradable cationic random copolymers may find potential applications in biomedical fields and personal care products.

CHAPTER 6

CATIONIC SALT-RESPONSIVE BOTTLE-BRUSH POLYMERS[5]

[5]K. Yao, Y. Chen, J. Zhang, C. Bunyard and C. Tang. *Macromolecular Rapid Communications* 34: 645–651.

Reprinted here with permission of publisher.

6.1 Abstract

We prepared a class of cationic bottle brush polymers that show ionic strength dependent stimuli-responsiveness. Brush polymers with norbornene as backbone and quaternary ammonium (QA)-containing polycaprolactone copolymers as side chains were synthesized by a combination of ring-opening metathesis polymerization, ring-opening polymerization and click reaction. Brush polymers containing 20mol% cationic QA groups showed excellent salt responsive property in aqueous solution, as confirmed by both UV-Vis and atomic force microscopy measurements. In DI water or water with low ionic strength, brush polymers were stretched and soluble due to the strong electrostatic repulsion interactions between cationic QA groups. As the addition of salt to increase ionic strength, single brush polymers underwent a transition from extended conformation to collapsed state and finally became insoluble in solution due to the screening effect of salts that yielded the once-dominant electrostatic interactions among QA species to hydrophobic-hydrophobic interactions.

6.2 Introduction

In the last decades, bottle-brush polymers, also called molecular brushes, have drawn a lot of attention due to their nanoscale sizes and unique unimolecular properties that lead to potential applications in various areas such as drug delivery, bioengineering, and molecular devices.[62, 214-217] Bottle-brush polymers are a special class of graft copolymers that usually contain a linear polymer backbone and densely grafted side chains.[218, 219] Synthetically, bottle-brush polymers can be prepared by three major approaches: (1) grafting to;[220-224] (2) grafting from;[225-229] and (3) grafting through.[219, 230-233] Each approach has intrinsic advantages and disadvantages. Particularly, the "grafting

through" method allows the preparation of molecular brushes with full grafting density and high molecular unity by controlled/living polymerization. Ring-opening metathesis polymerization (ROMP) is a very powerful polymerization strategy to prepare various polymer brushes with controlled molecular weight and low polydispersity index (PDI). Grubbs and coworkers recently reported norbornene-based bottle-brush polymers with various side chains prepared by ROMP and investigated their intriguing self-assembly behaviors.[234-236] The Wooley group prepared well-defined norbornene-based bottle-brush polymers by combining RAFT and ROMP.[237] Coates and coworkers reported the polymerization of norbornenyl-terminated poly(cyclohexene carbonate) via ROMP.[238]

Stimuli-responsive polymers are of great interest because of their promising applications in the biomedical field.[53, 54, 57, 58, 187, 188, 191, 194, 196, 239] Physical properties of these polymers, particularly macromolecular chain conformation, can be affected by external stimuli such as pH, temperature, light, electric and magnetic field.[64-67, 70, 73, 197] Generally, small environmental variations would result in dramatic conformational or other property changes. Similar to many other stimuli-responsive polymer systems, molecular brushes can be designed to respond to external stimuli. Since molecular brushes are single molecules, the driving forces for the conformational change in response to external stimuli are unique, often with specific advantages. For example, stimuli-responsive unimolecular micelles from molecular brushes could be used as controlled encapsulation and release of therapeutic agents. The normal critical micelle concentrations, which are a prerequisite for the formation of amphiphilic block copolymer micelles to avoid premature drug release, are not required for unimolecular micelles. A lot of work has been focused on the development of thermoresponsive

molecular brushes, which contain temperature-responsive side chains such as poly(*N*-isopropylacrylamide) (PNIPAAm),[240] poly(2-(dimethylamino)-ethyl methacrylate) (PDMAEMA), oligo(ethylene glycol), or their copolymers. pH-Responsive molecular brushes usually have ionic side chain including polyacids (i.e. poly(styrene sulfonate), poly(acrylic acid))[241] and polybases (i.e. PDMAEMA). Mechanically responsive molecular brushes are other emerging molecular brushes that can change their shape upon lateral compression or spreading on flat substrates. The Sheiko and Matyjaszewski groups have done a lot of fascinating pioneering work on this class of molecular brushes.[242-244]

Among stimuli-responsive molecular brushes, salt-responsive molecular brushes are much less explored. Mueller et al. found that quaternized PDMAEMA brushes exhibited conformational switch in response to concentrations of mono-, di- tri-valent salts through electrostatic screening or anionic surfactant through ionic complexation.[245] Other limited studies on salt-responsive polymers (non-brushes) have been primarily focused on ionic block copolymers for the benefits of micellar formation.[200-202, 246] Similarly, these block copolymers suffer potential micellar instability, which is strongly dictated by the critical micelle concentrations. In addition to these fundamental studies, salt-responsive polymers actually have extensive applications in personal-care products (i.e. wet tissue and hygiene-diapers), as mostly reported in patents[209, 210] and in one of our recent works.[246] Basically, in the wet state with higher ionic strength, the ionic charges of polymers are screened by salts and consequently the polymer chains are insoluble in water, therefore providing strength to the product. On the other hand, due to electrostatic

repulsions, these polymers are soluble in DI water or water with lower ionic strength and thus product can be flushed away.

Herein we report the first degradable cationic bottle-brush polymers that exhibits strong salt-responsiveness. We combine ROMP, ring-opening polymerization (ROP) and click chemistry to prepare a series of cationic molecular brushes with a QA-containing caprolactone random copolymer as the side chain. These molecular brushes are soluble in DI water or water with low ionic strength due to the overwhelming domination of electrostatic repulsion interactions between cationic QA species over attractive hydrophobic-hydrophobic interactions between polycaprolactone segments. The decrease in solubility of brushes with the increase of ionic strength is due to the screening effect of salts to shield the repulsion interactions between QA species and thus significant change of macromolecular conformations, which were directly observed by atomic force microscopy.

6.3 Experimental Section

6.3.1 Materials

Toluene and tetrahydrofuran (THF) were refluxed with sodium and distilled under a nitrogen atmosphere just before use. Grubbs III catalyst was synthesized following an earlier report.[247] ε-Caprolactone was dried over calcium hydride and purified by vacuum distillation before polymerization. α-Chloro-ε-caprolactone (αClεCL) was prepared according to our early work.[137, 185] All other chemicals were purchased from Sigma-Aldrich and used as received.

6.3.2 Characterization

^{1}H (300 MHz) NMR spectra were recorded on a Varian Mercury spectrometer with tetramethylsilane (TMS) as an internal reference. Fourier Transform Infrared Spectrometry (FTIR) spectra were recorded on a PerkinElmer spectrum 100 FTIR spectrometer. Mass spectra were conducted on a Waters Micromass Q-Tof mass spectrometer. The ionization source is positive ion electrospray. Gel Permeation Chromatography (GPC) was performed in DMF at a flow rate of 1.0 mL/min at 50 ^{o}C on a Varian system equipped with a Varian 356-LC refractive index detector and a Prostar 210 pump. The columns were STYRAGEL HR1, HR2 (300×7.5 mm) from Waters. DMF and polymer solutions were filtered over microfilters with a pore size of 0.2 μm (Nylon, Millex-HN 13 mm Syringes Filters, Millipore, USA). The columns were calibrated against polystyrene standards. Optical turbidity (at 818 nm) of random copolymers in aqueous solution was measured using a UV-visible spectrophotometer (UV-2450, SHIMADZU) at room temperature. The samples were placed in 1 cm path length quartz cells, and de-ionized water was used as control. Atomic force microscopy (AFM) measurements were performed on a Nanoscope V Multimode instrument, using tapping mode. Polymer brush solution in water was drop-cast onto fresh-cleaved mica substrates and visualized by AFM after dryness.

6.3.3 Synthesis

Synthesis of *N*-[3-hydroxylpropyl]-*cis*-5-norbornene-*exo*-2,3-dicarboximide (NPH): NPH was prepared according to our early work.[248] Briefly, *Cis*-5-norbornene-*exo*-2,3-dicarboxylic anhydride (NDA) (1.0 g, 6.0 mmol) was dissolved in 20 mL dichloromethane (DCM) and 3-amino-1-propanol (0.50 g, 6.7 mmol) was added

dropwise to the DCM solution under stirring. Then the solvent was evaporated and the mixture was heated at 110 ºC overnight. Finally the mixture was passed through an alumina column to give the product NPH. ^{1}H NMR ($CDCl_3$) δ: 6.27 (s, 2H, C*H*=C*H*), 3.64 (t, 2H, NC*H*$_2$CH$_2$), 3.53 (CH$_2$*CH*$_2$OH), 3.26 (s, 2H, C*H*CON), 2.71 (m, 2H, CH$_2$C*H*), 1.77 (m, 2H, CH$_2$C*H*$_2$CH$_2$), 1.23, 1.54 (m, 2H, C*H*$_2$CH). ^{13}C NMR ($CDCl_3$) δ: 178.6 (*C*ON), 137.6 (*C*H=*C*H), 58.9 (*C*H$_2$OH), 47.7 (CH$_2$*C*HCHCO), 45.0 (CH$_2$CH*C*HCO), 42.6 (*C*H$_2$CHCHCO), 34.9 (N*C*H$_2$CH$_2$), 30.4 (NCH$_2$*C*H$_2$). MS (ESI, m/z): theoretical 221.25, found 221.

Synthesis of ethyl dimethyl propargyl quaternary ammonium bromide (EDPQA): 3-Dimethylamino-1-propyne (5.00 g, 60.1 mmol) was added in a round bottom flask containing 20 mL THF, followed by the addition of 1-bromoethane (7.90 g, 72.2 mmol). The reaction mixture was stirred at 35 ºC for 2 days.[138] Then the solvent and excess bromoethane were evaporated. The mixture was washed with diethyl ether three times to remove unreacted 3-dimethylamion-1-propyne. The quaternary ammonium bromide was finally dried in vacuum. ^{1}H NMR (CD_4O) δ: 4.35 (m, 2H, C*H*$_2$N$^+$); 3.55 (q, 2H, N$^+$C*H*$_2$CH$_3$); 3.30 (m, 1H, C*H*≡C); 3.15 (s, 6H, N$^+$C*H*$_3$); 1.40 (t, 3H, N$^+$CH$_2$C*H*$_3$). ^{13}C NMR (CD_4O) δ: 82.7 (CH≡*C*), 72.3 (*C*H≡C), 60.9 (N$^+$*C*H$_2$CH$_3$), 54.5 (*C*H$_2$ N$^+$), 50.5 (N$^+$*C*H$_3$), 8.6 (N$^+$CH$_2$*C*H$_3$). MS (ESI, m/z): theoretical 192.10, found 112 (without Br$^-$ anion).

Synthesis of NPH-PCL-*co*-P(αClεCL) macromonomer by ROP: NPH-PCL-*co*-P(αClεCL) macromonomers with different degree of polymerization (DP) were prepared by ROP. As an example**,** εCL (0.91 g, 8.0 mmol) and αClεCL (0.30 g, 2.0 mmol) were dissolved in 1 mL dry toluene and added into a Schlenk flask along with NPH initiator

(0.044 g, 0.2 mmol). The mixture was purged with nitrogen for 10 min. $Sn(OCt)_2$ (0.008 g, 0.02 mmol) was dissolved in 0.2 mL dry toluene and transferred into the Schlenk flask under the protection of nitrogen. Finally the reaction mixture was stirred at 110 °C under nitrogen for 24 h. After reaction, the mixture was cooled to room temperature, diluted with toluene, precipitated twice into cold methanol, and dried overnight under vacuum to constant weight.

Synthesis of PNPH-*g*-[PCL-*co*-P (αClεCL)] molecular brushes by ROMP: As an example, in a nitrogen-filled reaction flask, macromonomer NPH-*g*-[PCL-co-P(αClεCL)] (400 mg, 61.5 μmol) was dissolved in 5 mL dry toluene. The flask was tightly sealed and purged with nitrogen for 15 min. Then a solution of Grubbs III catalyst (0.9 mg, 1.23 μmol) in 2 mL of degassed toluene was added to the flask under the protection of nitrogen. The mixture was stirred at 60 ^{o}C for 4 h and the polymerization was quenched by the addition of 1 mL ethyl vinyl ether. The solution was stirred for another 30 min and then precipitated in excess methanol. The polymer was isolated by filtration and dried under vacuum to constant weight.

Synthesis of PNPH-*g*-[PCL-*co*-P(αN$_3$CL)] molecular brushes: PNPH-*g*-[PCL-*co*-P(αClεCL)] (0.4 g, 0.65 mmol αClεCL) was dissolved in DMF in a round bottom flask with a stirring bar. NaN_3 (0.21 g, 3.25 mmol) was then added and the mixture was stirred at room temperature overnight. After the reaction, the solid was filtered and the DMF was evaporated under reduced pressure. Then the mixture was dissolved in toluene and the insoluble solid was removed by centrifugation (5000 rpm at 25^{o}C for 15 min). Finally the copolymer was recovered by evaporation of the solvent under reduced pressure.

Synthesis of PNPH-*g*-[PCL-*co*-P(CL-*g*-QA)] molecular brushes by click reaction: PNPH-*g*-[PCL-*co*-P(αN$_3$εCL)] (0.22 g, 0.36 mmol αN$_3$εCL) and EDPQA (0.076 g, 0.40 mmol) were added into a round bottom flask containing DMF and the mixture was purged with nitrogen for 10 min. DBU (0.0055 g, 0.036 mmol) and CuI (0.0068 g, 0.036 mmol) were then added, and the reaction mixture was stirred at 35 ºC for 4h. After the reaction, the copolymer was precipitated in cold diethyl ether and dried in vacuum. The filtered solid was then dissolved in water and dialyzed against deionized water for 6 h to remove the remaining small molecules and other impurities. The final copolymers were recovered by freeze-drying.

6.3.4 Degradation Test of Brush Polymers

10 mg Molecular brush PNPH-*g*-[PCL-*co*-P(CL-*g*-QA)] (20 mol% QA) was dissolved in 1 mL THF to give a 10 mg/mL solution. Then 0.2 mL $HCl_{(aq)}$ (0.3M) was added to the solution and the mixture was stirred at room temperature overnight. The solvent was evaporated under reduced pressure and the degradation residue was dried under vacuum.

6.4 Results and Discussion

Synthesis of Cationic Caprolactone Molecular Brushes: As shown in Figure6.1, cationic molecular brushes were synthesized by a combination of ROMP, ROP and click reaction. A macromonomer was first prepared by ROP of ε-caprolactone (εCL) and α-chloro-ε-caprolactone (αClεCL) using *N*-[3-hydroxylpropyl]-*cis*-5-norbornene-*exo*-2,3-dicarboximide (NPH) as initiator. The macromonomer was then polymerized via ROMP using Grubbs III catalyst followed by the conversion of chlorine groups to azide groups.

Finally a copper-catalyzed cycloaddition reaction was employed to give cationic brushes PNPH-*g*-(PCL-*co*-P(CL-*g*-QA)). Compared with the synthesis of other salt-responsive polymer brushes, our approach to prepare PNPH-*g*-(PCL-*co*-P(CL-*g*-QA)) brushes has some advantages. First, ROMP has high tolerance to functional groups and allows high reaction conversion without inducing chain crosslinking. Second, the high efficient click reaction can ensure the synthesis of molecular brushes with controlled molar fractions of salt-responsive cationic groups.

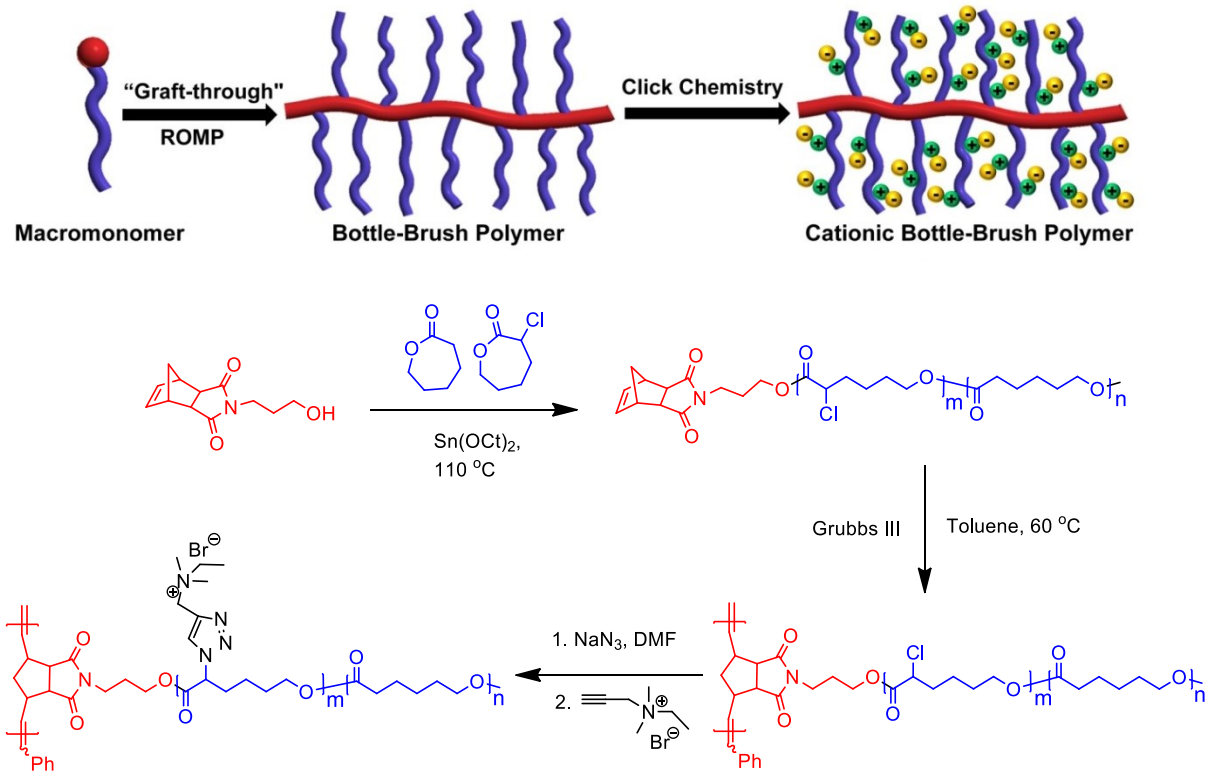

Figure 6.1 Preparation of PNPH-*g*-(PCL-*co*-P(CL-*g*-QA)) molecular brushes by ROMP, ROP and click chemistry

Macromonomers NPH-*g*-[PCL-*co*-P(αClεCL)] were prepared by ROP of εCL and αClεCL with various molar feed ratios using $Sn(Oct)_2$ and NPH as catalyst and initiator, respectively. ROP was controlled with conversion < 95% to minimize transesterification.

The macromonomer structures were characterized by ^{1}H NMR as shown in Figure 6.2, the peak at 6.25 ppm corresponded to the vinyl protons at the norbornene. The peak for the proton adjacent to the chlorine group was located at 4.25 ppm. Peaks at 4.14 ppm and 4.05 ppm represented the protons adjacent to oxygen in αClεCL and CL units, respectively. The proton next to the ester group in CL units gave a peak at 2.30 ppm. The molecular weights of macromonomers were determined by comparing the integration areas of proton **a** in the end group and protons **b, e** in the repeat units (representing the protons in αClεCL and CL units). Table 6.1 lists results of macromonomers with different polymer chain lengths.

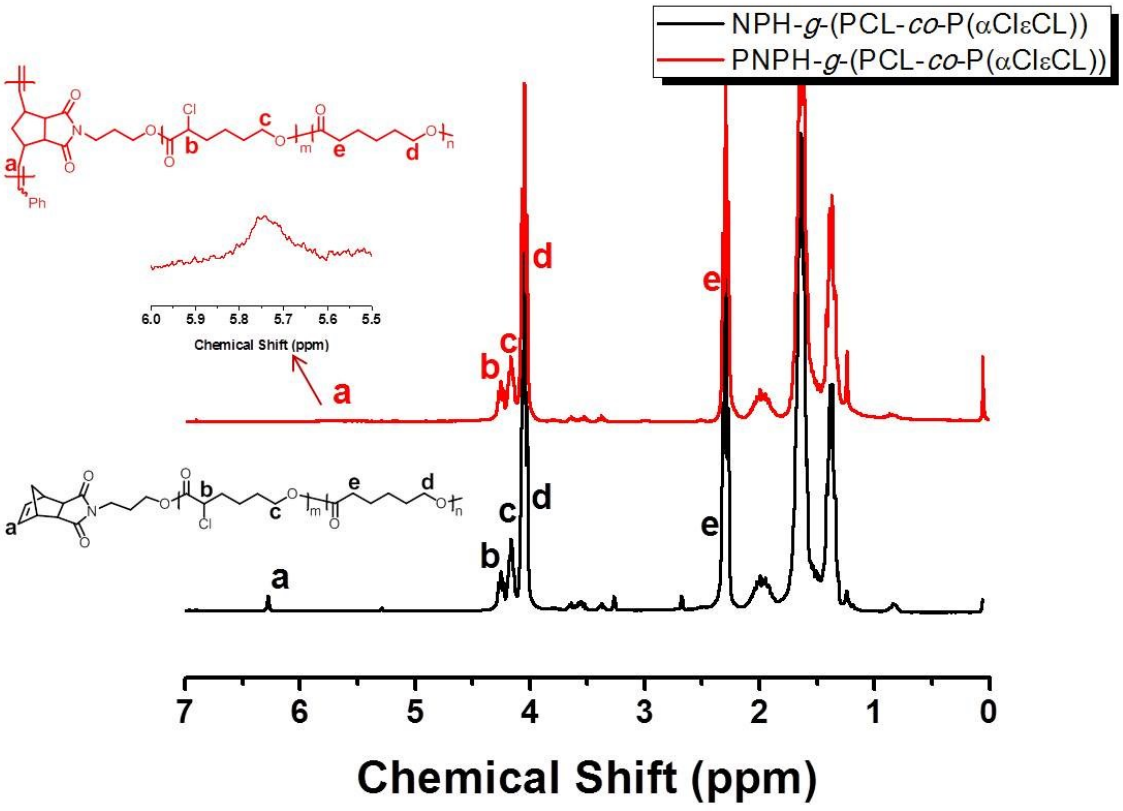

Figure 6.2 ^{1}H NMR spectra of macromonomer NPH-*g*-[PCL-*co*-P(αClεCL)] (Table 6.1, MM2) and polymer brush PNPH-*g*-[PCL-*co*-P(αClεCL)] (Table 6.2, Entry 1)

Table 6.1 Characterization of macromonomer NPH-*g*-[PCL-*co*-P(αClεCL)] by ROP

MM	[Monomer]:[NPH]:[Sn(Oct)$_2$]	f $_{\alpha Cl\varepsilon CL}$(%)[a]	Conversion (%)[b]	$M_{n,theo}$[c] (g/mol)	$M_{n,NMR}$ (g/mol)	$M_{n,GPC}$ (g/mol)	PDI $_{GPC}$
MM-1	100:1:0.1	20	94	11,600	15,900	23,600	1.13
MM-2	50:1:0.1	20	92	5,700	6,500	10,800	1.18
MM-3	25:1:0.1	20	90	2,900	3,900	6,800	1.22
MM-4	50:1:0.1	30	91	5,900	6,600	7,600	1.18
MM-5	100:1:0.1	30	95	12,000	13,700	19,400	1.16
MM-6	50:1:0.1	15	93	5,800	6,800	9,400	1.25

[a] molar composition of monomer feed ratio; [b] Conversion was determined by ^{1}H NMR; [c] $M_{n,\ theo}$= M_n (NPH) + M_n(monomer) × [monomer]/[NPH] × Conversion (%).

We performed "graft-through" polymerization of NPH-*g*-[PCL-*co*-P(αClεCL)] macromonomer via ROMP with the aid of Grubbs III catalysts.[249] The macromonomer was employed to run ROMP with different ratios of [macromonomer]/[catalyst]. All polymerizations had very high monomer conversions (~100%). Table 6.2 summarizes the results of polymer brushes PNPH-*g*-[PCL-*co*-P(αClεCL)] by ROMP. PNPH-*g*-[PCL-*co*-P(αClεCL)] brushes with high molecular weight and relatively low PDI were achieved. ^{1}H NMR spectra of polymer brushes showed that the signals of vinyl protons on the norbornene at 6.25 ppm disappeared and a new flat peak at 5.75 ppm appeared, indicating that the macromonomers were polymerized via ROMP (Figure 6.2). Compared with the protons in the macromonomers, the other protons did not show significant changes in their chemical shifts, suggesting that ROMP did not affect molecular structures of PCL-*co*-P(αClεCL) side chains. The molecular weight of polymer brushes showed a clear shift towards higher molecular weights in GPC traces compared to that of macromonomer, indicating successful polymerization of the macromonomer (Figure 6.3).

Table 6.2 Synthesis of molecular brushes PNPH-*g*-[PCL-*co*-P(αClεCL)] by "grafting-through" ROMP

Entry	MM[a]	[MM]:[Catalyst]	$M_{n,\,theo}$[b]	$M_{n,\,GPC}$[c]	PDI $_{GPC}$
1	MM-2	50:1	325,000	363,000	1.45
2	MM-2	25:1	162,500	182,000	1.33
3	MM-2	10:1	65,000	41,000	1.24
4	MM-4	50:1	330,000	173,000	1.45
5	MM-6	50:1	340,000	400,000	1.61

[a] see Table 6.1; [b] $M_{n,theo}$= $M_{n,NMR}$ (Macromonomer)×([MM]/[Catalyst]); [c] PS standard.

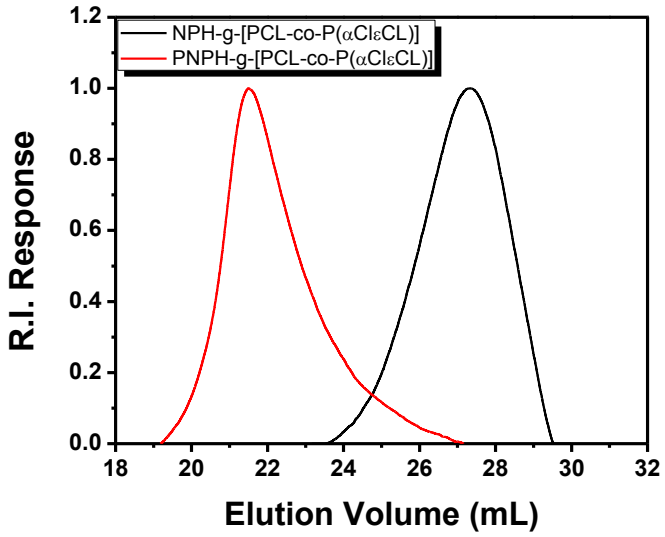

Figure 6.3 GPC traces of macromonomer NPH-*g*-[PCL-*co*-P(αClεCL)] (Table 6.1, MM-2) and polymer brush PNPH-*g*-[PCL-*co*-P(αClεCL)] (Table 6.2, Entry 1)

The chloro-substituted group in polymer brush PNPH-*g*-[PCL-*co*-P(αClεCL)] was further converted to azide group by reacting with NaN_3 in DMF at room temperature. Resultant PNPH-*g*-[PCL-*co*-P(αN_3εCL)] was characterized by both ^{1}H NMR and FT-IR. According to the ^{1}H NMR spectra (Figure 6.4), a new peak at 3.80 ppm in the PNPH-*g*-[PCL-*co*-P(αN_3εCL)] appeared, representing the proton next to the azide group, while the previous peak at 4.25 ppm (proton next to chlorine) completely disappeared, indicating that all chlorine groups were replaced by azide groups. The FT-IR spectra of polymer brushes showed a strong characteristic absorption at 2100 cm^{-1}, corresponding to the azide groups in the side chains of polymer brushes (Figure 6.5). Furthermore, the GPC traces of polymer brushes PNPH-*g*-[PCL-*co*-P(αN_3εCL)] showed similar molecular weight to that of PNPH-*g*-[PCL-*co*-P(αClεCL)] (Figure 6.6), indicating that the PCL side chains of polymer brushes didn't degrade during the reaction.

QA groups were finally installed onto molecular brushes by a click reaction between azide-containing PNPH-*g*-[PCL-*co*-P(αN$_3$εCL)] and alkyne-containing QA ethyl dimethyl propargyl quaternary ammonium bromide (EDPQA) with the aid of catalyst CuI and ligand 1,8-diazabicycloundec-7-ene (DBU), yielding the final cationic molecular brushes PNPH-*g*-[PCL-*co*-P(CL-*g*-QA)]. According to ^{1}H NMR spectra (Figure 6.4), a new chemical shift at 8.65 ppm was assigned to the proton from the newly formed triazole group. The peak at 3.80 ppm disappeared and a new peak at 5.70 ppm was assigned to the proton (on the caprolactone unit) next to the triazole group, indicating that all azide groups in polymer brushes reacted with alkyne to form triazole during the click reaction. FT-IR spectra (Figure 6.5) further confirmed the high efficiency of click reaction, as the azide absorption at 2100 cm^{-1} disappeared completely after reaction.

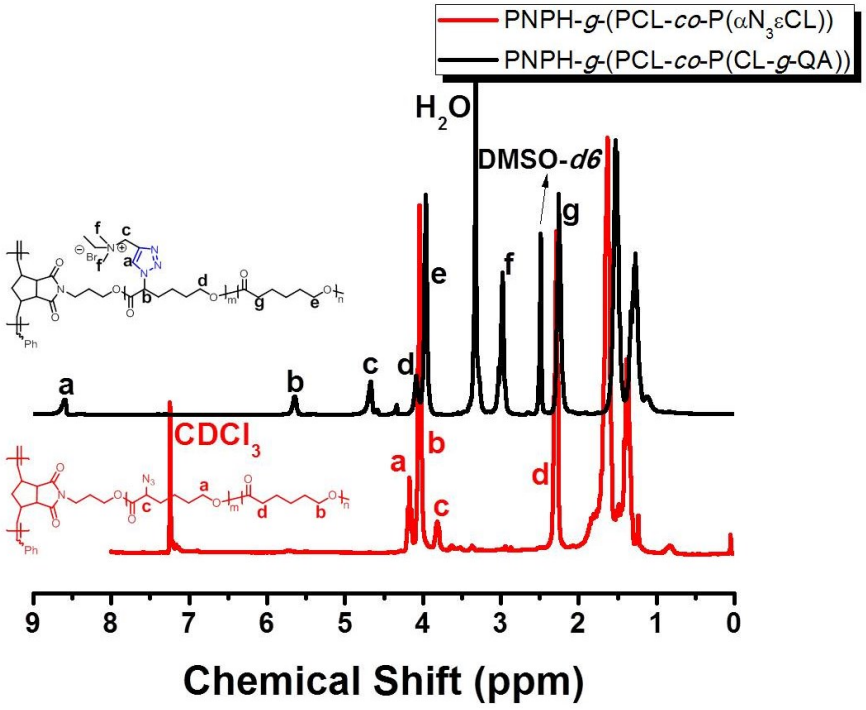

Figure 6.4 ^{1}H NMR spectra of PNPH-*g*-[PCL-*co*-P(αN3εCL)] and PNPH-*g*-[PCL-*co*-P(CL-*g*-QA)]

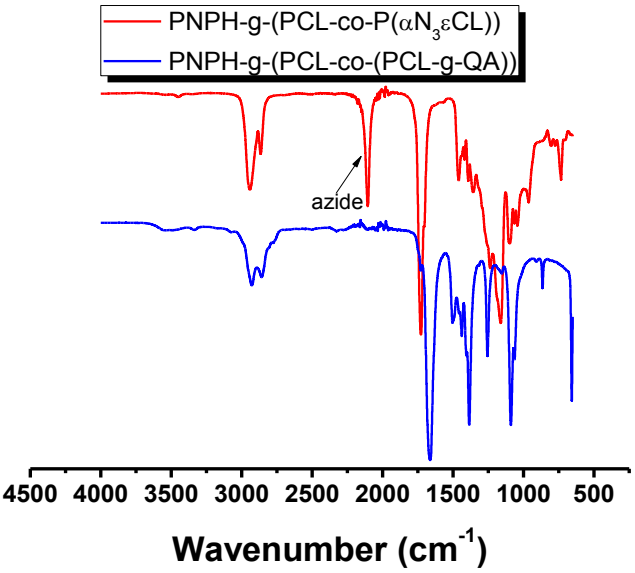

Figure 6.5 FT-IR spectra of PNPH-*g*-[PCL-*co*-P(αN3εCL)] and PNPH-*g*-[PCL-*co*-P(CL-*g*-QA)]

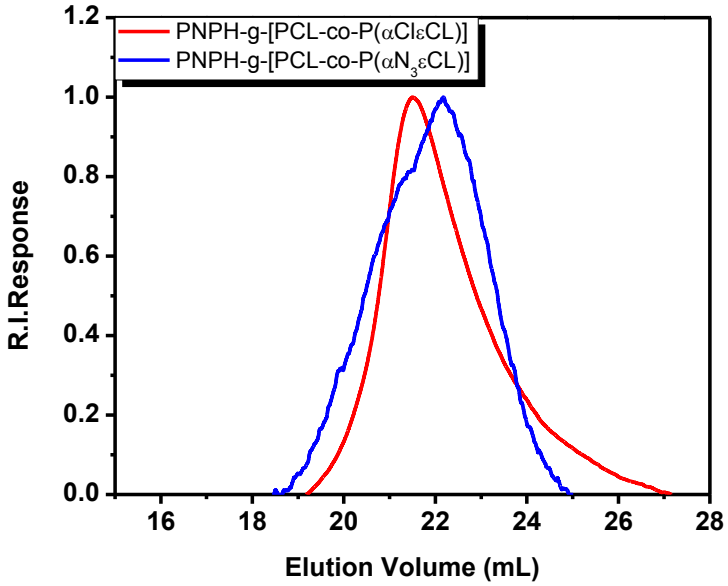

Figure 6.6 GPC traces of PNPH-*g*-[PCL-*co*-P(αClεCL)] and PNPH-*g*-[PCL-*co*-P(αN3εCL)]

Salt Response of Bottle-Brush Polymers: Salt-responsive property of molecular brushes PNPH-*g*-[PCL-*co*-P(CL-*g*-QA)] was characterized with the aid of UV-Vis spectroscopy and AFM. [211] The brushes were dissolved in DI water with a concentration

of 1 mg/mL (or 0.1 wt%). Then a series of copolymer solutions with different salt concentrations were prepared by adding NaCl into the solutions. Figure 6.7(a) shows the visual appearance of the polymer brush solutions.

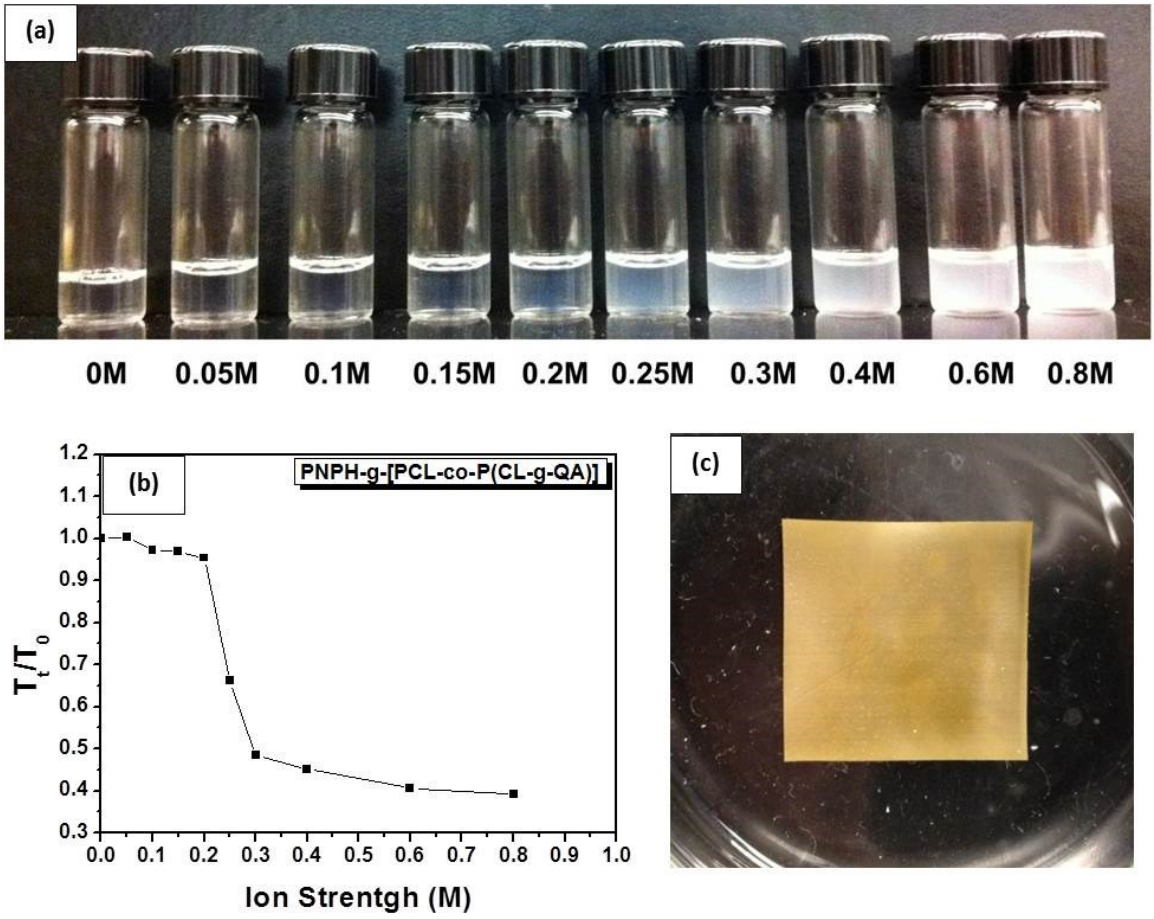

Figure 6.7 (a) PNPH-*g*-[PCL-*co*-P(CL-*g*-QA)] (20 mol% QA) solutions in water (1 mg/ mL) containing different ionic strength of NaCl solution. (b) Dependence of turbidity of molecular brush PNPH-*g*-[PCL-*co*-P(CL-*g*-QA)] with 20 mol% QA groups (Table 6.2, Entry 1) solutions (at 800 nm) on ionic strength of NaCl solution. (c) Films of PNPH-*g*-[PCL-*co*-P(CL-*g*-QA)] brush (Table 6.2, Entry 1)

PNPH-*g*-[PCL-*co*-P(CL-*g*-QA)] molecular brush with 20 mol% QA groups was well dissolved in salt-free water to produce a transparent aqueous solution. With the increase of NaCl concentration, the polymer brush solutions turned increasingly turbid. When the ionic strength of NaCl solution was between 0.15 M and 0.3 M, the solution

changed from slightly unclear and turbid to milky. As the ionic strength of NaCl solution reached 0.4 M or higher, the solution formed an opaque suspension with some precipitation at the bottom of vials. It is worthy to mention that due to the sufficiently high molecular weight, this molecular brush can produce nice films, which are important for applications in personal-care products (Figure 6.7 (c)). Thorough studies of the mechanical properties of prepared molecular brushes is beyond the scope of this paper. It should be pointed out that we also tested the salt response of molecular brushes with different fraction of QA groups. Brushes with less charged groups (e.g. 15 mol% QA) have limited solubility in DI water (Figure 6.8 (a)). For the brush with more ionic groups (30 mol% QA), brush solutions were transparent and did not show much change with the increase of ionic strength (Figure 6.8 (b) and Figure 6.9).

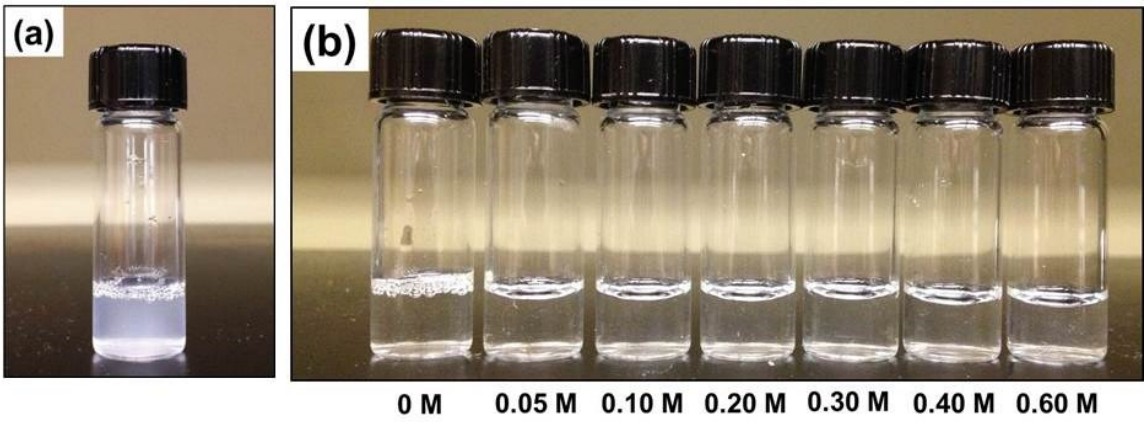

Figure 6.8 (a) PNPH-*g*-[PCL-*co*-P(CL-*g*-QA)] with 15 mol% QA groups **(**Table 6.2, Entry 5**)** solutions in water (1 mg/ mL). (b) PNPH-*g*-[PCL-*co*-P(CL-*g*-QA)] with 30 mol% QA groups (Table 6.2, Entry 4) solutions in water (1 mg/ mL) containing different ionic strength of NaCl solution

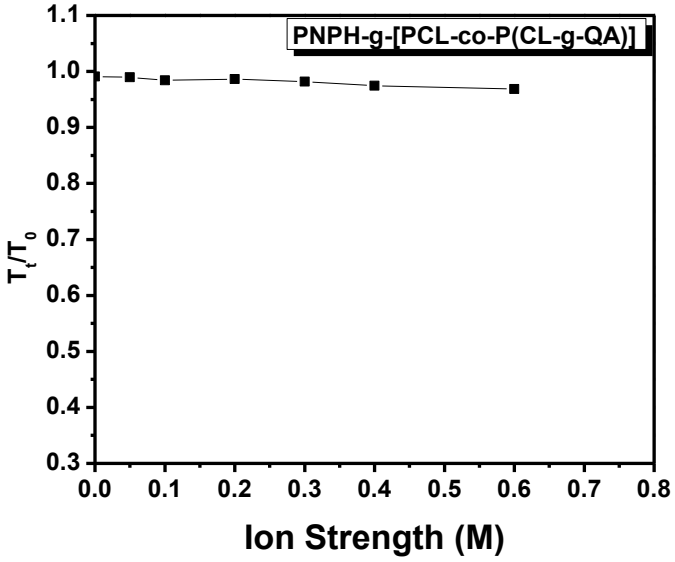

Figure 6.9 Dependence of turbidity of molecular brush PNPH-*g*-[PCL-*co*-P(CL-*g*-QA)] with 30 mol% QA groups (Table 6.2, Entry 4) solutions (at 800 nm) on ionic strength of NaCl solution

The optical turbidity (at 800 nm) of PNPH-*g*-[PCL-*co*-P(CL-*g*-QA)] brushes was then measured by a UV-Visible spectrophotometer at room temperature. We tested the transmittance of the solutions (T_t) and compared with that of DI water (T_0), as shown by solution transmittance ratio (T_t/T_0) as a function of ionic strength of salt solution in Figure 6.7 (b). The transmittance ratio showed an obvious sharp decrease when the ionic strength of NaCl solution was more than 0.2 M, which corresponded to the formation of slightly turbid solution. When the ionic strength of NaCl solution reached higher than 0.4M, the T_t/T_0 value dropped to less than 0.45, corresponding to the opaque suspension solution in Figure 6.7 (a).

To further confirm the salt responsive property of molecular brushes PNPH-*g*-[PCL-*co*-P(CL-*g*-QA)] with 20 mol% QA groups, we used AFM to image the morphologies of molecular brushes. First, polymer brush solutions with 0.1 mg/mL

concentration were prepared, and then NaCl was added to tune the final solutions with different salt concentrations. As shown in Figure 6.10, the polymer brushes from DI water solution showed typical extended worm-like morphology, since these brushes are completely soluble in water due to the electrostatic repulsion interactions between QA groups. The average length of single polymer brushes was around 100 ± 30 nm. Zoomed AFM image (inset in Figure 6.10 (A)) clearly showed the presence of halo around the backbone, corresponding to the extended side chains of polymer brushes. In salt-free water or diluted solution with low ionic strength, the extended conformation of molecular brushes is due to the overwhelming domination of electrostatic repulsive Coulomb interactions between cationic QA species over attractive hydrophobic-hydrophobic interactions between PCL segments. When salt was introduced into the polymer solution with a concentration of 0.05M, the polymer brushes started to shrink and curve inward, while the persistent length became much shorter (Figure 6.10(B)). In addition, the halo from side chains was not observable. When the salt concentration increased to 0.1-0.2M, a collapsed rod-like or sphere-like morphology was observed (Figure 6.10 (C)-6.10 (D)). Completely collapsed polymer brushes were observed when the salt concentration was ≥ 0.3M (Figure 6.10 (E)-6.10 (F)). With the addition of salt into the aqueous solution of copolymers, the ionic screening effect will be intensified by the free ions in water to reduce the above electrostatic repulsive Coulomb interactions between QA charges (the electric field lines between QA charges are terminated in the presence of many free ions). The polymer brushes gradually became insoluble with the increase of ionic strength, resulting in the increase of turbidity of the solution observed. Our results suggested that the free-ion screening effect can play a major role in the solubility of molecular brushes

only when there is an optimal composition range of QA groups in the brushes, mostly due to the balance of hydrophilic and hydrophobic components in the brush chain. All of these observations from AFM further confirmed the salt responsiveness results by UV-Vis spectroscopy.

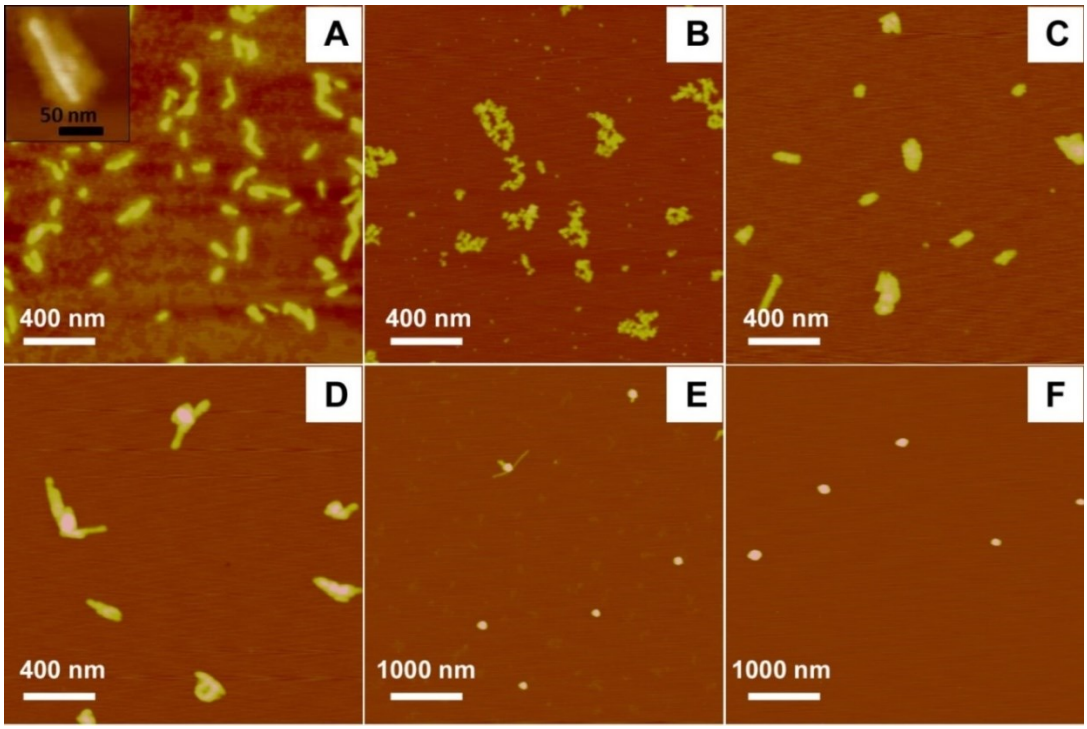

Figure 6.10 AFM images of molecular brush PNPH-*g*-[PCL-*co*-P(CL-*g*-QA)] with 20 mol% QA groups from aqueous solutions with different ionic strength: (A) 0 M; (B) 0.05M; (C) 0.1M; (D) 0.2M; (E) 0.3M; (F) 0.4 M

Degradability of Molecular Brushes: The degradability of cationic polymer brush PNPH-*g*-[PCL-*co*-P(CL-*g*-QA)] was tested under acidic condition (aq. HCl). The acid and polymer concentrations were at 0.05M and 8.3 mg/mL respectively. After the degradation in acid solution, GPC was employed to measure the molecular weight of degraded products. Since the final cationic polymer brush PNPH-*g*-[PCL-*co*-P(CL-*g*-QA)] was difficult to characterize by GPC, due to the strong interaction between polyelectrolytes and GPC column, we compared the molecular weight of degraded

products with that of PNPH-*g*-[PCL-*co*-P(αClεCL)] polymer brush. The GPC traces (Figure 6.11) showed that after degradation, the high molecular weight peak completely disappeared and a very lower molecular weight peak appeared, indicating the excellent degradability of molecular brushes.

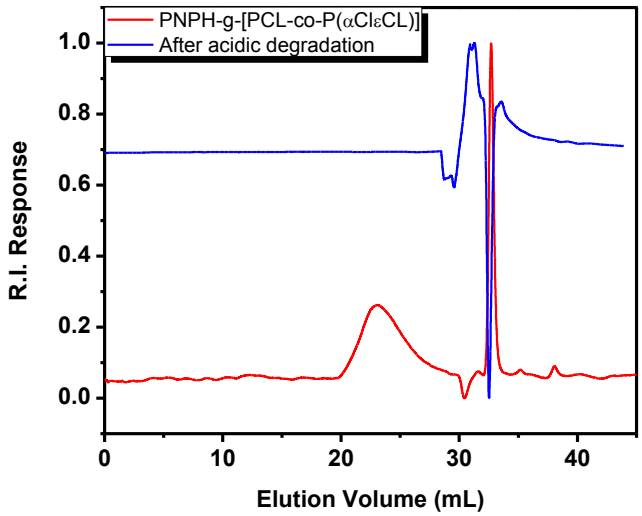

Figure 6.11 GPC traces of PNPH-*g*-[PCL-*co*-P(αClεCL)] and acid-degraded products from PNPH-*g*-[PCL-*co*-P(CL-*g*-QA)]

6.5 Conclusions

In conclusion, we have demonstrated the successful synthesis of cationic PNPH-*g*-[PCL-*co*-P(CL-*g*-QA)] molecular brushes using a "grafting-through" ROMP strategy coupled with ROP and click reaction. The versatility of ROMP and high efficiency of click reaction allowed us to obtain high molecular weight brushes with controlled PDI and controlled fractions of cationic groups. Solution test, UV-Vis and AFM analysis showed that these cationic molecular brushes exhibited excellent responsiveness to the ionic strength in aqueous solutions, given that the compositions of hydrophobic and hydrophilic components are balanced. This new class of cationic molecular brushes with

excellent salt responsive property could find potential applications in biomedical fields and personal care products.

CHAPTER 7

SUMMARY AND OUTLOOK

In this dissertation, two major research goals were achieved. First, renewable rosin acids were used to develop a series of new polymer materials containing rosin moieties via controlled/living radical polymerization techniques and "click" chemistry. (1) The rosin derived (meth) acrylate monomers were polymerized by ATRP and RAFT polymerization. The rosin homopolymers show tunable thermal property depending on the linker space between rosin and (meth) acrylate double bonds. (2) The rosin containing polyesters were prepared by ROP and click reaction and the new polyesters exhibit excellent hydrophobicity, elevated glass transition temperature, low water uptake while retaining full degradability. (3) Graft copolymers with cellulose as backbone and rosin and/or fatty acid derivatives as side chains were synthesized via "grafting from" ATRP. By adjusting the rosin content, polymers with various T_g were obtained. These graft copolymers based on renewable natural resources show good elastomeric properties and thermal stability, making them potential candidates for use as next-generation thermoplastic elastomer materials.

The second research objective is to develop degradable sat-responsive copolymers for binder applications in personal care products. First polycarprolactone containing quaternary ammonium side groups were prepared by a combination of ROP and click reaction. By adjusting the compositions of salt groups in polymers, good salt-responsive properties were observed and these polymers also show good degradability in acid solutions indicating their possible applications in biomedical field and personal care products. In order to improve the mechanical strength of degradable salt-responsive copolymers, new synthetic strategies involving ROMP, ROP, and click reaction were used to prepare salt-responsive bottle-brush polymers. These bottle brush polymers

showed good salt-responsive properties. These high molecular weight salt-responsive brush polymers exhibit improved mechanical properties, while keeping the similar salt-responsive properties.

Research on renewable bio-based polymer materials has drawn a lot of interest in the last decade and will keep growing in the future. Although the research on rosin-based monomers and polymers has been growing rapidly in the past several years, rosin is still not widely used to prepare various functional polymers compared with other renewable biomass. Due to the existence of functional groups (conjugated diene and carboxyl acid groups) in rosin acids, the preparation of new monomers derived from rosin acids for different polymerization techniques should be continuously pursued. New synthetic routes with high efficiency and less purification process are essential and favorable in the future. Our work on graft copolymers from renewable rosin and cellulose is an example how we combine renewable natural polymers (cellulose) and molecular biomass (rosin) together to get new polymers with new properties. In future research, combination of natural polymers and natural molecular biomass to prepare new materials would be a direction worthy for more attention, since it is less explored. Such combination would maximize the use of natural resources and enhance the material properties.

For the degradable salt-responsive copolymers system, we have demonstrated that these new ionic random copolymers and bottle-brush polymer can provide good salt-responsive properties in aqueous solutions. In future research, preparation of polymers with even higher molecular weight would be a potential objective. Although the bottle-brush polymers have achieved high molecular weight compared with random copolymers, their mechanical properties are still not high enough to be directly used as

binder composition in personal care paper products. New polymerization techniques with high efficiency are required to prepare high molecular weight salt-responsive polymers. Also other polyesters such as polylactide acid (PLA), polyhydroxyalkanoate (PHA) should be explored as new polymer backbones for the degradable salt-responsive polymeric materials. By post-polymerization modification or new functional monomer preparation, the new degradable polyester skeletons can be prepared and integrated with salt-responsive groups via different synthetic reactions (CuAAC, thiol-ene reaction, esterification, etc.). Besides the application in personal care products, the salt-responsive polymers should be combined with other stimuli-responsive systems (pH and temperature-responsive polymers) and further explored as potential candidates in drug delivery system for biomedical applications.

REFERENCES

1. *The Technology Roadmap for Plant/Crop-Based Renewable Resources 2020*; Renewables Vision 2020, Executive Steering Group, DOE and USDA: 1999.

2. *U.S. Biobased Products: Market Potential and Projections Through 2025*; Office of the Chief Economist, Office of Energy Policy and New Uses, U.S. Department of Agriculture: 2008.

3. Beach, E. S.; Cui, Z.; Anastas, P. T., Green Chemistry: A design framework for sustainability. *Energy & Environmental Science* **2009,** *2* (10), 1038-1049.

4. Anastas, P.; Eghbali, N., Green Chemistry: Principles and Practice. *Chemical Society Reviews* **2010,** *39* (1), 301-312.

5. Anastas, P. T.; Kirchhoff, M. M., Origins, Current Status, and Future Challenges of Green Chemistry. *Accounts Of Chemical Research* **2002,** *35* (9), 686-694.

6. Okada, M., Chemical syntheses of biodegradable polymers. *Prog. Polym. Sci.* **2002,** *27* (1), 87-133.

7. Williams, C. K.; Hillmyer, M. A., Polymers from Renewable Resources: A Perspective for a Special Issue of Polymer Reviews. *Polymer Reviews* **2008,** *48* (1), 1-10.

8. Huber, G. W.; Iborra, S.; Corma, A., Synthesis of Transportation Fuels from Biomass: Chemistry, Catalysts, and Engineering. *Chemical Reviews* **2006,** *106* (9), 4044-4098.

9. Ragauskas, A. J.; Williams, C. K.; Davison, B. H.; Britovsek, G.; Cairney, J.; Eckert, C. A.; Frederick, W. J.; Hallett, J. P.; Leak, D. J.; Liotta, C. L.; Mielenz, J. R.; Murphy, R.; Templer, R.; Tschaplinski, T., The Path Forward for Biofuels and Biomaterials. *Science* **2006,** *311* (5760), 484-489.

10. Coates, G. W.; Hillmyer, M. A., A Virtual Issue of Macromolecules: "Polymers from Renewable Resources". *Macromolecules* **2009,** *42* (21), 7987-7989.

11. Corma, A.; Iborra, S.; Velty, A., Chemical Routes for the Transformation of Biomass into Chemicals. *Chemical Reviews* **2007,** *107* (6), 2411-2502.

12. Gandini, A., The Irruption of Polymers from Renewable Resources on the Scene of Maacromolecular Science and Technology. *Green Chem.* **2011,** *13* (5), 1061-1083.

13. Gandini, A., Monomers and Macromonomers from Renewable Resources. In *Biocatalysis in Polymer Chemistry*, Loos, P. K., Ed. Wiley-VCH Verlag GmbH & Co.: Weinheim, Germany, 2011; pp 1-33.

14. Mathers, R. T., How well can renewable resources mimic commodity monomers and polymers? *Journal of Polymer Science Part A: Polymer Chemistry* **2012,** *50* (1), 1-15.

15. Mathers, R. T.; Meier, M. A. R., *Green Polymerization Methods: Renewable Starting Materials, Catalysis and Waste Reduction*. Wiley-VCH: Weinheim, 2011.

16. Mecking, S., Nature or Petrochemistry?—Biologically Degradable Materials. *Angew. Chem. Int. Ed.* **2004,** *43* (9), 1078-1085.

17. Dodds, D. R.; Gross, R. A., Chemicals from Biomass. *Science* **2007,** *318* (5854), 1250-1251.

18. Gandini, A., Polymers from Renewable Resources: A Challenge for the Future of Macromolecular Materials. *Macromolecules* **2008,** *41* (24), 9491-9504.

19. Eichhorn, S. J.; Dufresne, A.; Aranguren, M.; Marcovich, N. E.; Capadona, J. R.; Rowan, S. J.; Weder, C.; Thielemans, W.; Roman, M.; Renneckar, S.; Gindl, W.; Veigel, S.; Keckes, J.; Yano, H.; Abe, K.; Nogi, M.; Nakagaito, A. N.; Mangalam, A.; Simonsen, J.; Benight, A. S.; Bismarck, A.; Berglund, L. A.; Peijs, T., Review: current international research into cellulose nanofibres and nanocomposites. *J. Mater. Sci.* **2010,** *45* (1), 1-33.

20. Kubo, S.; Gilbert, R. D.; Kadla, J. F., Lignin-Based Polymer Blends and Bicomposte Materials. In *Natural Fibers, Biopolymers, and Biocomposites*, Mohanty, A. K.; Misra, M.; Drzal, L. T., Eds. CRC Press: Boca Raton, Florida, 2005; pp 671-698.

21. Kumar, M. N. V. R.; Muzzarelli, R. A. A.; Muzzarelli, C.; Sashiwa, H.; Domb, A. J., Chitosan Chemistry and Pharmaceutical Perspectives. *Chem. Rev.* **2004,** *104* (12), 6017-6084.

22. Pillai, C.; Paul, W.; Sharma, C., Chitin and chitosan polymers: Chemistry, solubility, and fiber formation. *Prog. Polym. Sci.* **2009,** *34* (7), 641-678.

23. Rinaudo, M., Chitin and chitosan: Properties and applications. *Prog. Polym. Sci.* **2006,** *31* (7), 603-632.

24. Rose, M.; Palkovits, R., Cellulose-Based Sustainable Polymers: State of the Art and Future Trends. *Macromol. Rapid Commun.* **2011,** *32* (17), 1299-1311.

25. Samir, M. A. S. A.; Alloin, F.; Dufresne, A., Review of Recent Research into Cellulosic Whiskers, Their Properties and Their Application in Nanocomposite Field. *Biomacromolecules* **2005,** *6* (2), 612-626.

26. Gandini, A.; Belgacem, M. N., Furans in polymer chemistry. *Prog. Polym. Sci.* **1997,** *22* (6), 1203-1379.

27. Meier, M. A. R.; Metzger, J. O.; Schubert, U. S., Plant oil renewable resources as green alternatives in polymer science. *Chemical Society Reviews* **2007,** *36* (11), 1788-1802.

28. Montero de Espinosa, L.; Meier, M. A. R., Plant oils: The perfect renewable resource for polymer science?! *European Polymer Journal* **2011,** *47* (5), 837-852.

29. Mutlu, H.; Meier, M. A. R., Castor oil as a renewable resource for the chemical industry. *European Journal Of Lipid Science And Technology* **2010,** *112* (1), 10-30.

30. Seniha Güner, F.; Yağcı, Y.; Tuncer Erciyes, A., Polymers from triglyceride oils. *Prog. Polym. Sci.* **2006,** *31* (7), 633-670.

31. Silvestre, A. J. D.; Gandini, A., Rosin: Major Sources, Properties and Applications. In *Monomers, Polymers and Composites from Renewable Resources*, Belgacem, M.; Gandini, A., Eds. Elsevier: Amsterdam, 2008; pp 67-88.

32. Silvestre, A. J. D.; Gandini, A., Terpenes: Major Sources, Properties and Applications. In *Monomers, Polymers and Composites from Renewable Resources*, Belgacem, M. N.; Gandini, A., Eds. Elsevier: Amsterdam, 2008; pp 17-38.

33. Trzaskowski, J.; Quinzler, D.; Bährle, C.; Mecking, S., Aliphatic Long-Chain C_{20} Polyesters from Olefin Metathesis. *Macromol. Rapid Commun.* **2011,** *32* (17), 1352-1356.

34. Türünç, O.; Meier, M. A. R., Fatty Acid Derived Monomers and Related Polymers Via Thiol-ene (Click) Additions. *Macromol. Rapid Commun.* **2010,** *31* (20), 1822-1826.

35. Wilbon, P.; Chu, F.; Tang, C., Progress in Renewable Polymers from Natural Terpenes, Terpenoids and Rosin. *Macromol. Rapid Commun.* **2013,** *34* (1), 8-37.

36. Zhang, J., *Rosin-based Chemicals and Polymers*. ISmithers: Shawbury, UK, 2012.

37. Yao, K.; Tang, C., Controlled Polymerization of Next-Generation Renewable Monomers and Beyond. *Macromolecules* **2013,** *46* (5), 1689-1712.

38. Chen, G.-Q., A microbial polyhydroxyalkanoates (PHA) based bio- and materials industry. *Chemical Society Reviews* **2009,** *38* (8), 2434-2446.

39. Chen, G.-Q.; Patel, M. K., Plastics Derived from Biological Sources: Present and Future: A Technical and Environmental Review. *Chemical Reviews* **2012,** *112* (4), 2082-2099.

40. Poirier, Y., Green chemistry yields a better plastic. *Nature Biotechnology* **1999,** *17* (10), 960-961.

41. Biermann, U.; Bornscheuer, U.; Meier, M. A. R.; Metzger, J. O.; Schäfer, H. J., Oils and Fats as Renewable Raw Materials in Chemistry. *Angewandte Chemie International Edition* **2011,** *50* (17), 3854-3871.

42. Maiti, S.; Ray, S. S.; Kundu, A. K., Rosin: a renewable resource for polymers and polymer chemicals. *Prog. Polym. Sci.* **1989,** *14*, 297-338.

43. Sinha Roy, S.; Kundu, A. K.; Maiti, S., Polymers from renewable resources--13. Polymers from rosin acrylic acid adduct. *European Polymer Journal* **1990,** *26* (4), 471-474.

44. Atta, A. M.; Nassar, I. F.; Bedawy, H. M., Unsaturated polyester resins based on rosin maleic anhydride adduct as corrosion protections of steel. *React. Funct. Polym.* **2007,** *67*, 617-626.

45. Lee, J. S.; Hong, S., Synthesis of acrylic rosin derivatives and application as negative photoresist. *European Polymer Journal* **2002,** *38*, 387-392.

46. Zhang, Y.; Heath, R. J.; Hourston, D. J., Morphology, mechanical properties, and thermal stability of polyurethane–epoxide resin interpenetrating polymer network rigid foams. *Journal of Applied Polymer Science* **2000,** *75* (3), 406-416.

47. Bicu, I.; Mustata, F., Water soluble polymers from Diels-Alder adducts of abietic acid as paper additives. *Macromol. Mater. Eng.* **2000,** *280-281*, 47-53.

48. Do, H.-S.; Park, J.-H.; Kim, H.-J., Synthesis and characteristics of photoactive-hydrogenated rosin epoxy methacrylate for pressure sensitive adhesives. *Journal of Applied Polymer Science* **2009,** *111*, 1172-1176.

49. Le Thi Nhut, H.; Pascault, J. P.; Lam Thanh, M.; Chu Pham Ngoc, S., Unsaturated polyester prepolymer from rosin. *European Polymer Journal* **1993,** *29* (4), 491-495.

50. Kim, S. J.; Kim, B. J.; Jang, D. W.; Kim, S. H.; Park, S. Y.; Lee, J.-H.; Lee, S.-D.; Choi, D. H., Photoactive polyamideimides synthesized by the polycondensation of azo-dye diamines and rosin derivative. *Journal of Applied Polymer Science* **2001,** *79* (4), 687-695.

51. Bicu, I.; Mustata, F., Polymers from a levopimaric acid–acrylonitrile Diels–Alder adduct: Synthesis and characterization. *Journal of Polymer Science Part A: Polymer Chemistry* **2005,** *43* (24), 6308-6322.

52. Wang, J.-F.; Lin, M.-T.; Wang, C.-P.; Chu, F.-X., Study on the synthesis, characterization and kinetic of bulk polymerization of disproportionated rosin (acryloxyl ethyl) ester. *Journal of Applied Polymer Science* **2009,** *113*, 3757-3765.

53. Alarcon, C. d. l. H.; Pennadam, S.; Alexander, C., Stimuli responsive polymers for biomedical applications. *Chemical Society Reviews* **2005,** *34* (3), 276-285.

54. Li, M.-H.; Keller, P., Stimuli-responsive polymer vesicles. *Soft Matter* **2009,** *5* (5), 927-937.

55. Liu, F.; Urban, M. W., Recent advances and challenges in designing stimuli-responsive polymers. *Prog. Polym. Sci.* **2010,** *35* (1–2), 3-23.

56. Meng, F.; Zhong, Z.; Feijen, J., Stimuli-Responsive Polymersomes for Programmed Drug Delivery. *Biomacromolecules* **2009,** *10* (2), 197-209.

57. Smith, A. E.; Xu, X.; McCormick, C. L., Stimuli-responsive amphiphilic (co)polymers via RAFT polymerization. *Prog. Polym. Sci.* **2010,** *35* (1–2), 45-93.

58. Stuart, M. A. C.; Huck, W. T. S.; Genzer, J.; Muller, M.; Ober, C.; Stamm, M.; Sukhorukov, G. B.; Szleifer, I.; Tsukruk, V. V.; Urban, M.; Winnik, F.; Zauscher, S.; Luzinov, I.; Minko, S., Emerging applications of stimuli-responsive polymer materials. *Nat. Mater.* **2010,** *9*, 101-113.

59. Tokarev, I.; Orlov, M.; Minko, S., Responsive Polyelectrolyte Gel Membranes. *Adv. Mater.* **2006,** *18* (18), 2458-2460.

60. Urban, M. W., Intelligent Polymeric Coatings; Current and Future Advances. *J. Macromol. Sci. Part C: Polym. Rev.* **2006,** *46* (4), 329-339.

61. Alexander, C.; Shakesheff, K. M., Responsive Polymers at the Biology/Materials Science Interface. *Adv. Mater.* **2006,** *18* (24), 3321-3328.

62. Lee, H.-i.; Pietrasik, J.; Sheiko, S. S.; Matyjaszewski, K., Stimuli-responsive molecular brushes. *Prog. Polym. Sci.* **2010,** *35* (1â€“2), 24-44.

63. Hu, J.; Liu, S., Responsive Polymers for Detection and Sensing Applications: Current Status and Future Developments. *Macromolecules* **2010,** *43* (20), 8315-8330.

64. Du, J.; Tang, Y.; Lewis, A. L.; Armes, S. P., pH-Sensitive Vesicles Based on a Biocompatible Zwitterionic Diblock Copolymer. *J. Am. Chem. Soc.* **2005,** *127* (51), 17982-17983.

65. Guice, K. B.; Marrou, S. R.; Gondi, S. R.; Sumerlin, B. S.; Loo, Y.-L., pH Response of Model Diblock and Triblock Copolymer Networks Containing Polystyrene and Poly(2-hydroxyethyl methacrylate-co-2-(dimethylamino)ethyl methacrylate). *Macromolecules* **2008,** *41* (12), 4390-4397.

66. Darcos, V.; El Habnouni, S.; Nottelet, B.; El Ghzaoui, A.; Coudane, J., Well-defined PCL-graft-PDMAEMA prepared by ring-opening polymerisation and click chemistry. *Polym. Chem.* **2010,** *1*, 280-282.

67. Li, Y.; Zhang, Y.; Yang, D.; Li, Y.; Hu, J.; Feng, C.; Zhai, S.; Lu, G.; Huang, X., PAA-g-PPO Amphiphilic Graft Copolymer: Synthesis and Diverse Micellar Morphologies. *Macromolecules* **2009,** *43* (1), 262-270.

68. Xiong, Z.; Peng, B.; Han, X.; Peng, C.; Liu, H.; Hu, Y., Dual-stimuli responsive behaviors of diblock polyampholyte PDMAEMA-b-PAA in aqueous solution. *Journal of Colloid and Interface Science* **2011,** *356* (2), 557-565.

69. Zhang, W.; He, J.; Liu, Z.; Ni, P.; Zhu, X., Biocompatible and pH-responsive triblock copolymer mPEG-b-PCL-b-PDMAEMA: Synthesis, self-assembly, and application. *Journal of Polymer Science Part A: Polymer Chemistry* **2010,** *48* (5), 1079-1091.

70. De, P.; Li, M.; Gondi, S. R.; Sumerlin, B. S., Temperature-Regulated Activity of Responsive Polymerâ˜Protein Conjugates Prepared by Grafting-from via RAFT Polymerization. *J. Am. Chem. Soc.* **2008,** *130* (34), 11288-11289.

71. Vogt, A. P.; Sumerlin, B. S., Tuning the Temperature Response of Branched Poly(N-isopropylacrylamide) Prepared by RAFT Polymerization. *Macromolecules* **2008,** *41* (20), 7368-7373.

72. Wang, D.; Liu, T.; Yin, J.; Liu, S., Stimuli-Responsive Fluorescent Poly(N-isopropylacrylamide) Microgels Labeled with Phenylboronic Acid Moieties as Multifunctional Ratiometric Probes for Glucose and Temperatures. *Macromolecules* **2011,** *44* (7), 2282-2290.

73. Wu, T.; Ge, Z.; Liu, S., Fabrication of Thermoresponsive Cross-Linked Poly(N-isopropylacrylamide) Nanocapsules and Silver Nanoparticle-Embedded Hybrid Capsules with Controlled Shell Thickness. *Chem. Mater.* **2011,** *23* (9), 2370-2380.

74. Li, L.-Y.; He, W.-D.; Li, J.; Zhang, B.-Y.; Pan, T.-T.; Sun, X.-L.; Ding, Z.-L., Shell-Cross-Linked Micelles from PNIPAM-b-(PLL)2 Y-Shaped Miktoarm Star Copolymer as Drug Carriers. *Biomacromolecules* **2010,** *11* (7), 1882-1890.

75. Scherzinger, C.; Lindner, P.; Keerl, M.; Richtering, W., Cononsolvency of Poly(N,N-diethylacrylamide) (PDEAAM) and Poly(N-isopropylacrylamide) (PNIPAM) Based Microgels in Water/Methanol Mixtures: Copolymer vs Core−Shell Microgel. *Macromolecules* **2010,** *43* (16), 6829-6833.

76. Buss, F.; Roberts, C. C.; Crawford, K. S.; Peters, K.; Francis, L. F., Effect of soluble polymer binder on particle distribution in a drying particulate coating. *Journal of Colloid and Interface Science* **2011,** *359* (1), 112-120.

77. Gill, E.; Arshak, A.; Arshak, K.; Korostynska, O., Response mechanism of novel polyaniline composite conductimetric pH sensors and the effects of polymer binder, surfactant and film thickness on sensor sensitivity. *European Polymer Journal* **2010,** *46* (10), 2042-2050.

78. Molhoek, L. J. N.; Wories, H. J. N. Binder composition based on an acrylate polymer and a crosslinking agent based on an acetoacetate compound. May 06, 1992.

79. Matyjaszewski, K., Atom Transfer Radical Polymerization (ATRP): Current Status and Future Perspectives. *Macromolecules* **2012,** *45* (10), 4015-4039.

80. Siegwart, D. J.; Oh, J. K.; Matyjaszewski, K., ATRP in the design of functional materials for biomedical applications. *Prog. Polym. Sci.* **2012,** *37* (1), 18-37.

81. Wang, J.-S.; Matyjaszewski, K., Controlled/"living" radical polymerization. atom transfer radical polymerization in the presence of transition-metal complexes. *J. Am. Chem. Soc.* **1995,** *117* (20), 5614-5615.

82. Chiefari, J.; Mayadunne, R. T. A.; Moad, C. L.; Moad, G.; Rizzardo, E.; Postma, A.; Thang, S. H., Thiocarbonylthio Compounds (SC(Z)S−R) in Free Radical Polymerization with Reversible Addition-Fragmentation Chain Transfer (RAFT Polymerization). Effect of the Activating Group Z. *Macromolecules* **2003,** *36* (7), 2273-2283.

83. Chiefari, J.; Chong, Y. K.; Ercole, F.; Krstina, J.; Jeffery, J.; Le, T. P. T.; Mayadunne, R. T. A.; Meijs, G. F.; Moad, C. L.; Moad, G.; Rizzardo, E.; Thang, S. H., Living Free-Radical Polymerization by Reversible Addition−Fragmentation Chain Transfer: The RAFT Process. *Macromolecules* **1998,** *31* (16), 5559-5562.

84. Barner-Kowollik, C., *Handbook of RAFT Polymerization*. Wiley: 2008.

85. Meijs, G. F.; Rizzardo, E.; Thang, S. H., Preparation of controlled-molecular-weight, olefin-terminated polymers by free radical methods. Chain transfer using allylic sulfides. *Macromolecules* **1988,** *21* (10), 3122-3124.

86. Nuyken, O.; Pask, S., Ring-Opening Polymerization—An Introductory Review. *Polymers* **2013,** *5* (2), 361-403.

87. Sutar, A. K.; Maharana, T.; Dutta, S.; Chen, C.-T.; Lin, C.-C., Ring-opening polymerization by lithium catalysts: an overview. *Chemical Society Reviews* **2010,** *39* (5), 1724-1746.

88. Albertsson, A.-C.; Varma, I. K., Recent Developments in Ring Opening Polymerization of Lactones for Biomedical Applications. *Biomacromolecules* **2003,** *4* (6), 1466-1486.

89. Hejl, A.; Scherman, O. A.; Grubbs, R. H., Ring-Opening Metathesis Polymerization of Functionalized Low-Strain Monomers with Ruthenium-Based Catalysts. *Macromolecules* **2005,** *38* (17), 7214-7218.

90. Atallah, P.; Wagener, K. B.; Schulz, M. D., ADMET: The Future Revealed. *Macromolecules* **2013,** *46* (12), 4735-4741.

91. Bielawski, C. W.; Grubbs, R. H., Living ring-opening metathesis polymerization. *Prog. Polym. Sci.* **2007,** *32* (1), 1-29.

92. Sumerlin, B. S.; Vogt, A. P., Macromolecular Engineering through Click Chemistry and Other Efficient Transformations. *Macromolecules* **2009,** *43* (1), 1-13.

93. Hein, J. E.; Fokin, V. V., Copper-catalyzed azide-alkyne cycloaddition (CuAAC) and beyond: new reactivity of copper(i) acetylides. *Chemical Society Reviews* **2010,** *39* (4), 1302-1315.

94. Rostovtsev, V. V.; Green, L. G.; Fokin, V. V.; Sharpless, K. B., A Stepwise Huisgen Cycloaddition Process: Copper(I)-Catalyzed Regioselective "Ligation" of Azides and Terminal Alkynes. *Angewandte Chemie International Edition* **2002,** *41* (14), 2596-2599.

95. Tornøe, C. W.; Christensen, C.; Meldal, M., Peptidotriazoles on Solid Phase: [1,2,3]-Triazoles by Regiospecific Copper(I)-Catalyzed 1,3-Dipolar Cycloadditions of Terminal Alkynes to Azides. *The Journal of Organic Chemistry* **2002,** *67* (9), 3057-3064.

96. Wu, P.; Feldman, A. K.; Nugent, A. K.; Hawker, C. J.; Scheel, A.; Voit, B.; Pyun, J.; Fréchet, J. M. J.; Sharpless, K. B.; Fokin, V. V., Efficiency and Fidelity in a Click-Chemistry Route to Triazole Dendrimers by the Copper(I)-Catalyzed Ligation of Azides and Alkynes. *Angewandte Chemie International Edition* **2004,** *43* (30), 3928-3932.

97. O'Reilly, R. K.; Joralemon, M. J.; Hawker, C. J.; Wooley, K. L., Fluorogenic 1,3-Dipolar Cycloaddition within the Hydrophobic Core of a Shell Cross-Linked Nanoparticle. *Chemistry – A European Journal* **2006,** *12* (26), 6776-6786.

98. Mantovani, G.; Ladmiral, V.; Tao, L.; Haddleton, D. M., One-pot tandem living radical polymerisation-Huisgens cycloaddition process ("click") catalysed by N-alkyl-2-pyridylmethanimine/Cu(i)Br complexes. *Chemical Communications* **2005,** (16), 2089-2091.

99. Golas, P. L.; Tsarevsky, N. V.; Matyjaszewski, K., Structure–Reactivity Correlation in "Click" Chemistry: Substituent Effect on Azide Reactivity. *Macromol. Rapid Commun.* **2008,** *29* (12-13), 1167-1171.

100. Altintas, O.; Hizal, G.; Tunca, U., ABC-type hetero-arm star terpolymers through "Click" chemistry. *Journal of Polymer Science Part A: Polymer Chemistry* **2006,** *44* (19), 5699-5707.

101. Gunera, F. S.; Yagci, Y.; Erciyes, A. T., Polymers from triglyceride oils. *Prog. Polym. Sci.* **2006,** *31*, 633-670.

102. Wool, R. P.; Knot, S. N.; LaScala, J. J.; Bunker, S. P.; Lu, J.; Thielemans, W.; Can, E.; Morye, S. S.; Williams, G. I., Affordable composites and plastics from renewable resources: part 1: synthesis of monomers and polymers. In *Advancing sustainability through green chemistry and engineering*, Lankey, R. L., Ed. American Chemical Society: Washington, D.C., 2002; Vol. 823, pp 177-204.

103. Lowe, J. R.; Tolman, W. B.; Hillmyer, M. A., Oxidized dihydrocarvone as a renewable multifunctional monomer for the synthesis of shape memory polyesters. *Biomacromolecules* **2009,** *10*, 2003-2008.

104. Kobayashi, S.; Lu, C.; Hillmyer, M. A., *J. Am. Chem. Soc.* **2009,** *131*, 7960-7961.

105. Maiti, S.; Das, S.; Maiti, M.; Ray, A., In *Polymer Application of Renewable-Resource Materials*, Carraher, C. E.; Sperling, L. H., Eds. Plenum Press: New York, 1983; p 129.

106. Lu, X.; Gong, S.; Meng, L.; Li, C.; Yang, S.; Zhang, L., Controllable synthesis of poly(N-vinylpyrrolidone) and its block copolymers by atom transfer radical polymerization. *Polymer* **2007,** *48* (10), 2835-2842.

107. Mustata, F.; Bicu, I., A novel route for synthesizing esters and polyesters from the Diels-Alder adduct of levopimaric acid and acrylic acid. *European Polymer Journal* **2010,** *46*, 1316-1327.

108. Matyjaszewski, K.; Xia, J., Atom Transfer Radical Polymerization. *Chemical Reviews* **2001,** *101* (9), 2921-2990.

109. Hawker, C. J.; Bosman, A. W.; Harth, E., New polymer synthesis by nitroxide mediated living radical polymerizations. *Chemical Reviews* **2001,** *101* (12), 3661-3688.

110. Moad, G.; Rizzardo, E.; Thang, S. H., Living radical polymerization by the RAFT process. *Aust. J. Chem.* **2005,** *58*, 379-410.

111. Xia, J.; Gaynor, S. G.; Matyjaszewski, K., Controlled/"Living" Radical Polymerization. Atom Transfer Radical Polymerization of Acrylates at Ambient Temperature. *Macromolecules* **1998,** *31* (17), 5958-5959.

112. Guo, T.-Y.; Liu, P.; Zhu, J.-W.; Song, M.-D.; Zhang, B.-H., Well-Defined Lactose-Containing Polymer Grafted onto Silica Particles. *Biomacromolecules* **2006,** *7* (4), 1196-1202.

113. Moad, G.; Chiefari, J.; Chong, Y. K.; Krstina, J.; Mayadunne, R. T. A.; Postma, A.; Rizzardo, E.; Thang, S. H., Living free radical polymerization with reversible addition – fragmentation chain transfer (the life of RAFT). *Polym. Int.* **2000,** *49* (9), 993-1001.

114. Zheng, Y.; Yao, K.; Lee, J.; Chandler, D.; Wang, J.; Wang, C.; Chu, F.; Tang, C., Well-Defined Renewable Polymers Derived from Gum Rosin. *Macromolecules* **2010,** *43* (14), 5922-5924.

115. Huang, C.-F.; Nicolay, R.; Kwak, Y.; Chang, F.-C.; Matyjaszewski, K., Homopolymerization and Block Copolymerization of N-Vinylpyrrolidone by ATRP and RAFT with Haloxanthate Inifers. *Macromolecules* **2009,** *42* (21), 8198-8210.

116. Matyjaszewski, K.; Nakagawa, K.; Jasieczek, C. G., Polymerization of n-Butyl Acrylate by Atom Transfer Radical Polymerization. Remarkable Effect of Ethylene Carbonate and Other Solvents. *Macromolecules* **1998,** *31*, 1535-1541.

117. Pascual, S.; Coutin, B.; Tardi, M.; Polton, A.; Vairon, J. P., *Macromolecules* **1999,** *32*, 1432-1437.

118. Jeong, W.; Shin, E. J.; Culkin, D. A.; Hedrick, J. L.; Waymouth, R. M., Zwitterionic Polymerization: A Kinetic Strategy for the Controlled Synthesis of Cyclic Polylactide. *J. Am. Chem. Soc.* **2009,** *131* (13), 4884-4891.

119. Jiang, X.; Smith, M. R.; Baker, G. L., Water-Soluble Thermoresponsive Polylactides. *Macromolecules* **2007,** *41* (2), 318-324.

120. Van Horn, B. A.; Iha, R. K.; Wooley, K. L., Sequential and Single-Step, One-Pot Strategies for the Transformation of Hydrolytically Degradable Polyesters into Multifunctional Systems. *Macromolecules* **2008,** *41* (5), 1618-1626.

121. Petrović, Z. S.; Milić, J.; Xu, Y.; Cvetković, I., A Chemical Route to High Molecular Weight Vegetable Oil-Based Polyhydroxyalkanoate. *Macromolecules* **2010,** *43* (9), 4120-4125.

122. Van de Velde, K.; Kiekens, P., Biopolymers: overview of several properties and consequences on their applications. *Polymer Testing* **2002,** *21* (4), 433-442.

123. Gross, R. A.; Kalra, B., Biodegradable Polymers for the Environment. *Science* **2002,** *297* (5582), 803-807.

124. Amass, W.; Amass, A.; Tighe, B., A review of biodegradable polymers: uses, current developments in the synthesis and characterization of biodegradable polyesters, blends of biodegradable polymers and recent advances in biodegradation studies. *Polym. Int.* **1998,** *47* (2), 89-144.

125. Siracusa, V.; Rocculi, P.; Romani, S.; Rosa, M. D., Biodegradable polymers for food packaging: a review. *Trends In Food Science & Technology* **2008,** *19* (12), 634-643.

126. Ravi Kumar, M. N. V., A review of chitin and chitosan applications. *React. Funct. Polym.* **2000,** *46* (1), 1-27.

127. Haynes, D.; Abayasinghe, N. K.; Harrison, G. M.; Burg, K. J.; Smith, D. W., In Situ Copolyesters Containing Poly(l-lactide) and Poly(hydroxyalkanoate) Units. *Biomacromolecules* **2007,** *8* (4), 1131-1137.

128. Woodruff, M. A.; Hutmacher, D. W., The return of a forgotten polymer--Polycaprolactone in the 21st century. *Prog. Polym. Sci.* **2010,** *35* (10), 1217-1256.

129. Villarroya, S.; Zhou, J.; Duxbury, C. J.; Heise, A.; Howdle, S. M., Synthesis of Semifluorinated Block Copolymers Containing Poly(ε-caprolactone) by the Combination of ATRP and Enzymatic ROP in scCO2. *Macromolecules* **2005,** *39* (2), 633-640.

130. Lecomte, P.; Riva, R.; Schmeits, S.; Rieger, J.; Van Butsele, K.; Jérôme, C.; Jérôme, R., New Prospects for the Grafting of Functional Groups onto Aliphatic Polyesters. Ring-Opening Polymerization of α- or γ-Substituted ε-Caprolactone Followed by Chemical Derivatization of the Substituents. *Macromolecular Symposia* **2006,** *240* (1), 157-165.

131. Riva, R.; Lenoir, S.; Jérôme, R.; Lecomte, P., Functionalization of poly([epsilon]-caprolactone) by pendant hydroxyl, carboxylic acid and epoxide groups by atom transfer radical addition. *Polymer* **2005,** *46* (19), 8511-8518.

132. Pounder, R. J.; Dove, A. P., Towards poly(ester) nanoparticles: recent advances in the synthesis of functional poly(ester)s by ring-opening polymerization. *Polym. Chem.* **2010,** *1* (3), 260-271.

133. Jiang, X.; Vogel, E. B.; Smith, M. R.; Baker, G. L., "Clickable" Polyglycolides: Tunable Synthons for Thermoresponsive, Degradable Polymers. *Macromolecules* **2008,** *41* (6), 1937-1944.

134. Wilbon, P. A.; Zheng, Y.; Yao, K.; Tang, C., Renewable Rosin Acid-Degradable Caprolactone Block Copolymers by Atom Transfer Radical Polymerization and Ring-Opening Polymerization. *Macromolecules* **2010,** *43* (21), 8747-8754.

135. Jayachandran, K. N.; Takacs-Cox, A.; Brooks, D. E., Synthesis and Characterization of Polymer Brushes of Poly(N,N-dimethylacrylamide) from Polystyrene Latex by Aqueous Atom Transfer Radical Polymerization. *Macromolecules* **2002,** *35* (11), 4247-4257.

136. Lenoir, S.; Riva, R.; Lou, X.; Detrembleur, C.; Jérôme, R.; Lecomte, P., Ring-Opening Polymerization of α-Chloro-ε-caprolactone and Chemical Modification of Poly(α-chloro-ε-caprolactone) by Atom Transfer Radical Processes. *Macromolecules* **2004,** *37* (11), 4055-4061.

137. Riva, R.; Schmeits, S.; Jérôme, C.; Jérôme, R.; Lecomte, P., Combination of Ring-Opening Polymerization and "Click Chemistry": Toward Functionalization and Grafting of Poly(ε-caprolactone). *Macromolecules* **2007,** *40* (4), 796-803.

138. Riva, R.; Lussis, P.; Lenoir, S.; Jérôme, C.; Jérôme, R.; Lecomte, P., Contribution of "click chemistry" to the synthesis of antimicrobial aliphatic copolyester. *Polymer* **2008,** *49* (8), 2023-2028.

139. Opsteen, J. A.; van Hest, J. C. M., Modular synthesis of block copolymers via cycloaddition of terminal azide and alkyne functionalized polymers. *Chemical Communications* **2005,** (1), 57-59.

140. Iha, R. K.; Wooley, K. L.; Nyström, A. M.; Burke, D. J.; Kade, M. J.; Hawker, C. J., Applications of Orthogonal "Click" Chemistries in the Synthesis of Functional Soft Materials. *Chemical Reviews* **2009,** *109* (11), 5620-5686.

141. Kolb, H. C.; Finn, M. G.; Sharpless, K. B., Click Chemistry: Diverse Chemical Function from a Few Good Reactions. *Angewandte Chemie International Edition* **2001,** *40* (11), 2004-2021.

142. Riva, R.; Schmeits, S.; Stoffelbach, F.; Jerome, C.; Jerome, R.; Lecomte, P., Combination of ring-opening polymerization and "click" chemistry towards functionalization of aliphatic polyesters. *Chemical Communications* **2005,** (42), 5334-5336.

143. Martin, V. J. J.; Yu, Z.; Mohn, W. W., Recent advances in understanding resin acid biodegradation: microbial diversity and metabolism. *Archives of Microbiology* **1999,** *172* (3), 131-138.

144. Wanamaker, C. L.; Tolman, W. B.; Hillmyer, M. A., Hydrolytic Degradation Behavior of a Renewable Thermoplastic Elastomer. *Biomacromolecules* **2009,** *10* (2), 443-448.

145. Grijpma, D. W.; Hou, Q.; Feijen, J., Preparation of biodegradable networks by photo-crosslinking lactide, [epsilon]-caprolactone and trimethylene carbonate-based oligomers functionalized with fumaric acid monoethyl ester. *Biomaterials* **2005,** *26* (16), 2795-2802.

146. Södergård, A., Preparation of poly(ε-caprolactone)-co-poly(acrylic acid) by radiation-induced grafting. *Journal of Polymer Science Part A: Polymer Chemistry* **1998,** *36* (11), 1805-1812.

147. Miller, S. A., Sustainable Polymers: Opportunities for the Next Decade. *ACS Macro Letters* **2013,** *2* (6), 550-554.

148. Tang, C., Next-generation renewable polymers. *Green Materials* **2013,** *1*, 62-63.

149. Bhowmick, A. K.; Stephens, H., *Handbook of Elastomers, Second Edition*. Taylor & Francis: 2000.

150. Lewis, P. R.; Price, C., Electron microscopy of sym-SBS block polymers. *Polymer* **1972,** *13* (1), 20-26.

151. McIntyre, D.; Campos-Lopez, E., The Macrolattice of a Triblock Polymer. *Macromolecules* **1970,** *3* (3), 322-327.

152. Campos-Lopez, E.; McIntyre, D.; Fetters, L. J., Thermodynamic and Structural Properties of Polystyrene-Polybutadiene-Polystyrene Block Copolymers. *Macromolecules* **1973,** *6* (3), 415-423.

153. Nese, A.; Mosnáček, J.; Juhari, A.; Yoon, J. A.; Koynov, K.; Kowalewski, T.; Matyjaszewski, K., Synthesis, Characterization, and Properties of Starlike Poly(n-butyl acrylate)-b-poly(methyl methacrylate) Block Copolymers. *Macromolecules* **2010,** *43* (3), 1227-1235.

154. Tong, J. D.; Moineau, G.; Leclère, P.; Brédas; Lazzaroni, R.; Jérôme, R., Synthesis, Morphology, and Mechanical Properties of Poly(methyl methacrylate)-b-poly(n-butyl acrylate)-b-poly(methyl methacrylate) Triblocks. Ligated Anionic Polymerization vs Atom Transfer Radical Polymerization. *Macromolecules* **1999,** *33* (2), 470-479.

155. Tsarevsky, N. V.; Matyjaszewski, K., "Green" Atom Transfer Radical Polymerization: From Process Design to Preparation of Well-Defined Environmentally Friendly Polymeric Materials. *Chemical Reviews* **2007,** *107* (6), 2270-2299.

156. Matyjaszewski, K.; Tsarevsky, N. V., Nanostructured functional materials prepared by atom transfer radical polymerization. *Nat Chem* **2009,** *1* (4), 276-288.

157. Mosnáček, J.; Matyjaszewski, K., Atom Transfer Radical Polymerization of Tulipalin A: A Naturally Renewable Monomer. *Macromolecules* **2008,** *41* (15), 5509-5511.

158. Mosnáček, J.; Yoon, J. A.; Juhari, A.; Koynov, K.; Matyjaszewski, K., Synthesis, morphology and mechanical properties of linear triblock copolymers based on poly(α-methylene-γ-butyrolactone). *Polymer* **2009,** *50* (9), 2087-2094.

159. Juhari, A.; Mosnáček, J.; Yoon, J. A.; Nese, A.; Koynov, K.; Kowalewski, T.; Matyjaszewski, K., Star-like poly (n-butyl acrylate)-b-poly (α-methylene-γ-butyrolactone) block copolymers for high temperature thermoplastic elastomers applications. *Polymer* **2010,** *51* (21), 4806-4813.

160. Frick, E. M.; Zalusky, A. S.; Hillmyer, M. A., Characterization of Polylactide-b-polyisoprene-b-polylactide Thermoplastic Elastomers. *Biomacromolecules* **2003,** *4* (2), 216-223.

161. Shin, J.; Martello, M. T.; Shrestha, M.; Wissinger, J. E.; Tolman, W. B.; Hillmyer, M. A., Pressure-Sensitive Adhesives from Renewable Triblock Copolymers. *Macromolecules* **2010,** *44* (1), 87-94.

162. Wanamaker, C. L.; O'Leary, L. E.; Lynd, N. A.; Hillmyer, M. A.; Tolman, W. B., Renewable-Resource Thermoplastic Elastomers Based on Polylactide and Polymenthide. *Biomacromolecules* **2007,** *8* (11), 3634-3640.

163. Wanamaker, C. L.; Bluemle, M. J.; Pitet, L. M.; O'Leary, L. E.; Tolman, W. B.; Hillmyer, M. A., Consequences of Polylactide Stereochemistry on the Properties of Polylactide-Polymenthide-Polylactide Thermoplastic Elastomers. *Biomacromolecules* **2009,** *10* (10), 2904-2911.

164. Iatrou, H.; Mays, J. W.; Hadjichristidis, N., Regular Comb Polystyrenes and Graft Polyisoprene/Polystyrene Copolymers with Double Branches ("Centipedes"). Quality of (1,3-Phenylene)bis(3-methyl-1-phenylpentylidene)dilithium Initiator in the Presence of Polar Additives. *Macromolecules* **1998,** *31* (19), 6697-6701.

165. Zhu, Y.; Burgaz, E.; Gido, S. P.; Staudinger, U.; Weidisch, R.; Uhrig, D.; Mays, J. W., Morphology and Tensile Properties of Multigraft Copolymers with Regularly Spaced Tri-, Tetra-, and Hexafunctional Junction Points. *Macromolecules* **2006,** *39* (13), 4428-4436.

166. Duan, Y.; Thunga, M.; Schlegel, R.; Schneider, K.; Rettler, E.; Weidisch, R.; Siesler, H. W.; Stamm, M.; Mays, J. W.; Hadjichristidis, N., Morphology and Deformation Mechanisms and Tensile Properties of Tetrafunctional Multigraft Copolymers. *Macromolecules* **2009,** *42* (12), 4155-4164.

167. Weidisch, R.; Gido, S. P.; Uhrig, D.; Iatrou, H.; Mays, J.; Hadjichristidis, N., Tetrafunctional Multigraft Copolymers as Novel Thermoplastic Elastomers. *Macromolecules* **2001,** *34* (18), 6333-6337.

168. Schneider, Y.; Lynd, N. A.; Kramer, E. J.; Bazan, G. C., Novel Elastomers Prepared by Grafting n-Butyl Acrylate from Polyethylene Macroinitiator Copolymers. *Macromolecules* **2009,** *42* (22), 8763-8768.

169. Jiang, F.; Wang, Z.; Qiao, Y.; Wang, Z.; Tang, C., A Novel Architecture toward Third-Generation Thermoplastic Elastomers by a Grafting Strategy. *Macromolecules* **2013,** *46* (12), 4772-4780.

170. Klemm, D.; Heublein, B.; Fink, H.-P.; Bohn, A., Cellulose: Fascinating Biopolymer and Sustainable Raw Material. *ChemInform* **2005,** *36* (36), 10.1002/chin.200536238.

171. Kobayashi, S.; Kashiwa, K.; Shimada, J.; Kawasaki, T.; Shoda, S.-i., Enzymatic polymerization: The first in vitro synthesis of cellulose via nonbiosynthetic path catalyzed by cellulase. *Makromolekulare Chemie. Macromolecular Symposia* **1992,** *54-55* (1), 509-518.

172. Wagner, T. E.; Chai, H. G.; Warfield, A. S., Cellulose polymer supported sequential analysis of polyribonucleotides. *J. Am. Chem. Soc.* **1969,** *91* (9), 2388-2389.

173. Favier, V.; Chanzy, H.; Cavaille, J. Y., Polymer Nanocomposites Reinforced by Cellulose Whiskers. *Macromolecules* **1995,** *28* (18), 6365-6367.

174. Wang, J.; Yu, J.; Liu, Y.; Chen, Y.; Wang, C.; Tang, C.; Chu, F., Synthesis and characterization of a novel rosin-based monomer: free-radical polymerization and epoxy curing. *Green Materials* **2013,** *1*, 105-113.

175. Wilbon, P.; Gulledge, A. L.; Benicewicz, B. C.; Tang, C., Renewable rosin fatty acid polyesters: the effect of backbone structure on thermal properties. *Green Materials* **2013,** *1*, 96-104.

176. Chen, Y.; Wilbon, P. A.; Zhou, J.; Nagarkatti, M.; Wang, C.; Chu, F.; Tang, C., Multifunctional self-fluorescent polymer nanogels for label-free imaging and drug delivery. *Chemical Communications* **2013,** *49* (3), 297-299.

177. Chen, Y.; Wilbon, P. A.; Chen, Y. P.; Zhou, J.; Nagarkatti, M.; Wang, C.; Chu, F.; Decho, A. W.; Tang, C., Amphipathic antibacterial agents using cationic methacrylic polymers with natural rosin as pendant group. *RSC Advances* **2012,** *2* (27), 10275-10282.

178. Wang, J.; Chen, Y. P.; Yao, K.; Wilbon, P. A.; Zhang, W.; Ren, L.; Zhou, J.; Nagarkatti, M.; Wang, C.; Chu, F.; He, X.; Decho, A. W.; Tang, C., Robust antimicrobial compounds and polymers derived from natural resin acids. *Chemical Communications* **2012,** *48* (6), 916-918.

179. Wang, J.; Yao, K.; Wang, C.; Tang, C.; Jiang, X., Synthesis and drug delivery of novel amphiphilic block copolymers containing hydrophobic dehydroabietic moiety. *Journal of Materials Chemistry B* **2013,** *1* (17), 2324-2332.

180. Çayli, G.; Meier, M. A. R., Polymers from renewable resources: Bulk ATRP of fatty alcohol-derived methacrylates. *European Journal Of Lipid Science And Technology* **2008,** *110* (9), 853-859.

181. Dutertre, F.; Pennarun, P.-Y.; Colombani, O.; Nicol, E., Straightforward synthesis of poly(lauryl acrylate)-b-poly(stearyl acrylate) diblock copolymers by ATRP. *European Polymer Journal* **2011,** *47* (3), 343-351.

182. Meng, T.; Gao, X.; Zhang, J.; Yuan, J.; Zhang, Y.; He, J., Graft copolymers prepared by atom transfer radical polymerization (ATRP) from cellulose. *Polymer* **2009,** *50* (2), 447-454.

183. Shin, J.; Lee, Y.; Tolman, W. B.; Hillmyer, M. A., Thermoplastic Elastomers Derived from Menthide and Tulipalin A. *Biomacromolecules* **2012,** *13* (11), 3833-3840.

184. Ferry, J. D., Viscoelastic Properties of Polymers. John Wiley & Sons: New York, 1980; pp 35-129.

185. Yao, K.; Wang, J.; Zhang, W.; Lee, J. S.; Wang, C.; Chu, F.; He, X.; Tang, C., Degradable Rosin-Ester–Caprolactone Graft Copolymers. *Biomacromolecules* **2011,** *12* (6), 2171-2177.

186. Wang, J.; Yao, K.; Korich, A. L.; Li, S.; Ma, S.; Ploehn, H. J.; Iovine, P. M.; Wang, C.; Chu, F.; Tang, C., Combining renewable gum rosin and lignin: Towards hydrophobic polymer composites by controlled polymerization. *Journal of Polymer Science Part A: Polymer Chemistry* **2011,** *49* (17), 3728-3738.

187. Dai, S.; Ravi, P.; Tam, K. C., pH-Responsive polymers: synthesis, properties and applications. *Soft Matter* **2008,** *4* (3), 435-449.

188. Jochum, F. D.; zur Borg, L.; Roth, P. J.; Theato, P., Thermo- and Light-Responsive Polymers Containing Photoswitchable Azobenzene End Groups. *Macromolecules* **2009,** *42* (20), 7854-7862.

189. Morishima, Y., Thermally Responsive Polymer Vesicles. *Angewandte Chemie International Edition* **2007,** *46* (9), 1370-1372.

190. Tam, T. K.; Ornatska, M.; Pita, M.; Minko, S.; Katz, E., Polymer Brush-Modified Electrode with Switchable and Tunable Redox Activity for Bioelectronic Applications. *The Journal of Physical Chemistry C* **2008,** *112* (22), 8438-8445.

191. Azzaroni, O.; Brown, A. A.; Huck, W. T. S., UCST Wetting Transitions of Polyzwitterionic Brushes Driven by Self-Association. *Angewandte Chemie International Edition* **2006,** *45* (11), 1770-1774.

192. Toomey, R.; Freidank, D.; RÃ¼he, J. r., Swelling Behavior of Thin, Surface-Attached Polymer Networks. *Macromolecules* **2004,** *37* (3), 882-887.

193. Itano, K.; Choi, J.; Rubner, M. F., Mechanism of the pH-Induced Discontinuous Swelling/Deswelling Transitions of Poly(allylamine hydrochloride)-Containing Polyelectrolyte Multilayer Films. *Macromolecules* **2005,** *38* (8), 3450-3460.

194. Binks, B. P.; Murakami, R.; Armes, S. P.; Fujii, S., Temperature-Induced Inversion of Nanoparticle-Stabilized Emulsions. *Angewandte Chemie International Edition* **2005,** *44* (30), 4795-4798.

195. Gillies, E. R.; Jonsson, T. B.; FrÃ©chet, J. M. J., Stimuli-Responsive Supramolecular Assemblies of Linear-Dendritic Copolymers. *J. Am. Chem. Soc.* **2004,** *126* (38), 11936-11943.

196. Dupin, D.; Armes, S. P.; Fujii, S., Stimulus-Responsive Liquid Marbles. *J. Am. Chem. Soc.* **2009,** *131* (15), 5386-5387.

197. Woodcock, J. W.; Jiang, X.; Wright, R. A. E.; Zhao, B., Enzyme-Induced Formation of Thermoreversible Micellar Gels from Aqueous Solutions of Multiresponsive Hydrophilic ABA Triblock Copolymers. *Macromolecules* **2011,** *44*, 5764-5775.

198. Jiang, X.; Jin, S.; Zhong, Q.; Dadmun, M. D.; Zhao, B., Stimuli-Induced Multiple Solâ^'Gelâ^'Sol Transitions of Aqueous Solution of a Thermo- and Light-Sensitive Hydrophilic Block Copolymer. *Macromolecules* **2009,** *42*, 8468-8476.

199. Karg, M.; Pastoriza-Santos, I.; Rodriguez-González, B.; von Klitzing, R.; Wellert, S.; Hellweg, T., Temperature, pH, and Ionic Strength Induced Changes of the Swelling Behavior of PNIPAM−Poly(allylacetic acid) Copolymer Microgels. *Langmuir* **2008,** *24* (12), 6300-6306.

200. Wang, D.; Wu, T.; Wan, X.; Wang, X.; Liu, S., Purely Salt-Responsive Micelle Formation and Inversion Based on a Novel Schizophrenic Sulfobetaine Block Copolymer: Structure and Kinetics of Micellization. *Langmuir* **2007,** *23* (23), 11866-11874.

201. Behrens, M. A.; Lopez, M.; Kjøniksen, A.-L.; Zhu, K.; Nyström, B.; Pedersen, J. S., Structure and Interactions of Charged Triblock Copolymers Studied by Small-Angle X-ray Scattering: Dependence on Temperature and Charge Screening. *Langmuir* **2011,** *28* (2), 1105-1114.

202. Kellum, M. G.; Smith, A. E.; York, S. K.; McCormick, C. L., Reversible Interpolyelectrolyte Shell Cross-Linked Micelles from pH/Salt-Responsive Diblock Copolymers Synthesized via RAFT in Aqueous Solution†. *Macromolecules* **2010,** *43* (17), 7033-7040.

203. Arnal, M. L.; Balsamo, V.; López-Carrasquero, F.; Contreras, J.; Carrillo, M.; Schmalz, H.; Abetz, V.; Laredo, E.; Müller, A. J., Synthesis and Characterization of Polystyrene-b-poly(ethylene oxide)-b-poly(ε-caprolactone) Block Copolymers. *Macromolecules* **2001,** *34* (23), 7973-7982.

204. Bogdanov, B.; Vidts, A.; Van Den Buicke, A.; Verbeeck, R.; Schacht, E., Synthesis and thermal properties of poly(ethylene glycol)-poly(ϵ-caprolactone) copolymers. *Polymer* **1998,** *39* (8–9), 1631-1636.

205. Hua, C.; Dong, C.-M.; Wei, Y., Versatile Strategy for the Synthesis of Dendronlike Polypeptide/Linear Poly(ε-caprolactone) Block Copolymers via Click Chemistry. *Biomacromolecules* **2009,** *10* (5), 1140-1148.

206. Motala-Timol, S.; Jhurry, D.; Zhou, J.; Bhaw-Luximon, A.; Mohun, G.; Ritter, H., Amphiphilic Poly(l-lysine-b-caprolactone) Block Copolymers: Synthesis, Characterization, and Solution Properties. *Macromolecules* **2008,** *41* (15), 5571-5576.

207. Brahim, S.; Narinesingh, D.; Guiseppi-Elie, A., Synthesis and Hydration Properties of pH-Sensitive p(HEMA)-Based Hydrogels Containing 3-(Trimethoxysilyl)propyl Methacrylate. *Biomacromolecules* **2003,** *4* (3), 497-503.

208. Sun, G.; Zhang, M.; He, J.; Ni, P., Synthesis of amphiphilic cationic copolymers poly[2-(methacryloyloxy)ethyl trimethylammonium chloride-co-stearyl methacrylate] and their self-assembly behavior in water and water-ethanol mixtures. *Journal of Polymer Science Part A: Polymer Chemistry* **2009,** *47* (18), 4670-4684.

209. Branham, K. D.; Bunyard, C. W.; Lang, F. J.; Possell, K.; Schultz, W. T.; Schick, K. G. Ion triggerable, cationic polymers, a method of making same and items using same. Feb 7, 2006.

210. Chang, Y.; Lang, F. J.; Wang, K. Y.; Chen, F. M.; Branham, K. D.; Schick, K. G.; Schultz, W. T. Water-dispersible, cationic polymers, a method of making same and items using same. July 4, 2006.

211. Chang, Y.; McLandsborough, L.; McClements, D. J., Interactions of a Cationic Antimicrobial (ε-Polylysine) with an Anionic Biopolymer (Pectin): An Isothermal Titration Calorimetry, Microelectrophoresis, and Turbidity Study. *J. Agri. Food Chem.* **2011,** *59* (10), 5579-5588.

212. Behrens, M. A.; Kjøniksen, A.-L.; Zhu, K.; Nyström, B.; Pedersen, J. S., Small-Angle X-ray Scattering Study of Charged Triblock Copolymers as a Function of Polymer Concentration, Temperature, and Charge Screening. *Macromolecules* **2011,** *45* (1), 246-255.

213. Kjøniksen, A.-L.; Zhu, K.; Behrens, M. A.; Pedersen, J. S.; Nyström, B., Effects of Temperature and Salt Concentration on the Structural and Dynamical Features in Aqueous Solutions of Charged Triblock Copolymers. *The Journal of Physical Chemistry B* **2011,** *115* (10), 2125-2139.

214. Lin, X.; He, Q.; Li, J., Complex polymer brush gradients based on nanolithography and surface-initiated polymerization. *Chemical Society Reviews* **2012,** *41* (9), 3584-3593.

215. Azzaroni, O., Polymer brushes here, there, and everywhere: Recent advances in their practical applications and emerging opportunities in multiple research fields. *Journal of Polymer Science Part A: Polymer Chemistry* **2012,** *50* (16), 3225-3258.

216. Zhang, M.; Müller, A. H. E., Cylindrical polymer brushes. *Journal of Polymer Science Part A: Polymer Chemistry* **2005,** *43* (16), 3461-3481.

217. Sheiko, S. S.; Sumerlin, B. S.; Matyjaszewski, K., Cylindrical molecular brushes: Synthesis, characterization, and properties. *Prog. Polym. Sci.* **2008,** *33* (7), 759-785.

218. Bhattacharya, A.; Misra, B. N., Grafting: a versatile means to modify polymers: Techniques, factors and applications. *Prog. Polym. Sci.* **2004,** *29* (8), 767-814.

219. Wintermantel, M.; Gerle, M.; Fischer, K.; Schmidt, M.; Wataoka, I.; Urakawa, H.; Kajiwara, K.; Tsukahara, Y., Molecular Bottlebrushes†. *Macromolecules* **1996,** *29* (3), 978-983.

220. Subbotin, A.; Saariaho, M.; Ikkala, O.; ten Brinke, G., Elasticity of Comb Copolymer Cylindrical Brushes. *Macromolecules* **2000,** *33* (9), 3447-3452.

221. Ryu, S. W.; Hirao, A., Anionic Synthesis of Well-Defined Poly(m-halomethylstyrene)s and Branched Polymers via Graft-onto Methodology. *Macromolecules* **2000,** *33* (13), 4765-4771.

222. Schappacher, M.; Deffieux, A., New Polymer Chain Architecture: Synthesis and Characterization of Star Polymers with Comb Polystyrene Branches. *Macromolecules* **2000,** *33* (20), 7371-7377.

223. Gao, H.; Matyjaszewski, K., Synthesis of Molecular Brushes by "Grafting onto" Method: Combination of ATRP and Click Reactions. *J. Am. Chem. Soc.* **2007,** *129* (20), 6633-6639.

224. Lanson, D.; Ariura, F.; Schappacher, M.; Borsali, R.; Deffieux, A., Application of living ionic polymerizations to the design of AB-type comb-like copolymers of various topologies and organizations. *Macromol. Res.* **2007,** *15* (2), 173-177.

225. Beers, K. L.; Gaynor, S. G.; Matyjaszewski, K.; Sheiko, S. S.; Möller, M., The Synthesis of Densely Grafted Copolymers by Atom Transfer Radical Polymerization. *Macromolecules* **1998,** *31* (26), 9413-9415.

226. Sumerlin, B. S.; Neugebauer, D.; Matyjaszewski, K., Initiation Efficiency in the Synthesis of Molecular Brushes by Grafting from via Atom Transfer Radical Polymerization. *Macromolecules* **2005,** *38* (3), 702-708.

227. Tang, C.; Dufour, B.; Kowalewski, T.; Matyjaszewski, K., Synthesis and Morphology of Molecular Brushes with Polyacrylonitrile Block Copolymer Side Chains and Their Conversion into Nanostructured Carbons. *Macromolecules* **2007,** *40* (17), 6199-6205.

228. Qin, S.; Matyjaszewski, K.; Xu, H.; Sheiko, S. S., Synthesis and Visualization of Densely Grafted Molecular Brushes with Crystallizable Poly(octadecyl methacrylate) Block Segments. *Macromolecules* **2003,** *36* (3), 605-612.

229. Neugebauer, D.; Sumerlin, B. S.; Matyjaszewski, K.; Goodhart, B.; Sheiko, S. S., How dense are cylindrical brushes grafted from a multifunctional macroinitiator? *Polymer* **2004,** *45* (24), 8173-8179.

230. Ohno, S.; Matyjaszewski, K., Controlling grafting density and side chain length in poly(n-butyl acrylate) by ATRP copolymerization of macromonomers. *Journal of Polymer Science Part A: Polymer Chemistry* **2006,** *44* (19), 5454-5467.

231. Berry, G. C.; Kahle, S.; Ohno, S.; Matyjaszewski, K.; Pakula, T., Viscoelastic and dielectric studies on comb- and brush-shaped poly(n-butyl acrylate). *Polymer* **2008,** *49* (16), 3533-3540.

232. Vogt, A. P.; Sumerlin, B. S., An Efficient Route to Macromonomers via ATRP and Click Chemistry. *Macromolecules* **2006,** *39* (16), 5286-5292.

233. Pantazis, D.; Chalari, I.; Hadjichristidis, N., Anionic Polymerization of Styrenic Macromonomers. *Macromolecules* **2003,** *36* (11), 3783-3785.

234. Xia, Y.; Olsen, B. D.; Kornfield, J. A.; Grubbs, R. H., Efficient Synthesis of Narrowly Dispersed Brush Copolymers and Study of Their Assemblies: The Importance of Side Chain Arrangement. *J. Am. Chem. Soc.* **2009,** *131* (51), 18525-18532.

235. Johnson, J. A.; Lu, Y. Y.; Burts, A. O.; Lim, Y.-H.; Finn, M. G.; Koberstein, J. T.; Turro, N. J.; Tirrell, D. A.; Grubbs, R. H., Core-Clickable PEG-Branch-Azide Bivalent-Bottle-Brush Polymers by ROMP: Grafting-Through and Clicking-To. *J. Am. Chem. Soc.* **2010,** *133* (3), 559-566.

236. Miyake, G. M.; Weitekamp, R. A.; Piunova, V. A.; Grubbs, R. H., Synthesis of Isocyanate-Based Brush Block Copolymers and Their Rapid Self-Assembly to Infrared-Reflecting Photonic Crystals. *J. Am. Chem. Soc.* **2012,** *134* (34), 14249-14254.

237. Li, A.; Ma, J.; Sun, G.; Li, Z.; Cho, S.; Clark, C.; Wooley, K. L., One-pot, facile synthesis of well-defined molecular brush copolymers by a tandem RAFT and ROMP, "Grafting-through" strategy. *Journal of Polymer Science Part A: Polymer Chemistry* **2012,** *50* (9), 1681-1688.

238. Kim, J. G.; Coates, G. W., Synthesis and Polymerization of Norbornenyl-Terminated Multiblock Poly(cyclohexene carbonate)s: A Consecutive Ring-Opening Polymerization Route to Multisegmented Graft Polycarbonates. *Macromolecules* **2012,** *45* (19), 7878-7883.

239. Ding, X.; Yang, C.; Lim, T. P.; Hsu, L. Y.; Engler, A. C.; Hedrick, J. L.; Yang, Y.-Y., Antibacterial and antifouling catheter coatings using surface grafted PEG-b-cationic polycarbonate diblock copolymers. *Biomaterials* **2012,** *33* (28), 6593-6603.

240. Li, C.; Gunari, N.; Fischer, K.; Janshoff, A.; Schmidt, M., New Perspectives for the Design of Molecular Actuators: Thermally Induced Collapse of Single Macromolecules from Cylindrical Brushes to Spheres. *Angewandte Chemie-International Edition* **2004,** *43* (9), 1101-1104.

241. Lee, H.-i.; Boyce, J. R.; Nese, A.; Sheiko, S. S.; Matyjaszewski, K., pH-induced conformational changes of loosely grafted molecular brushes containing poly(acrylic acid) side chains. *Polymer* **2008,** *49* (25), 5490-5496.

242. Nese, A.; Li, Y.; Averick, S.; Kwak, Y.; Konkolewicz, D.; Sheiko, S. S.; Matyjaszewski, K., Synthesis of Amphiphilic Poly(N-vinylpyrrolidone)-b-poly(vinyl acetate) Molecular Bottlebrushes. *ACS Macro Letters* **2011,** *1* (1), 227-231.

243. Nese, A.; Lebedeva, N. V.; Sherwood, G.; Averick, S.; Li, Y.; Gao, H.; Peteanu, L.; Sheiko, S. S.; Matyjaszewski, K., pH-Responsive Fluorescent Molecular Bottlebrushes Prepared by Atom Transfer Radical Polymerization. *Macromolecules* **2011,** *44* (15), 5905-5910.

244. Nese, A.; Kwak, Y.; Nicolaÿ, R.; Barrett, M.; Sheiko, S. S.; Matyjaszewski, K., Synthesis of Poly(vinyl acetate) Molecular Brushes by a Combination of Atom Transfer Radical Polymerization (ATRP) and Reversible Addition−Fragmentation Chain Transfer (RAFT) Polymerization. *Macromolecules* **2010,** *43* (9), 4016-4019.

245. Xu, Y.; Bolisetty, S.; Drechsler, M.; Fang, B.; Yuan, J.; Ballauff, M.; Müller, A. H. E., pH and salt responsive poly(N,N-dimethylaminoethyl methacrylate) cylindrical brushes and their quaternized derivatives. *Polymer* **2008,** *49* (18), 3957-3964.

246. Yao, K.; Tang, C.; Zhang, J.; Bunyard, C., Degradable and salt-responsive random copolymers. *Polym. Chem.* **2013,** *4* (3), 528-535.

247. Sanford, M. S.; Love, J. A.; Grubbs, R. H., A Versatile Precursor for the Synthesis of New Ruthenium Olefin Metathesis Catalysts. *Organometallics* **2001,** *20* (25), 5314-5318.

248. Ren, L.; Zhang, J.; Bai, X.; Hardy, C. G.; Shimizu, K. D.; Tang, C., Preparation of cationic cobaltocenium polymers and block copolymers by "living" ring-opening metathesis polymerization. *Chemical Science* **2012,** *3* (2), 580-583.

249. Xie, M.; Dang, J.; Han, H.; Wang, W.; Liu, J.; He, X.; Zhang, Y., Well-Defined Brush Copolymers with High Grafting Density of Amphiphilic Side Chains by Combination of ROP, ROMP, and ATRP. *Macromolecules* **2008,** *41* (23), 9004-9010.

APPENDIX A – PERMISSION TO REPRINT

RightsLink®

Home | Account Info | Help

Title: Controlled Polymerization of Next-Generation Renewable Monomers and Beyond

Author: Kejian Yao and Chuanbing Tang

Publication: Macromolecules

Publisher: American Chemical Society

Date: Mar 1, 2013

Logged in as:
Kejian Yao
Account #:
3000625163

LOGOUT

PERMISSION/LICENSE IS GRANTED FOR YOUR ORDER AT NO CHARGE

This type of permission/license, instead of the standard Terms & Conditions, is sent to you because no fee is being charged for your order. Please note the following:

- Permission is granted for your request in both print and electronic formats, and translations.
- If figures and/or tables were requested, they may be adapted or used in part.
- Please print this page for your records and send a copy of it to your publisher/graduate school.
- Appropriate credit for the requested material should be given as follows: "Reprinted (adapted) with permission from (COMPLETE REFERENCE CITATION). Copyright (YEAR) American Chemical Society." Insert appropriate information in place of the capitalized words.
- One-time permission is granted only for the use specified in your request. No additional uses are granted (such as derivative works or other editions). For any other uses, please submit a new request.

BACK | CLOSE WINDOW

RightsLink®

Home | Account Info | Help

Title: Well-Defined Renewable Polymers Derived from Gum Rosin

Author: Yijun Zheng, Kejian Yao, James Lee, David Chandler, Jifu Wang, Chunpeng Wang, Fuxiang Chu, and Chuanbing Tang

Publication: Macromolecules

Publisher: American Chemical Society

Date: Jul 1, 2010

Logged in as:
Kejian Yao
Account #:
3000625163

LOGOUT

PERMISSION/LICENSE IS GRANTED FOR YOUR ORDER AT NO CHARGE

This type of permission/license, instead of the standard Terms & Conditions, is sent to you because no fee is being charged for your order. Please note the following:

- Permission is granted for your request in both print and electronic formats, and translations.
- If figures and/or tables were requested, they may be adapted or used in part.
- Please print this page for your records and send a copy of it to your publisher/graduate school.
- Appropriate credit for the requested material should be given as follows: "Reprinted (adapted) with permission from (COMPLETE REFERENCE CITATION). Copyright (YEAR) American Chemical Society." Insert appropriate information in place of the capitalized words.
- One-time permission is granted only for the use specified in your request. No additional uses are granted (such as derivative works or other editions). For any other uses, please submit a new request.

BACK | CLOSE WINDOW

RSC | Advancing the Chemical Sciences

Royal Society of Chemistry
Thomas Graham House
Science Park
Milton Road
Cambridge
CB4 0WF

Tel: +44 (0)1223 420 066
Fax: +44 (0)1223 423 623
Email: contracts-copyright@rsc.org

www.rsc.org

Acknowledgements to be used by RSC authors

Authors of RSC books and journal articles can reproduce material (for example a figure) from the RSC publication in a non-RSC publication, including theses, without formally requesting permission providing that the correct acknowledgement is given to the RSC publication. This permission extends to reproduction of large portions of text or the whole article or book chapter when being reproduced in a thesis.

The acknowledgement to be used depends on the RSC publication in which the material was published and the form of the acknowledgements is as follows:

- For material being reproduced from an article in *New Journal of Chemistry* the acknowledgement should be in the form:
  - [Original citation] - Reproduced by permission of The Royal Society of Chemistry (RSC) on behalf of the Centre National de la Recherche Scientifique (CNRS) and the RSC
- For material being reproduced from an article *Photochemical & Photobiological Sciences* the acknowledgement should be in the form:
  - [Original citation] - Reproduced by permission of The Royal Society of Chemistry (RSC) on behalf of the European Society for Photobiology, the European Photochemistry Association, and RSC
- For material being reproduced from an article in *Physical Chemistry Chemical Physics* the acknowledgement should be in the form:
  - [Original citation] - Reproduced by permission of the PCCP Owner Societies
- For material reproduced from books and any other journal the acknowledgement should be in the form:
  - [Original citation] - Reproduced by permission of The Royal Society of Chemistry

The acknowledgement should also include a hyperlink to the article on the RSC website.

The form of the acknowledgement is also specified in the RSC agreement/licence signed by the corresponding author.

Except in cases of republication in a thesis, this express permission does not cover the reproduction of large portions of text from the RSC publication or reproduction of the whole article or book chapter.

A publisher of a non-RSC publication can use this document as proof that permission is granted to use the material in the non-RSC publication.

VAT Registration Number: GB 342 1764 71 Registered Charity Number: 207890

JOHN WILEY AND SONS LICENSE TERMS AND CONDITIONS

Oct 20, 2013

This is a License Agreement between Kejian Yao ("You") and John Wiley and Sons ("John Wiley and Sons") provided by Copyright Clearance Center ("CCC"). The license consists of your order details, the terms and conditions provided by John Wiley and Sons, and the payment terms and conditions.

All payments must be made in full to CCC. For payment instructions, please see information listed at the bottom of this form.

License Number	3253350596715
License date	Oct 20, 2013
Licensed content publisher	John Wiley and Sons
Licensed content publication	Macromolecular Rapid Communications
Licensed content title	Cationic Salt-Responsive Bottle-Brush Polymers
Licensed copyright line	Copyright © 2013 WILEY-VCH Verlag GmbH & Co. KGaA, Weinheim
Licensed content author	Kejian Yao,Ying Chen,Jun Zhang,Clay Bunyard,Chuanbing Tang
Licensed content date	Mar 13, 2013
Start page	645
End page	651
Type of use	Dissertation/Thesis
Requestor type	Author of this Wiley article
Format	Print and electronic
Portion	Full article
Will you be translating?	No
Total	0.00 USD
Terms and Conditions	

TERMS AND CONDITIONS

This copyrighted material is owned by or exclusively licensed to John Wiley & Sons, Inc. or one of its group companies (each a "Wiley Company") or a society for whom a Wiley Company has exclusive publishing rights in relation to a particular journal (collectively "WILEY"). By clicking "accept" in connection with completing this licensing transaction, you agree that the following terms and conditions apply to this transaction (along with the billing and payment terms and conditions established by the Copyright Clearance Center Inc., ("CCC's Billing and Payment terms and conditions"), at the time that you opened your RightsLink account (these are available at any time at http://myaccount.copyright.com).